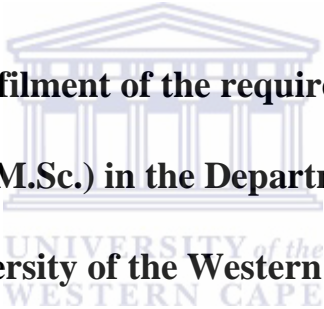


Microbial Diversity of the Namib Desert Salt Pans

By

Melissa Cloete



**Submitted in partial fulfilment of the requirements for the degree of
Magistrate Scientiae (M.Sc.) in the Department of Biotechnology,
University of the Western Cape**

Supervisor: Prof. I. M Trindade

Co-Supervisor: Dr. B.M. Kirby

December 2015

Declaration

I declare that ‘The Microbial Diversity of the Namib Desert Salt Pans’ is my own work, that is has not been submitted for any degree or examination in any other university, and that all the resources I have used or quoted have been indicated and acknowledged by complete references.



Melissa (Du Plessis) Cloete



Abstract

Salt pans are a characteristic feature of many dry deserts. The microbial communities inhabiting salt pans are thought to be particularly complex and are generally dominated by halophilic microorganisms. Although saline pools are frequently found within the hyper-arid Namib Desert, the microbial communities of these saline sites have been scarcely investigated. The aim of the present study was to characterise the archaeal, bacterial and cyanobacterial diversity inhabiting these extreme saline pools using three culture independent molecular techniques (DGGE, T-RFLP and 16S rRNA clone libraries). The physiochemical results, mainly the conductivity readings recorded from the sampling sites, indicated that the Gobabeb (103.0mS/cm) region was less saline than the two Swakopmund [(Sps01) (150.0mS/cm) and Sps02 (180.0mS/cm)] sites. Results obtained from DGGE and T-RFLP data were in agreement for both bacterial and cyanobacterial analysis indicating that the Gobabeb site was more diverse than the two Swakopmund sites (Sps01 and Sps02). In comparison, the archaeal community profiles for DGGE and T-RFLP analysis were in agreement illustrating that the archaeal community were more abundant in the two extreme Swakopmund saline sites. Phylogenetic data obtained from 16S rRNA gene clone libraries identified halophilic phylotypes (*Rhodothermaceae*, *Idiomarinaceae*, *Puniceicoccaceae* and *Cyanobacteria/Chloroplast*, Family VII) normally associated with salt rich sites. In addition, a large number of unclassified taxa were identified. To conclude, the study highlighted the presence of a rich microbial diversity present within the salt pans of the Namib Desert and establishes a platform for future investigations.

Publications originating from this thesis

Poster/Presentations

1. Melissa Du Plessis, Angel Valverde, Marla Tuffin and Don Cowan. *Microbial Diversity of the Namib Desert Salt Pans*. Biotechnology Department Open day, October 2012 (Poster)
2. Melissa Du Plessis, Angel Valverde, Marla Tuffin* and Don Cowan. *Microbial Diversity of the Namib Desert Salt Pans*. 9th International Congress on Extremophiles, Sevilla, Spain, September 2012 (Poster) (* presenting author)
3. Melissa Du Plessis, Francesca Stomeo, Marla Tuffin and Don Cowan. *Microbial Diversity of the Namib Desert Salt Pans*. South African Society for Microbiology (SASM), Cape Town, South Africa, November 2011 (Poster)



Acknowledgements

This has truly been a long winding road to complete this thesis, this degree, but it would not have been possible if not for the long list of individuals who guided, motivated and pushed me over the finish line. To them I owe a great deal of gratitude that I never would be able to pay in full. All I can give them is my heartfelt thanks to their teachings and patients that I will take with to all my future endeavours.

My thanks are extended to:

- 1) Supervisors- Prof IM Trindade and Prof. D Cowan (past supervisor)
- 2) Past co-supervisors: Dr. Francesca Stomeo and Dr. Angel Valverde
- 3) Present co-supervisor- Dr. Bronwyn Kirby, the completion of this thesis and my degree would not have been possible if not for your guidance and patience. Many, many thanks!
- 4) To my family and especially my husband Kevin thank you for your support, patience and encouragement, I know it wasn't easy
- 5) The funders, NRF for their financial assistance and to the Gobabeb Research Centre for allowing access to the sampling sites.

Dedication

To my Creator, for never allowing me to quit!



Table of Contents

Declaration	ii
Abstract.....	iii
Publications originating from this thesis.....	iv
Acknowledgements	v
Dedication	vi
Table of Contents	vii
List of Tables	xiii
List of Figures.....	xiv
List of Abbreviations	xxii
Chapter 1: Literature review	1
1.1 The Namib Desert	1
1.1.2 Climate	1
1.1.3 Salt weathering.....	2
1.1.4 Saline environments	3
1.1.5 Salt Pans	3
1.1.6 Namib Desert salt pans.....	4
1.2 Microbial diversity in salt pans	5
1.2.1 Halophiles and halotolerant microorganisms.....	5
1.2.2 Adaptions of halophiles to saline environment.....	5
1.2.3 The halophilic communities of saline habitats	7
1.2.3.1 Archaeal diversity.....	8
1.2.3.2 Bacterial diversity.....	8
1.2.3.3 Cyanobacterial diversity.....	9
1.2.3.4 Eukaryotic diversity	10
1.3 The biotechnology application and role of halophiles in salt pans.....	10
1.4 The biodiversity of the Namib Desert salt pans.....	11
1.5 Culture independent techniques used to assess microbial diversity	12

1.5.1 16S rRNA gene in phylogenetic analysis.....	13
1.5.2 16S rRNA gene clone libraries.....	14
1.5.3 Denaturing gradient gel electrophoresis.....	15
1.5.4 Terminal restriction fragment length polymorphism	17
1.6 Aims and objectives of the study	18
Chapter 2: Materials and Methods	19
2.1 Sampling procedures	19
2.1.1 Physio-Chemical Analysis	20
2.2 DNA extraction methods.....	20
2.2.1 Materials used for the modified Zhou et al. (1999) DNA extraction method.....	20
2.2.1.1 <i>Extraction buffer</i>	20
2.2.1.2 <i>DNA elution buffer/ TE</i>	20
2.2.1.3 <i>Methodology for the modified Zhou et al. (1999) DNA extraction method</i>	20
2.2.2 Commercial DNA extraction kit: UltraClean Soil DNA Extraction kit (MoBio laboratories, Inc.).....	21
2.3 DNA Quantification	21
2.4 Agarose gel electrophoresis	21
2.5 Denaturing gradient gel electrophoresis	21
2.5.1 Bacterial 16S rRNA PCR amplification for DGGE analysis	21
2.5.2 Archaeal 16S rRNA gene PCR amplification for DGGE analysis	22
2.5.3 DGGE gel assembly	24
2.5.4 Analysing DGGE banding patterns.....	24
2.5.5 Sequencing of DGGE bands	25
2.6.1 PCR amplification of the bacterial 16S rRNA gene	25
2.6.2 PCR amplification of the archaeal 16S rRNA gene	25
2.6.3 PCR amplification of the cyanobacterial 16S rRNA gene	26
2.6.4 Restriction digestion and T-RF peak analysis.....	26
2.7 Clone library construction.....	27

2.7.1 Media used for cloning.....	27
2.7.1.1 <i>Luria Broth (Sambrook and Russel, 2001)</i>	27
2.7.1.2 <i>Luria Agar (Sambrook and Russel, 2001)</i>	27
2.7.2 Preparation of chemical competent cells (Li et al., 2010).....	27
2.7.3 Ligation	28
2.7.4 Transformation of E.coli GeneHog competent cells.....	28
2.7.5 Screening of recombinant clones	28
2.7.5.1 Colony PCR	28
2.7.5.2 <i>Amplified ribosomal DNA Restriction Analysis (ARDRA) of clone libraries</i>	29
2.7.5.3 <i>Sequence analysis of clones</i>	29
2.7.5.4 <i>Statistical analysis of clones</i>	30
Chapter 3: Bacterial Diversity	31
3.1 Introduction	31
3.2 Results and discussion	31
3.2.1 Description of the sampling sites	31
3.2.2 Analysis of Metagenomic DNA extraction procedures	35
3.2.3 DGGE analysis.....	35
3.2.4 Statistical analysis of DGGE.....	36
3.2.4.1 Gobabeb site	36
3.2.4.2 <i>Swakopmund site 1</i>	37
3.2.4.3 <i>Swakopmund site 2</i>	39
3.2.5 T-RFLP analysis.....	40
3.2.6 Comparison of OTUs obtained by restriction analysis for the different sampling sites	40
3.2.6.1 <i>Analysis of Gobabeb site OTUs</i>	41
3.2.6.2 <i>Analysis of Swakopmund site 1 OTUs</i>	42
3.2.6.3 <i>Swakopmund site 2 OTUs</i>	43



3.2.7 Statistical analysis of T-RFs.....	44
3.2.7.1 Gobabeb site OTUs	45
3.2.7.2 Swakopmund site 1 OTUs.....	45
3.2.7.3 Swakopmund site 2 OTUs.....	46
3.2.8 Construction of bacterial 16S rRNA gene clone libraries.....	46
3.2.8.1 Clone library construction.....	46
3.2.8.2 ARDRA analysis of clone libraries	47
3.2.8.3 Analysis of 16S rRNA gene clone libraries	48
3.2.9 Sequence analysis of 16S rRNA gene clones.....	49
3.2.9.1 Phylogenetic analysis of Gobabeb site	50
3.2.9.2 Phylogenetic analysis of Swakopmund site 1	52
3.2.9.3 Phylogenetic analysis of Swakopmund site 2	53
3.3 Summary of bacterial diversity findings.....	60
3.3.1 Summary of the Gobabeb microbial diversity	60
3.3.2 Summary of the Swakopmund site 1 microbial diversity	61
3.3.3 Summary of Swakopmund site 2 microbial diversity	62
Chapter 4: Cyanobacteria.....	63
4.1 Introduction	63
4.2 Results and discussion	63
4.2.1 Community profile of Cyanobacteria.....	63
4.2.2 OTU Analysis of T-RFs	64
4.2.2.1 Gobabeb site OTUs	64
4.2.2.2 Swakopmund site 1 OTUs.....	65
4.2.2.3 Swakopmund site 2 OTUs.....	67
4.2.3 T-RF cluster analysis.....	68
4.2.3.1 Gobabeb site cluster analysis	68
4.2.3.2 Swakopmund site 1 sampling site cluster analysis	69

4.2.3.3 <i>Swakopmund site 2 cluster analysis</i>	70
4.2.4 Cyanobacteria 16S rRNA gene clone libraries	70
4.2.4.1 <i>ARDRA analysis of clones</i>	70
4.2.4.2 <i>Statistical analysis of 16S rRNA gene clone libraries</i>	71
4.2.5 Phylogenetic analysis of clones.....	72
4.2.5.1 <i>Gobabeb site</i>	72
4.2.5.2 <i>Swakopmund site 1</i>	74
4.2.5.3 <i>Swakopmund site 2</i>	74
4.2.6 Phylogenetic tree construction	75
4.3 Summary of cyanobacterial diversity findings	77
4.3.1 Cyanobacteria diversity findings of Gobabeb site	78
4.3.2 Cyanobacteria diversity findings of Swakopmund site 1	78
4.3.3 Cyanobacteria diversity findings of Swakopmund site 2.....	78
4.4 Concluding remarks	79
Chapter 5: Archaeal diversity	80
5.1 Introduction	80
5.2 Results and discussion	80
5.2.1 DGGE analysis	80
5.2.2 Statistical analysis of DGGE.....	81
5.2.2.1 <i>Gobabeb site</i>	81
5.2.2.2 <i>Swakopmund site 1</i>	82
5.2.2.3 <i>Swakopmund site 2</i>	83
5.2.3 Profiling of DGGE bands.....	84
5.2.4 T-RFLP analysis.....	86
5.2.4.1 <i>OTU analysis of T-RFs</i>	86
5.2.5 Assessment of Archaeal primers	87
5.2.6 Phylogenetic assignment of T-RFs	88
5.3 Summary of archaeal diversity findings	89

5.4 Concluding remarks.....	91
Chapter 6: General Discussion.....	92
6.1 Future Prospects	96
Appendices	97
Appendix A: Chapter 3-Gobabeb site. T-RFs matched to Blast results of clones obtained from Genbank for 16S rRNA gene bacterial libraries.....	98
Appendix B: Chapter 3- Swakopmund site 1. T-RFs matched to Blast results of clones obtained from Genbank for 16S rRNA gene bacterial libraries.....	102
Appendix C: Chapter 3-Swakopmund site 2. T-RFs matched to Blast results of clones obtained from Genbank for 16S rRNA gene bacterial libraries.....	105
Appendix D: Chapter 3-Phylogenetic affiliation of bacterial 16S rRNA gene clone based on RDP Classifier.....	107
Appendix E: Chapter 4-T-RFs matched to Blast results obtained from GenBank for 16S rRNA clone library created for Gobabeb site.....	112
Appendix F: Chapter 4-T-RFs matched from Blast results obtained from GenBank for 16S rRNA clone library created for Swakopmund site 1.....	114
Appendix G: Chapter 4-T-RFs matched to Blast results obtained from GenBank for 16S rRNA clone library created for Swakopmund site 2.....	115
Appendix H: Chapter 4, Phylogenetic affiliation of 16r RNA gene clones based on RDP Classifier.....	116
References.....	119

List of Tables

Table 1: The three different research sites chosen for this investigation with their respective GPS coordinates.....	19
Table 2: Summary of PCR primers used in this study.....	23
Table 3: Preparation of 0% and 100% denaturing stock solutions.....	24
Table 4: Denaturing gels prepared from 0% and 100% stock solutions.....	24
Table 5: Summary of the diversity indices.....	30
Table 6: Physiochemical evaluation of the Gobabeb (GOB) and Swakopmund (Sps01 and Sps02) sediment samples	34
Table 7: Origins of the bacterial 16S rRNA gene clone libraries.....	47
Table 8: Summary of results obtained from library richness estimates: S_{Chao1} and S_{ACE}	49
Table 9: Summary of the results obtained from both richness estimators S_{Chao1} and S_{ACE}	71
Table 10: Sequence identification of DGGE bands obtained from BLASTn, NCBI database.....	85
Table 11: Evaluation of the archaeal primer pairs A3Fa/Ab927R and 8Fa/1492R using Silva. Numerical value are given in percentages. Archaea phylotypes frequently isolated in saline environments are highlighted in yellow.....	88
Table 12: Phylotypic assignment of the OTU's obtained from T-RFs generated from enzymes <i>AluI</i> , <i>RsaI</i> , <i>HaellI</i> and <i>HpaII</i> using MiCA III (PAT+).....	89

List of Figures

- Figure 1:** The map illustrates the rainfall pattern observed in the central parts of the desert. “Low stratus cover regions” receive precipitation less than 75 days per year, while “average rainfall regions” receive rainfall of less than 100mm per year (Map taken from Eckhardt *et al.*, 2012).....2
- Figure 2:** Distribution of Namib salt pans, stretching from the coast to the central inland region of the desert (Eckhardt and Drake, 2011). A+B: the Silver Lake playas, C: Welwitschia Flat playas, D and E: Okahandja Lineament playas.....4
- Figure 3:** Graphic representation of the adaption of non-halophiles, extremophiles and moderate halophiles in saline environments. When non-halophiles are placed in high salt concentrations, water moves out of the cytoplasm into the surroundings causing the cell to lose its rigidity and shrink. An extreme halophile maintains its osmotic balance by means of the “salt in” strategy when placed in a high salt environment, it starts synthesising KCl molecules. Moderate halophiles sustain their cell turgor pressure by means of the “compatible solute strategy”, accumulating compatible solutes from the external environment (adapted from McGenity and Oren, 2010).....7
- Figure 4:** The three domains of life with halophilic families highlighted in red (Taken from Oren, 2007).....7
- Figure 5:** The diagram illustrates the different microbiota that dominates at the various salt levels found within salt crust of a solar saltern in Eilat, Israel (Sorenson *et al.* 2004).9
- Figure 6:** The two sampling sites. Gobabeb (near the Gobabeb Research Centre) and Swakopmund (near the coast) in the Namib Desert. Gobabeb and Swakopmund sampling sites are approximately 127km apart. (Adapted from Eckardt and Drake, 2011).....32
- Figure 7:** The sampling sites included in this study Gobabeb site (1, 2), Swakopmund site 1 (3, 4) and Swakopmund site 2 (5, 6), with their respective conductivity readings. Conductivity was measured in milliSiemens per centimetre (mS/cm), with $1\mu\text{S}/\text{cm}=0.6\text{mg}/\text{kg}$ of NaCl. The pictures of Gobabeb sampling site depict the soil with a layer of salt precipitates

on its surfaces together with green material, while Swakopmund site 1 represents the epidermal rivers. The soil of Swakopmund site 2 sampling site is surrounded by gypsum containing water with the crust containing distinct microbial stratification layers of orange, and green material. (Photos taken by the investigating team from IMBM).....33

Figure 8: The amplified bacterial 16S rRNA gene fragments separated on a 1% agarose gel. Lane 1: λ PstI marker, Lane 2-7 Gobabeb samples, Lane 8: positive control *E. coli* DNA, Lane 9: No template control.....36

Figure 9: The similarity dendrogram constructed for Gobabeb site. The software GelCompar (version5) was used with the similarity matrix DICE coefficient and the UPGMA cluster method. The similarity ruler is represented above the diagram. Sample GOB1, 2 and 3 formed a cluster, while GOB4 and GOB5 were found to cluster separately.....37

Figure 10: The MDS plot constructed from DGGE data for the five samples collected at the Gobabeb site from (GOB1-5) using GelCompar II (version5). The plot was constructed using the similarity matrix Pearson coefficient and the UPGMA cluster method. The MDS plot scale separates the samples at 0.02 intervals at the Z-axis and 0.05 intervals at both the X and Y-axis.....37

Figure 11: Similarity dendrogram constructed for Swakopmund site 1 samples. The software GelCompar II (version5) was used in combination with the similarity matrix DICE coefficient and the UPGMA cluster method. The dendrogram illustrates that Sp01A and Sp01D forms a cluster, whereas Sp01B and Sp01C do not cluster.....38

Figure 12: The MDS plot constructed from DGGE data for Swakopmund site 1 for the four samples (Sp01A-D) collected using GelCompar II (version5). Samples Sp01A and Sp01D cluster while Sp01C and Sp01B did not cluster. The MDS plot scale is scored at 0.1 intervals on all three axes (X, Y and Z).....38

Figure 13: Similarity dendrogram constructed for Swakopmund site 2. The software GelComparII (version5) was used in combination with the similarity matrix DICE coefficient and the UPGMA cluster method in the analysis. The similarity dendrogram shows how

samples Sps02B and Sps02D were clustered while Sps02A and Sps02C did not. The dominant band present in all samples is highlighted in orange.....39

Figure 14: The MDS plot constructed from DGGE data for the four samples collected from Swakopmund site 2 using GelCompar II (version5). Samples Sp02B and Sp02D cluster, while Sp02A and Sp02C do not. The MDS plot scale separates the samples at 0.05 intervals at the Y-axis and 0.1 intervals at both the X and Z-axis.....40

Figure 15: Distribution of OTUs within Gobabeb site. The graph represents the number of T-RFs generated from the restriction enzymes *HaeIII* and *HpaII* between the five samples (GOB1-GOB5). Three of the OTUs (76, 77, 120) were found to be shared among the five samples.....41

Figure 16: Venn-diagram illustrating the number of T-RFs shared between the samples obtained at Gobabeb site.....42

Figure 17: Distribution of OTUs within Swakopmund site 1. The graph represents the number of T-RFs obtains with restriction enzymes *HaeIII* and *HpaII* within Swakopmund site 1.....43

Figure 18: Venn-diagram illustrating the number of T-RFs shared between samples Sps01A and Sps01B obtained at Swakopmund site 1.....43

Figure 19: Distribution of OTUs within Swakopmund site 2. The restriction enzymes (*HaeIII* and *HpaII*) utilised generated 16 OTUs collectively. Only two of the T-RFs (76 and 77) were shared while the majority of the T-RFs were found to separately between the four samples, Sps02A-Sps02D obtained at this site.....44

Figure 20: Venn-diagram illustrating the number of T-RFs shared between the samples obtained at Swakopmund site 2.....44

Figure 21: The MDS plot constructed from T-RFLP data for Gobabeb site. Samples GOB1-GOB3 and GOB5 cluster at 40% similarity while GOB4 clusters separately, sharing only 20% similarity with the other samples.....45

Figure 22: The MDS plot constructed from T-RFLP data for Swakopmund site 2. The samples clustered in two groups (Sp02A and Sp02B; Sp02C and Sp02D) at the 60% similarity level. All four samples obtained from this site share 40 similarity.46

Figure 23: Restriction digests of amplicons of library 2 (GOB4) digested with enzyme *HpaII*. The amplicons were viewed on 2% agarose gel. Lane1 and 21: ladder $\lambda PstI$, Lane: 2-20 and lane 22-36 digested amplicons.....48

Figure 24: The coverage estimates obtained from both S_{Choa1} and S_{ACE} for libraries GOB, GOB4, Sps01 and Sps02.....49

Figure 25: Histogram representing the different phlotypes identified from the clone libraries GOB, GOB4, Sps01A, Sps01B and Sps02. The clones were assigned phylogenetic affiliation based on the RDP database.....51

Figure 26: Phylogenetic tree of 16S rRNA gene sequences that affiliated to Proteobacteria. One sequence per cluster was used in constructing the phylogenetic tree with the Mega 6 software. The evolutionary relationship between taxa was assessed using the maximum likelihood method and the Kimura 2-parameter model. A 1000 replicates were inferred based on the bootstrap consensus to analyse the evolutionary relationship between taxa. The sequences of Proteobacteria were clustered into their respective classes: Alphaproteobacteria and Gammaproteobacteria. Bootstrap values less than 50 were excluded from the tree.....55

Figure 27: Phylogenetic trees of 16S rRNA gene sequences that affiliated to Bacteroidetes (Figure 20). One sequence per cluster was used in constructing the phylogenetic tree with the Mega 6 software. The evolutionary relationship between taxa was assessed using the maximum likelihood method and the Kimura 2-parameter model (Kimura, 1980). A 1000 replicates were inferred based on the bootstrap consensus to analyse the evolutionary relationship between taxa.56

Figure 28: Phylogenetic trees of 16S rRNA gene sequences that affiliated to the minority groups: Firmicutes, Verrucomicrobia, *Planctomycetes*, *Nitrospira* and Cyanobacteria. One sequence per cluster was used in constructing the phylogenetic tree with the Mega 6 software. The evolutionary relationship between taxa was assessed using the maximum likelihood

method and the Kimura 2-parameter model (Kimura, 1980). A 1000 replicates were inferred based on the bootstrap consensus to analyse the evolutionary relationship between taxa.....57

Figure 29: Phylogenetic tree of 16S rRNA gene sequences that were isolated at Swakopmund site 1. One sequence per cluster was used in constructing the phylogenetic tree with the Mega 6 software. The evolutionary relationship between taxa was assessed using the maximum likelihood method and the Kimura 2-parameter model. A 1000 replicates were inferred based on the bootstrap consensus to analyse the evolutionary relationship between taxa. The sequences were clustered into their respective phyla of *Proteobacteria* (Alphaproteobacteria), Bacteroidetes, Cyanobacteria, Firmicutes and unclassified bacteria. Bootstrap values less than 50 were excluded from the tree.....58

Figure 30: Phylogenetic tree of 16S rRNA gene sequences that were isolated at Swakopmund site 2. One sequence per cluster was used in constructing the phylogenetic tree with the Mega 6 software. The evolutionary relationship between taxa was assessed using the maximum likelihood method and the Kimura 2-parameter model. A 1000 replicates were inferred based on the bootstrap consensus to analyse the evolutionary relationship between taxa. The sequences were clustered into their respective phyla of *Proteobacteria* (Alphaproteobacteria), Bacteroidetes, Cyanobacteria, Firmicutes and unclassified bacteria. Bootstrap values less than 50 were excluded from the tree.....59

Figure 31: The graph represents the OTU distribution between all the samples obtained at Gobabeb site. The asterisks (*) represents the OTU at its highest frequency.....65

Figure 32: The Venn-diagram shows the distribution of OTUs between the samples collected at the Gobabeb site.....65

Figure 33: The graph represents the number of OTUs obtained from the different T-RFs between the samples obtained at Swakopmund site 1.....66

Figure 34: The Venn-diagram shows the distribution of OTUs between the samples collected at the Swakopmund site 1.....67

Figure 35: The graph represents the OTU distribution between all the samples obtained at Swakopmund site 2.....67

Figure 36: The Venn-diagram shows the distribution of OTUs between the samples collected at Swakopmund site 2.....68

Figure 37: MDS plot created for Gobabeb. The Gobabeb samples, GOB1 and GOB3 cluster at 60% while GOB4, GOB5 and GOB2 cluster separately sharing 20% similarity.....69

Figure 38: MDS plot created for Swakopmund site 1. Samples were found to share 20% similarity with one another while Sps01B and Sp01C cluster at 40% while Sp01A and Sp01C cluster separately at 20%.....69

Figure 39: MDS plot created for Swakopmund site 2. The samples collected at Swakopmund, Sp02C and Sp02D cluster at 40% while Sp02B clustered at 20% similarity.....70

Figure 40: ARDRA analysis of the GOB cyanobacterial 16S rRNA gene clone library. Clones were digested with *HpaII*. Samples were separated on a 2% agarose gel. Lane 1 & 26: ladder λ *PstI*, Lane 2-25, 27-50: digested clones.....71

Figure 41: The coverage (Good's C) of the cyanobacterial 16S rRNA gene clone libraries (Sps01, Sps02 and GOB). The overall coverage is shown in the Y- axis and the number of clones per library in the x-axis.72

Figure 42: Histogram representing the distribution of ribotypes found in sampling sites GOB, Sps01 and Sps02. Clones were matched and grouped based on the data obtained from the RDP database.....73

Figure 43: Phylogenetic tree representing the evolutionary relationships between Cyanobacterial clone sequences for libraries constructed for Gobabeb, Swakopmund site 1 and Swakopmund site 2. Mega 6 software was used to construct the phylogenetic tree with the Maximum Likelihood method and the Kimura 2_{parameter} model. Bootstrap values were set at a 1000 replicates. One cluster per group was used to construct the tree, with the

outgroup being *Haloquadratum walsbyi* (NR_028207.1). Bootstrap values less than 50 are not indicated on the tree.....77

Figure 44: Similarity analysis for the Gobabeb samples. The dendrogram was constructed using the GelComparII (version 5) software, the similarity matrix DICE coefficient and the UPGMA cluster method. The four samples were found to be highly dissimilar, with the similarity between the samples being 15%.....81

Figure 45: MDS plot was constructed for Gobabeb site using GelComparII (version5) software. The four Gobabeb samples (GOB1, 2, 3 and 5) were found not to cluster. The scale for MDS plot separates the samples on the X, Y and Z plane at 0.2 intervals.....82

Figure 46: Similarity analysis for Swakopmund site 1. The dendrogram was constructed using the GelComparII (version 5) software, the similarity matrix DICE coefficient and the UPGMA cluster method. The four samples were found to contain different banding patterns with both Sps01A and Sps01C with 17 bands, Sps01B with 14 bands and Sps01D with five bands.....82

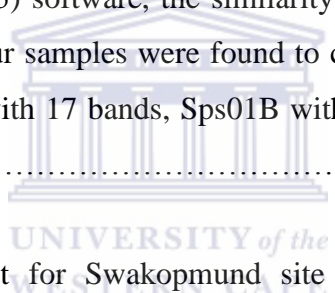


Figure 47: MDS plot construct for Swakopmund site 1 using GelComparII (version5) software. Samples Sps01A and Sps01B clustered separately from Sps01C and Sps01D. The scale of MDS plot is set at 0.2 intervals for both the X and Y plane while at the Z plane intervals are set at 0.05 intervals.....83

Figure 48: Similarity analysis for Swakopmund site 1. The dendrogram was constructed using the GelComparII (version 5) software, the similarity matrix DICE coefficient and the UPGMA cluster method. The four samples were found to contain different banding patterns with Sp02A with six bands, Sps02B with 19 bands, Sps02C with 11 bands and Sps02D with nine bands.....83

Figure 49: MDS plot constructed for Swakopmund site 2 using GelComparII (version5) software. Sample Sps02D and Sps02D clustered while Sps02B and Sps02C did not. The MDS plot scale separates the samples at 0.2 intervals for both the X and Y plane, while the Z plane separating samples at 0.1 intervals.....84

Figure 50: DGGE analysis from all three sites for community profiling. The six bands excised from the gel are marked84

Figure 51: PCR amplicons of metagenomic DNA generated using the universal archaeal primer pair 8fa/1492R. Lane1: $\lambda PstI$ ladder, Lane 2 and 3: GOB2, 4 and 5: GOB3, 6: Sps01A, 7: Sps01C, 8: Sps01B, 9 and 10: open soil, 11: Negative control, 12: Positive control: *S. sulfolobus*.....86

Figure 52: Comparison between the two different fingerprinting techniques (DGGE and T-RFLP) for three sampling sites. The OTUs obtained for DGGE is compared between the two restriction enzymes, *HpaII* and *HaeIII* used in T-RFLP analysis.....93

Figure 53: A summary of the number of archaea, bacteria and cyanobacteria OTU's obtained with T-RFLP analysis at the respective sampling sites.....95



List of Abbreviations

°C	degrees Celsius
%	percentage
µg	microgram
µl	microliter
µM	micromolar
ATP	adenosine triphosphate
Bp	base pairs
BSA	bovine serum albumin
Cl ⁻	chloride ions
CaCl ₂	calcium chloride
CaCO ₃	calcium carbonate
Cfu	colony forming units
Cm	centimetre
CTAB	cetyl trimethyl ammonium bromide
DGGE	denaturing gradient gel electrophoresis
DMSO	dimethyl sulfoxide
DNA	deoxyribonucleic acid
dNTP	deoxynucleotide triphosphosphate
EC	electronic conductivity
EDTA	ethylene diamine tetraacetic acid
Fig.	Figure
HCl	hydrochloric acid
Hrs	hours
IPTG	isopropyl β-D-thiogalactosidase
K ⁺	potassium ions
KCl	potassium chloride
Km	kilometre
l	litre
LB Luria	Bertoni medium
LB-amp	Luria Bertoni medium containing ampicillin
m	meter

M	molar
MDS	multidimensional scaling
MgCl ₂	magnesium chloride
MgSO ₄	magnesium sulphate
min	minutes
ml	millilitre
mm	millimetre
mM	millimolar
Na ⁺	sodium ions
NaCl	sodium chloride
NaH ₂ PO ₄	sodium dihydrogen orthophosphate
NaOH	sodium hydroxide
ng	nanogram
nm	nanometer
OTU's	operational taxonomic units
PCR	polymerase chain reaction
PCA	principal component analysis
Rpm	revolutions per minute
RFLP	restriction fragment length polymorphism
rRNA	ribosomal oxyribonucleic acid
s	seconds
SDS	sodium dodecyl sulphate
ssu	small sub unit
TAE	tris acetic acid EDTA
T-RFLP	terminal restriction length polymorphism
T-RFs	terminal restriction fragments
UV	ultraviolet
v/v	volume per volume
w/v	weight per volume
X-gal	5-bromo-4-chloro-3-indolyl-β-D-galactosidase

Chapter 1: Literature review

1.1 The Namib Desert

The Namib Desert is one of the oldest deserts in the world with an estimated age of 80 million years, with the hyper-arid central part of the desert being 50 million years old (van Damme, 1991). The Namib occupies about 15% of the Namibian landmass and stretches from the west-coast for approximately 120km inland where the Great Escarpment forms its border. The desert is further divided into four ecological regions ranging from the semi-arid districts covering the southern, western and eastern side, to its hyper-arid central parts. The prevailing arid conditions result in the formation of ephemeral rivers, dry river beds, salt pans and sand dunes. Although subjected to harsh environmental conditions, the desert is rich in both prokaryotic and eukaryotic life, and is host to a range of endemic plant species such as *Welwitschia mirabilis* and *Acanthosicyos horrida* (melons that are locally known as nara) (Van Damme, 1991; Hatchfield, 2000). The desert forms part of the Namibian National Conservation District and the biodiversity of this hyper-arid region is ultimately structured by the prevailing climatic conditions (Maartens, 2010).

1.1.2 Climate

The Namib Desert's climate ranges from arid to hyper-arid, with humidity and temperature increasing from the coastal region to the central parts. The desert's fluctuating environmental conditions are predominantly caused by the presence of the cold Benguela current along its western shore. Fog is the main water source in the central regions, with rainfall supplying the least amount of water. The fog is caused by the uprising of warm oceanic air, which is moved along by westerly winds over the cold Benguela currents. The resulting advection fog is then disseminated over a region of 100km inland from the coast (Eckhardt and Schemenauer, 1998). Precipitation due to fog is not homogenous over this region - fog accounts for 60mm of precipitation in areas 35km from the coast and declines to 30mm in areas 55km inland. The desert's rainfall patterns varies, with the coastal region receiving a minimum of 5-18mm per annum, while the westerly region receives approximately 10mm of rain and easterly areas receive approximately 60mm (Figure 1) (Eckhardt *et al.*, 2012).

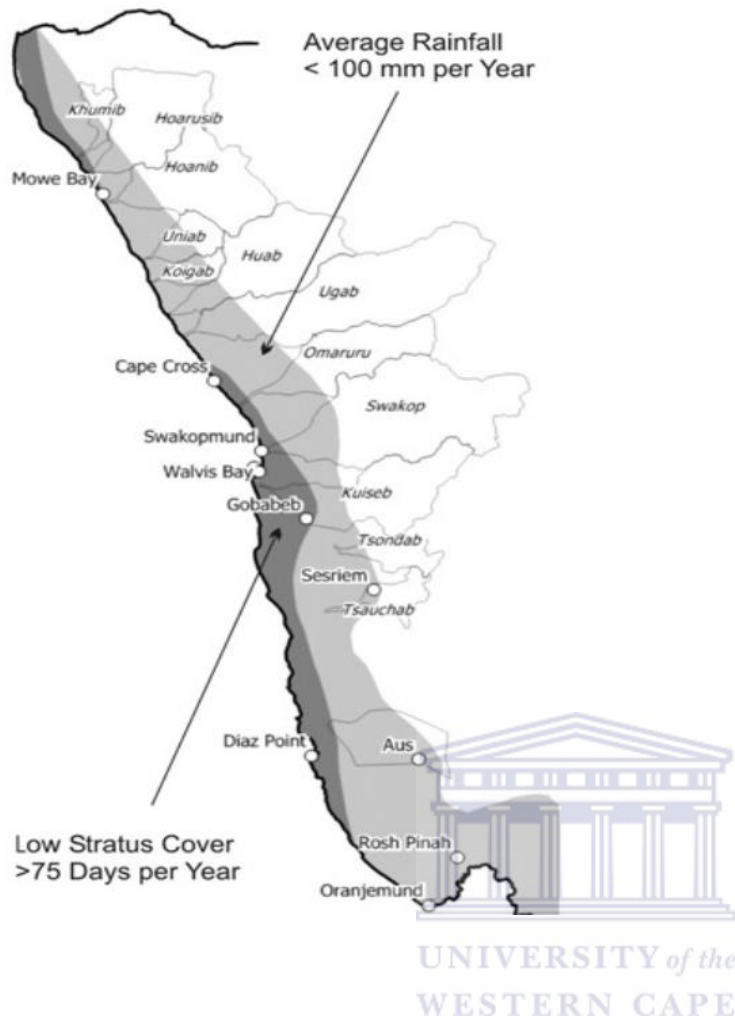


Figure 1: The map illustrates the rainfall pattern observed in the central parts of the desert. “Low stratus cover regions” receive precipitation less than 75 days per year, while “average rainfall regions” receive rainfall of less than 100mm per year (Map taken from Eckhardt *et al.*, 2012).

1.1.3 Salt weathering

Weathering refers to the mechanical and chemical processes involved in the abrasion of rocks, soils and minerals, while erosion refers to the geological displacement of these abraded products via wind, water or gravity (Cooke *et al.*, 1993). Most salt weathering occurs at the ground-air interface, and is caused by climatic conditions. Salt weathering plays a vital role in the Namib Desert mineral composition and its geomorphological structure (Viles, 2005; Viles and Goudie, 2007). Weathering in hot arid environments such as the Namib Desert is caused by the extreme environmental conditions associated with high temperatures and low humidity playing an important role (Cooke *et al.*, 1993).

These conditions are favourable for the promotion of crystal growth from evaporating saline waters (Cooke *et al.*, 1993). Salt weathering in the Namib coastal and central regions is caused mainly by fog precipitation. The repeated wetting and drying of bed rock surfaces causes the rocks to slowly crack and chip. Weathering takes about two to three years, depending on the chemical composition of the rock surface, before it has any sort of permanent effect. Salt weathering causes denudation of the desert's coastal regions and ultimately restructures microbial communities (Viles, 2005; Viles and Goudie, 2007). In addition, the salt springs found in the Namib Desert are vastly influenced by salt weathering processes (Viles and Goudie, 2007). This is evident by the high breakdown of Namibian blocks (marble and Bath stone blocks) in the region with the presence of halites at the bottom of these sediments (Viles and Goudie, 2007).

1.1.4 Saline environments

Saline environs are heterogeneous and are characterised by salinity concentrations greater than 3.5% (w/v) (Torsvik and Ovreas, 2008). These environments tend to be aquatic rather than edaphic. Aquatic hypersaline environments are classified as being either thalassohaline or athalassohaline (Grant & Gemmell, 1998). Thalassohaline habitats are marine in origin with the mineral composition being mostly NaCl, whereas athalassohaline habitats occur either naturally or artificially, and include solar salterns or salt pans. Athalassohaline habitats contain a range of salts such as MgCl₂, CaCO₃, KCl, CaSO₄ and NaCl. Even though thalassohaline environments are geographically more widespread it is the athalassohaline pools that are more extreme, containing varied concentrations of salts and minerals (Torsvik and Ovreas, 2008).

1.1.5 Salt Pans

Salt pans are evaporated pans of saline waters caused by the direct effect of environmental disturbances in desiccated regions (Shaw and Bryant, 2011). They are further categorised as containing clastic or non-clastic sediments. Clastic sediments are formed by the deposition of abraded sediments due to water- or wind currents, whereas non-clastic sediments are formed by the precipitation of saline deposits from groundwater (Cooke, 1993). Salt pans vary in size from a small dam or stream to a lake. Depending on their country of origin and physical location, salt pans are referred to by various names. In the Middle East they are referred to as sabkhas when located close to the coast, while inland salt pans are referred to as playas (Shaw and Bryant, 2011). In the Namib Desert the salt pans have more often been referred to

as salt springs in earlier studies (Day and colleagues (1993 and 1997) but presently they are more clearly defined as playas by Eckhardt and colleagues (2011 and 2012).

1.1.6 Namib Desert salt pans

The many salt pans found in the Namib Desert are scattered throughout its landscape and present mostly as salt springs (Figure 2). While several studies have investigated the geomorphology, distribution and mineralogy constituents of these pans (Day, 1993; Day *et al.*, 1997; Eckhardt and Drake, 2011) most salt pans remain uncharacterised. The pans investigated include those found north east of Swakopmund which form part of the Silver Lake playas, the Welwitschia Flats (near Swakop Canyon) and the Okahandja Lineament (Gobabeb) playas. The Silver Lake playas were formed by the obstruction of dolerite rock, while the Welwitschia Flats were formed by Precambrian marble. The Okahandja Lineament was formed by a combination of Damara bedrock, Tinkas schists and Salem granites. The outcrops of these bedrocks dam the drainage channels causing the ground water to pool (Eckhardt and Drake, 2011).

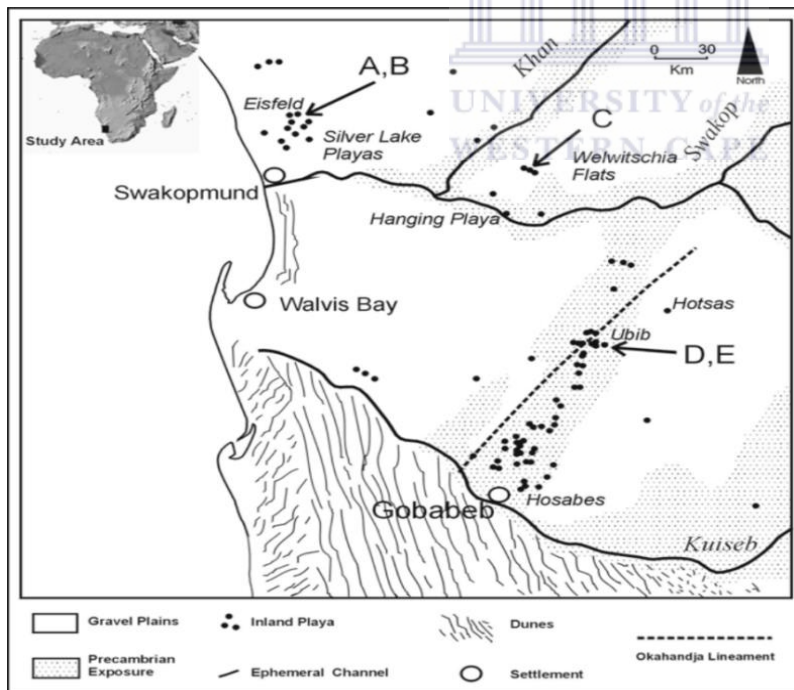


Figure 2: Distribution of Namib salt pans, stretching from the coast to the central inland region of the desert (Eckhardt and Drake, 2011). A+B: the Silver Lake playas, C: Welwitschia Flat playas, D and E: Okahandja Lineament playas.

The playas are shallow pools composed of clay sediments containing varying amounts of mineral salts and gypsum. The geochemistry of these pans indicates that the majority of the

saline springs in the Namib contain mostly Na^+ and Cl^- ions, and variable concentrations of Ca^{2+} and SO_4^{2-} ions (Day, 1993).

1.2 Microbial diversity in salt pans

Microorganisms isolated from evaporated ponds are best known as halophiles and are described as “salt loving” microorganisms. These microbes require NaCl for growth and are limited to hyper saline environments. Conversely, halotolerant microbes can survive in the presence or absence of salts. Halophilic organisms are classified according to their NaCl tolerance in growth media. Non-halophiles grow in media containing less than 1% NaCl, halotolerant organisms grow in medium up to 2.5% NaCl; moderate halophiles grow in media containing 3-15% NaCl; and extreme halophiles can survive in media of $\leq 25\%$ NaCl concentrations (Grant *et al.*, 1998; Ventosa, 2006).

1.2.1 Halophiles and halotolerant microorganisms

Studies have shown that these microbes which are isolated from evaporated ponds are frequently of marine origin (Ventosa *et al.*, 2006) and as the salt concentration of the ponds increases the organisms become more specialised. The changes in the saline content of the pans bring about changes in mineral composition and with it, alterations in the population structure (Lopzupone and Knight, 2007). One of the mechanisms that also influences the microbial structure in salt pans is the formation of halite crusts which is formed due to the evaporation of Na^+ , Cl^- , Mg^{2+} , SO_4^{2-} and Ca^{2+} ions (Howari *et al.*, 2002). The rate of evaporation experienced in salt pans brings about the dominance of different ions at different intervals ultimately selecting for the adaption of more specialised microbes (Alio, 2004).

1.2.2 Adaptions of halophiles to saline environment

Prokaryotes living at high salt concentration are adapted to keep their internal environment similar to the external environment, in order to maintain cellular turgor pressure (Oren, 1999). Two adaptive strategies used by halophiles to maintain turgor pressure are the “salt-in-cytoplasm” strategy and the “compatible solute” strategy.

The “salt-in-cytoplasm” strategy requires the intracellular and extracellular salt concentration to be osmotically equivalent, thus requiring all internal cellular compartments to be adapted to maintain a high concentration of salt (Figure 3). This method is adopted mainly by extreme halophilic archaea, but is also used by some aerobic and anaerobic bacteria (Anton *et al.*,

2002). These halophiles adapt to extreme salt environments by accumulating mainly potassium (K^+) and chloride (Cl^-) ions within the cells, although some species have been found to store sodium ions (Na^+). The ions increase the ionic strength of the cytoplasm thereby stabilizing the cells against hydration in high ionic environments. When placed in a relatively low salt environment the cations move out of the cytoplasm and destabilize the cellular membrane, causing it to collapse.

In the “compatible solute” adaption strategy the intracellular compartments have a low salt concentration and the osmotic pressure is balanced by the presence of osmolytes (compatible organic solutes also referred to as low molecular weight solutes) such as sugars (Figure 3). The osmolytes do not interfere with the cells normal metabolism, and act to protect the cell from dehydration. Solutes ultimately prevent the loss of intracellular fluids to the external environment (Roberts *et al.*, 2005). The “compatible solute” method is used mainly by halophilic bacteria and some halophilic methanogenic archaea (Oren, 1999). The principle of this method depends on the ability of the prokaryotes to either synthesize or obtain osmolytes from the external environment. Compatible organic solutes are either polar or zwitterionic molecules (zwitterionic compatible solutes are mostly favoured by archaea) enabling non-salt adapted enzymes to be active within the cells.

While both archaea and bacteria use osmolytes to maintain iso-osmosis within the cell, the taxa differ in the type of organic solutes used to maintain osmoregulation (Madigan and Oren, 1999). Examples of halophiles that use the salt-in-strategy are methanogenic archaea which have adapted to increasing osmotic stress by the *de novo* synthesis and accumulation of zwitterionic osmolytes such as glycine betaine, β -glutamate and N_ϵ -acetyl- β -lysine within their cells (Lai *et al.*, 1991). *Methanohalophilus* strains have been found to accumulate L- α -glutamate and N_ϵ -acetyl- β -lysine as the dominant organic solutes, whereas moderate and extreme *Methanohalophilus* and *Methanococcus* strains accumulate L- α -glutamate, N_ϵ -acetyl- β -lysine and glycine betaine. The concentration of osmolytes within cells differs at different NaCl concentrations (Lai *et al.*, 1991).

Examples of halophiles that have adapted by means of the compatible solute method can be observed by the halophilic strains of cyanobacteria, *Nodularia harveyana* and *Synechocystis* species. These moderate halophiles accumulate the compatible solutes β -glutamate and glycine betaine within their cytoplasm. Further investigations of halophilic strains of

cyanobacteria revealed the synthesis of glycosylglycerol as an osmoprotectant in increasing salinities (Mikkat *et al.*, 1996). The extreme halophilic bacterium *S. marasensis*, like archaea, synthesises zwitterionic glycine betaine *de novo* at NaCl concentrations from 10% to 25% (de Lourdes Morenoa *et al.*, 2010).

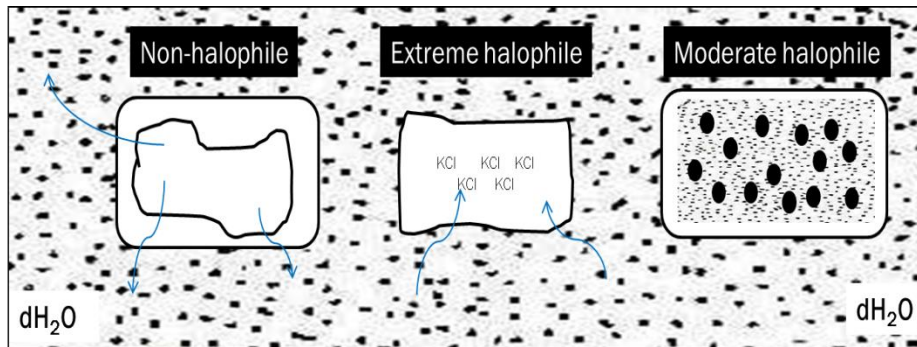


Figure 3: Graphic representation of the adaption of non-halophiles, extremophiles and moderate halophiles in saline environments. When non-halophiles are placed in high salt concentrations, water moves out of the cytoplasm into the surroundings causing the cell to lose its rigidity and shrink. An extreme halophile maintains its osmotic balance by means of the “salt in” strategy when placed in a high salt environment, it starts synthesising KCl molecules. Moderate halophiles sustain their cell turgor pressure by means of the “compatible solute strategy”, accumulating compatible solutes from the external environment (adapted from McGenity and Oren, 2010).

1.2.3 The halophilic communities of saline habitats

The majority of the halophiles found in saline pans are archaea, with bacteria, cyanobacteria and eukaryotic species (Figure 4) forming the minority groups (McGenity and Oren, 2010).

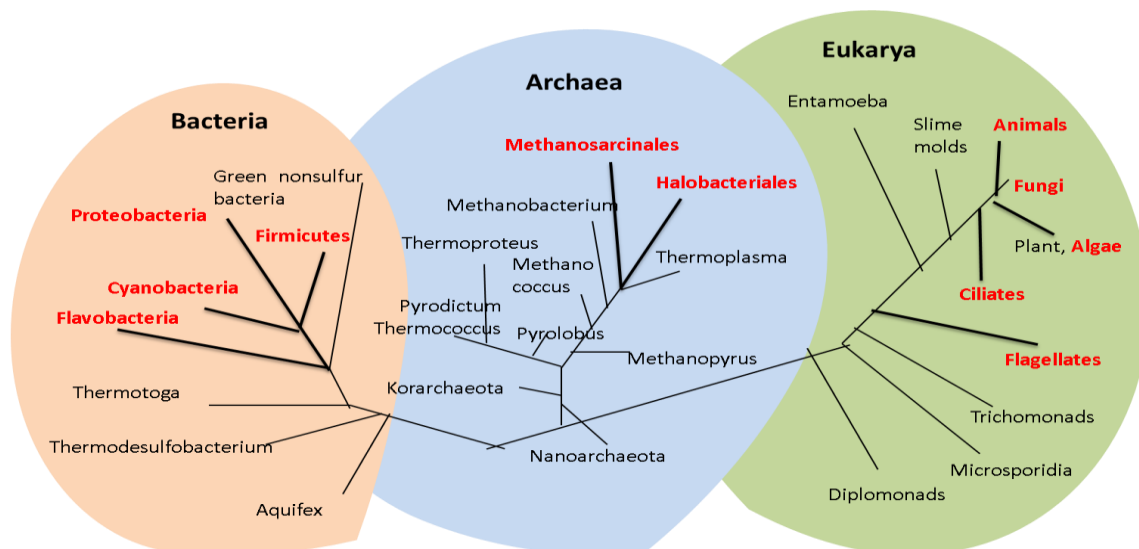


Figure 4: The three domains of life with halophilic families highlighted in red (Taken from Oren, 2007).

1.2.3.1 Archaeal diversity

Aerobic haloarchaea of the family *Halobacteriaceae* and methanogenic archaeobacteria are the most common archaea found in the saline soils of salt pans. *Halobacteriaceae* isolated from salt pans were originally characterised based on their red pigmentation (Ventosa, 2006), while the application of culture independent techniques resulted in the identification of 27 genera and 96 species of the family *Halobacteriaceae* (Oren *et al.*, 2009, Minegishi *et al.*, 2010.). Members of this group thrive at salt concentrations ranging from 2 to 7%.

Even though the family *Halobacteriaceae* recently has expanded from its previous 81 to 96 species it is likely that a large number of species within this family remain undiscovered (Youssef *et al.*, 2012). Culture independent studies conducted in the salt pans of Arpora (India) revealed uncultured members of the phyla *Crenarchaeota* and *Euryarchaeota* (Ahmed *et al.*, 2011). Another archaeal species which is frequently detected in salt pans is *Haloquadratum walsbyi* which has been identified by culture-independent techniques in both Maras salterns situated in Peruvian Andes (Maturrano *et al.*, 2006), and in salt pans situated in Australia and Spain. This species survives at salinity concentrations of 18% salt (Burns *et al.*, 2007).

1.2.3.2 Bacterial diversity

The most common bacteria isolated from salt pans are sulphur oxidizing and purple sulphur bacteria. The sulphur reducing clades form part of the alphaproteobacteria (family *Desulfobacteriaceae*), the sulphur oxidising clade forms part of both the gammaproteobacteria (*Ectothiorhodospiraceae*) and the *Firmicutes* (*Chromatiales*) and methanogenic archaea the *Methanomicrobiales* and *Methanosarcinales* clades (Montoya *et al.*, 2011).

Surveys of salt pans have resulted in the discovery of many novel microorganisms including the halophilic bacterium *Salinibacter ruber* (Anton *et al.*, 2002). This bacterium was initially isolated from the saline ponds of Alicante and Mallorca, Spain, and survives at saline concentrations between 20-30%. Another novel extremophilic bacterium, *Salicola marasensis*, isolated from crystallised ponds in Maras, Peru, thrives at 25% NaCl (de Lourdes Morena *et al.*, 2010). However, not all microorganisms isolated from salt pans are halophilic. For example a halotolerant bacterium, *Neptuniibacter halophilus* isolated from a

salt pan situated in Southern Taiwan is only able to survive in conditions of less than 4% salt (Chen *et al.*, 2012).

1.2.3.3 Cyanobacterial diversity

By using cultivation and microscopy methods, numerous cyanobacterial families including *Nostocaceae*, *Chroococcaceae* and *Oscillatoriaceae* have been identified from the salt pan habitats of Jodhpur, India, (Makandar and Bhatnagar, 2010), Petchaburi, Thailand (Chatchawan *et al.*, 2011); and from the Uppanar estuary, India (Nedumaran and Perumal, 2012). Furthermore, other investigations into the diversity of cyanobacteria in the Southern east coast of India salt pans, identified 21 halophilic cyanobacterial communities affiliated to the families of *Nostocaceae* and *Chroococcaceae* (Nagasathya and Thajuddin, 2008). Similarly, twelve species affiliated to the families *Oscillatoriaceae* and *Chroococcaceae* were identified in the salt pans of Cape Comorin, state of Tamil Nadu (Sugumar *et al.*, 2011). In salt crusts the cyanobacterial community may comprise at least two thirds of the microbial structure (Fig. 5) (Sorenson *et al.* 2004). When these salt crusts were microscopically evaluated, they were found to consist of Halothece-like cyanobacteria in the top brown layer, both *Halospirulina* and *Phormidium* like cyanobacteria in the bright green centre, Chromatium-like anoxygenic phototrophs in the purple layer and lastly, a grey layer which consisted of precipitated metal ions.

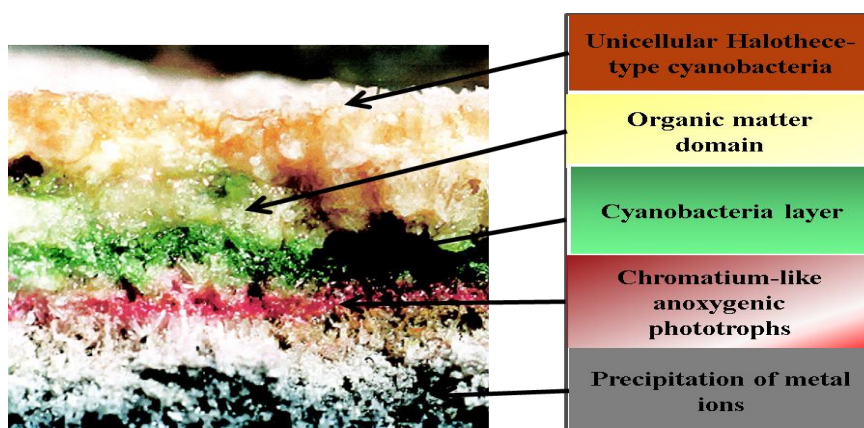


Figure 5: The diagram illustrates the different microbiota that dominates at the various salt levels found within salt crust of a solar saltern in Eilat, Israel (Sorenson *et al.* 2004).

1.2.3.4 Eukaryotic diversity

Other than archaea and bacteria, eukaryotic organisms including the green algae (*Chlorophyta*), protozoa (ciliates and flagellates) and fungi (*Aspergillus* and *Penicillium*) (Thamizhmani *et al.*, 2013) thrive in salt pans, but are less abundant than prokaryotic species. Although many species of green algae are present in saline habits, only species belonging to the red-pink pigmented genera *Dunaliella* (*Dunaliella salinia* and *Dunaliella bardawil*), which are the most abundant, and *Asteromonas* (*A. gracilis*) have been cultured from extreme saline waters (10-30% salinity) (Ventosa, 2006). Recently, the algae *Tetraselmis indica* has been isolated from salt pan in Goa, India with a salinity of 3.5 % (Arora, *et al.*, 2013).

1.3 The biotechnology application and role of halophiles in salt pans

While halophiles have several potential applications in biotechnology only a few have been successfully applied. The oldest and most traditional application of halophilic microbes is their function in the salt manufacturing processes, where they are used as indicators in salt harvesting (Javour, 2002). Salt has been utilised for centuries both as a preservative and for flavouring of various foods. Both the quality and quantity of salt is to a large degree determined by the presence of microbes in the solar saltern (Javour, 2002, Gomez *et al* 2003). The reddish colour observed in solar salterns is caused by the presence of carotenoids, which includes bacteriorubin from halobacteria and β -carotene from the green microalgae *Dunaliella*. The presence of these organisms in solar salterns can both be advantageous or detrimental to the salt manufacturing process (Davis and Giordano, 1996). While the presence of these halophiles is beneficial since they aid in the evaporation process, too large populations can result in a decrease in the absorption rate, thus increasing the amount of unwanted minerals such as magnesium chlorides, sulphates and calcium carbonates, where only sodium chloride is required in the manufacturing of salt (Javor, 2002).

Other than its application in salt manufacturing, the microalgae, *Dunaliella* has also shown its vast potential in various biotechnology applications such as a producer of β -carotene. β -carotene has been used as a food supplement, as the human body converts it into retinol (vitamin A). It has also been proposed as a chemopreventative agent as studies have shown that vitamin A and β -catotene increase the potency of the drug 5-Azc in the treatment of hepatocarcinogenesis in Wistar rats (Sampaio *et al*, 2007). Both vitamin A and provitamin β -

carotene has been previously proposed to play an essential role in prolonging human life, as well as being a putative candidate in cancer preventative treatments (Cutler, 1984).

Other industrial applications of halophiles mined from salt pans are the protein bacteriodopsin. Bacteriodopsin is isolated from the purple membranes of the archaean *Halobacterium salinarium*. It is an apoprotein which functions as a light driven proton pump in the bacterium. It harnesses the solar energy from the sun, stores it and generates energy in the form ATP which is then used in other molecular processes beneficial for the bacterium's survival. The protein's potential lies in its industrial application in bioelectronics and nanotechnology based on its photochemical and thermostability properties (Wagner *et al.*, 2013). For example, bacteriorhodopsin's chromophore can withstand high levels of chemical stress and photon influx thus making it an excellent candidate for biophotonic application (Wagner *et al.*, 2013). Bacteriodopsin could also be applied as a photosynthetic material in the manufacturing of biosensors and in biogenerated computers (Birge *et al.*, 1999, Braun *et al.*, 2006).

Ectoine is a compatible solute which is produced by moderate halophilic bacteria such as *Chromohalobacter salexigens* (Canovas *et al.*, 1997) and *S. coelicolor* (Bursy *et al.*, 2008) to aid in its survival in saturated brines. The compound has potential as a drug for the treatment of Alzheimer's disease, as it has been found to decrease amyloid formation (Kanapathipillaia *et al.*, 2005). Its protective function in extreme environmental conditions also makes it a putative candidate as a cellular protectant agent for human skin against aging and dehydration (Graf *et al.*, 2008).

Another application of halophiles is in the treatment of waste water and oil spills. *Halomonas meridian* produces α -amylase which has the potential to aid in the disposal of unwanted waste water products (Coronado *et al.*, 2000). Similarly *Marinbacter* species can degrade BETEX compounds such as benzene (Nicholson and Fathepure, 2004).

1.4 The biodiversity of the Namib Desert salt pans

The biodiversity inhabiting the Namib saline pools remains poorly understood. Preliminary investigations done by Brain (1980) documented the presence of ciliates in samples obtained from pools close to Walvis Bay, with salt concentrations up to 10.4%. These ciliates were

identified microscopically as *Fabrea salina* species, a group of salt dependant halophilic organisms within the eukaryotic domain. Day and Seely (1988) reported that a salt spring in Hosabes near the Gobabeb Research Centre had high concentrations of NaCl which acted as a precursor in the formation of the gypsum (CaSO₄) found in the surrounding area. In spite of the high salinity measured in Hosabes, researchers have identified a wide range of macroorganisms such as spiders (*Lycosid* and *Theriid*), beetles (*Hydraenidae* and *ptilid*) and flies (*Ceratopogonidae* and *Ephydrid*). They also noted the presence of microorganisms. Subsequent investigations identified a novel micro pseudocoelomate from the genus *Proales* (Rotifers) belonging to the animalia phylum (Brain and Koste, 1993). This species can survive in salinity concentrations of up to 50% (w/v). Thus far the species diversity composition in the Namib salt pans has mostly been documented by means of microscopic as well as macroscopic evaluation. The role of prokaryotic diversity in the saline pools of this remote extreme environment has been poorly investigated and may consist of novel microbes that can be applied in the field of biotechnology.

1.5 Culture independent techniques used to assess microbial diversity

The microbial soil community is estimated to be comprised of more than 10³ microbial species per gram of soil (Torsvik *et al.*, 1990). Culture-dependent techniques are estimated to identify less than 1% of these microbes (Boivin-Jahns *et al.*, 1995; Torsvik *et al.*, 1998). Culture-dependent methods rely on the creation of artificial soil-like conditions for the isolation of microbes *in vivo*. These techniques are laborious and time consuming, and generally detect the most dominant microbes from the environment, leaving rarer species undetected. Until the symbiotic inter-relationships that exist between microbes and their immediate environment are fully understood, culture dependent techniques will be unable to detect the full diversity spectrum within an environment. Culture independent techniques are necessary to identify those that remain uncultured under standard laboratory conditions.

Culture independent techniques are based on the use of universal phylogenetic markers. The rRNA gene is commonly used for this purpose as it is conserved within all species and can serve as a valid molecular chronometer in assigning evolutionary traits among species (Wilson *et al.*, 1990). Oligonucleotide primers targeting species- and domain-specific genomic hotspots (regions in the bacterial genome which has undergone increased rates of recombination) within the rRNA genes are used in polymerase chain reactions (PCR) and

have aided in the identification of the previously unclassified microbial taxa (Yahara *et al.*, 2014).

PCR is an analytical tool which allows for the amplification of DNA using target specific primers and a thermostable DNA polymerase enzyme. In molecular ecology, PCR is the primary tool in culture independent studies to ascertain microbial community structures (Wilson *et al.*, 1990). The application of PCR in culture independent techniques is advantageous since it provides a cost effective, rapid amplification tool which can detect rare phylotypes from complex biomes (Hill *et al.*, 2000).

1.5.1 16S rRNA gene in phylogenetic analysis

The rRNA genes are conserved within all species, with 16S-, 23S- and 5S rRNA genes located within the prokaryotic ribosomal operon (*rrn*), and are crucial for the translation of proteins. The 5S rRNA gene was one of the first genes used to obtain phylogenetic information on bacterial communities (MacDonell and Colwell, 1984; Lane *et al.*, 1985). However, the one disadvantage of using this gene for phylogenetic analysis is that the relatively short oligonucleotide sequence obtained fails to resolve relationships at the intra- and inter-genus level (Olsen *et al.*, 1986). The 16S rRNA gene subunit is more useful, since it is longer and therefore, increases the validity of assigning phylogenetic affiliations among prokaryotic groups. The 16S rRNA gene was first applied to identify microbes microscopically by means of fluorescently labelled probes (De Longe *et al.*, 1989). The applications of 16S rRNA-based probing widened when Wilson and colleagues (1990) used it as a tool for the rapid assessment of pathogenic bacterial communities in humans and also when oligonucleotide primers capable of amplifying full length 16S rRNA gene sequences in bacterial and archaeal communities were published (Weisburg *et al.*, 1991; De Longe, 1992). Since then fluorescently labelled probes have also been applied to assess microbial composition in hypersaline saline environs such as the solar salterns of Santa Pole (Alicante, Spain) (Anton *et al.*, 2000); the salterns of Peruvian, Andes (Maturrano *et al.*, 2006); and the microbial mats of the Lower Cane Cave, USA (Engel *et al.*, 2010).

Despite the wide spread use of 16S rRNA gene for phylogenetic analysis there are several limitations. The 16S rRNA gene cannot be used as a phylogenetic marker in genera where there is little variation between species or where variation in the rRNA copy number exists (Rainey *et al.*, 1996; Mevarech *et al.*, 1989). This because variation in rRNA operon copy

number causes sequence heterogeneity within a microorganism's genome. Furthermore, examples of bacterial genomes were found to display up to 15 operons per genome and Archaea a maximum of five operons per genome (Fox *et al.*, 1992; Stackebrandt and Goebel, 1994; Klappenbach *et al.*, 2000).

Despite discrepancies observed between 16S rRNA gene sequences among species, it still remains one of the most widely utilised housekeeping gene to date in classifying and differentiating species in complex and varied environs (Yousuf *et al.*, 2012; Campbell *et al.*, 2013; Zhang *et al.*, 2013; Wang *et al.*, 2014). It also represents the baseline for which new biotechnology applications can be developed for both single and multi-cellular organisms (Langille *et al.*, 2013). For example, Langille and colleagues (2013) found that a computational algorithm can be used to quantify and link function of gene families based on the use of the phylogenetic marker, 16S rRNA. The predictive metagenomic computation model is the first to compare 'functional stability across metagenomes' by comparing 16S rRNA genes across different environs by relating phylogenetic gene families (Langille *et al.*, 2013).

1.5.2 16S rRNA gene clone libraries

Clone libraries form part of the primary tools utilised in molecular diversity studies to characterise both prokaryotic and eukaryotic community structure within complex environs. It is especially useful since it allows one to detect both culturable and uncultivable organisms from the environment that are normally missed when only culture dependant techniques are applied (Leigh *et al.*, 2010). 16S rRNA gene clone library techniques are based on the principal of basic PCR and cloning methodology, whereby 16S rRNA genes are amplified from metagenomic DNA and cloned into a suitable commercial plasmid vector (Vergin *et al.*, 2000). The resultant clones consist of a library of 16S rRNA genes which are transformed into competent cells (e.g. *E. coli*). A final dereplication step can be included that differentiates the clones by means of restriction length polymorphisms, thereby identifying different operational taxonomic units. Representative clones are sequenced and characterised by means of *in silico* analysis (Leigh *et al.*, 2010).

16S rRNA gene clone libraries have been utilised in an array of microbial diversity studies, sometimes in conjunction with other fingerprinting techniques to characterise bacterial communities in complex environs. For example, 16S rRNA gene clone libraries were used in

conjunction with T-RFLP to characterise the archaeal communities from the Eastern Mediterranean Seas (Moeseneder *et al.*, 2001). Others have used 16S rRNA cloning to help characterise the functional role of microbes in methane oxidation process in Kazan's mud volcano also situated in Eastern Mediterranean seas (Heijs *et al.*, 2007). 16S rRNA clone libraries have also been used to assess archaeal composition in two salt pans situated in Arpora, Goa. The archaea communities are found to inhabit these salt pans related to phyla of Haloarchaea and Crenarchaeota (Ahmad *et al.*, 2011).

1.5.3 Denaturing gradient gel electrophoresis

Denaturing Gradient Gel Electrophoresis (DGGE), also referred to as PCR-DGGE, is a culture independent molecular tool in which metagenomic DNA can be used to assess microbial diversity patterns within complex environmental settings. The technique offers a rapid, cost effective and non-labour intensive approach for obtaining a semi-quantitative molecular fingerprint of microbial communities in complex environmental samples. DGGE was first used to investigate the community structure of anaerobic sulphate reducing bacteria under aerobic conditions (Myzer *et al.*, 1993). Subsequently, the technique has been applied to investigate microbial diversity within extreme complex settings such as saline brines (Diez *et al.* 2001; Sørensen *et al.*, 2009), highly acidic environments (Aguilera *et al.*, 2006) and in the Arctic Ocean (Gast *et al.*, 2004).

In PCR-DGGE, amplified 16S rRNA gene fragments are electrophoresed in a polyacrylamide gel containing an increasing gradient of a denaturant. DNA fragments with different nucleotide sequences are separated based on the composition of their melting domains (strings of purine and pyrimidine sequences). A transition from a double stranded molecule to a partially separated DNA strand occurs, whereby the melting domain with the lowest melting temperature ceases to migrate within the gel. This transition is caused by both the temperature in which the gel is electrophoresed, and the presence of denaturants such as urea and formamide which break the hydrogen bonds between the nucleotides. This variation in melting temperatures allows the fragments with different melting domains to separate at various positions within the gel (Muyzer *et al.*, 1993; Muyzer 1999). Furthermore, either the 5' or 3' primer can be modified to include a 30 to 40 bp GC-rich sequence which modifies the melting behaviour of the resulting amplicons by increasing the percentage of sequence variations detected from 50% up to 100% (Sheffield *et al.*, 1989; Top, 1992).

The DGGE fingerprinting technique has been applied to assess microbial diversity structure in extreme environs such as salt pans and artificial saline habitats. For example, DGGE was used in conjunction with 16S rRNA clone libraries to assess the microbial composition in a salt crust collected from the hypersaline microbial mat in Eilat, Israel. The result obtained from DGGE analysis indicated that the bacterial communities decreased “with depth in the crust”, while the archaeal communities stayed constant. Excision and sequencing of the DGGE bands further identified three additional bacteria phyla from the Bacteroidetes group and three phyla from the Halobacteriales, in comparison with the 16S rRNA clone libraries where various phyla from Cyanobacteria, Planctomycetes, Chloroflexi, Halaneorobiales, Alpha-, Beta-, Delta- and Gammaproteobacteria were isolated (Sorensen *et al.*, 2005). Other applications of DGGE were to assess the microbial structure in two batch reactors of increasing salt concentrations. DGGE analysis indicated a diverse bacterial community which decreases as the salinity concentration increases. Excising of the DGGE bands further identified microorganisms belonging to Proteobacteria, Chloroflexi, Bacteroidetes, Actinobacteria and Firmicutes (Bassin *et al.*, 2012).

Although the procedure allows for the rapid phylogenetic fingerprinting of both terrestrial and aquatic environments, the technique also has drawbacks. DGGE is a PCR based method and as such is subjected to PCR bias. DGGE is supposed to separate sequences of as little as one base pair difference, but a study done by Jackson and colleagues (2000) showed that the technique was only able to separate sequences that differed in at least two base pairs. They also indicated that the percentage of denaturing gradient used could also affect the separation of DGGE bands in the gel. Bands have been found to co-migrate in DGGE thus resulting in the under-representation of species diversity in environmental samples, with one band representing more than one phylotype. Excising and sequencing of these bands may help to identify the phylogenetic difference between fragments that co-migrate (Sekiguchi *et al.*, 2001; Yu *et al.*, 2008).

To increase the validity of the results obtained from this technique in community profiling, it is often used in conjunction with other culture independent techniques, such as T-RFLP or 16S rRNA gene clone libraries.

1.5.4 Terminal restriction fragment length polymorphism

Terminal restriction fragment length polymorphism (T-RFLP) analysis is employed in both the assessment of the diversity and spatial analysis of microbial communities. The technique involves the PCR amplification of DNA with at least one fluorescently labelled primer, followed by digestion of the amplified product with restriction endonucleases. The digested products are analysed using an automated capillary sequencer. The fluorescently labelled terminal fragments are assigned to phylogenetic groups based on *in silico* analysis of 16S rRNA gene sequences deposited in databases. The restriction length fragments resemble partial microbial sequences within the 16S rRNA gene database which allows for the identification of the acquired sequences to a known phylogenetic community. T-RFLP analysis resolution can be improved by increasing both the number of fluorescently labelled primers and the number of restriction endonucleases used (Marsh, 2005; Schutte *et al.*, 2008).

T-RFLP analysis is a cost effective approach to analysing microbial communities within complex environments. It enables analysis of both cultivated and uncultivated microbes using a high throughput automated system. The method has proven valuable in environmental studies in discerning community composition of both archaeal and bacterial organisms in extreme saline environs. Moeseneder and colleagues (2001) applied T-RFLP analysis to assess the archaeal diversity of the Eastern Mediterranean seas by comparing the restriction patterns of three tetrameric enzymes. They found with the application of T-RFLP fingerprinting novel archaeal marine groups I, II and III could be identified. More recently T-RFLP fingerprinting was utilised to assess Crenarchaeal heterotrophy in sediments obtained from salt marshes in Hooks Creek, New York City, USA (Seyler *et al.*, 2014). The authors used isotope probing to ascertain heterotrophy by using extracted DNA from C-labelled compounds (urea, acetate and glycine) and C-labelled biopolymers (proteins, lipids and complex growth media). By means of T-RFLP fingerprinting, Seyler and colleagues (2014) found that both heterotrophic bacteria and archaea compete for carbon sources and that this model can be used to assess both metabolic functions and diversity of crenarchaea in salt marshes.

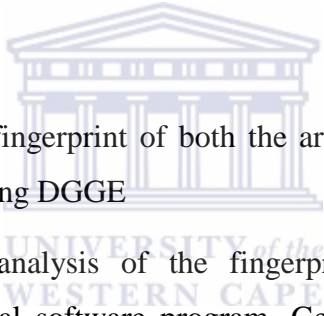
As with all methods T-RFLP analysis has advantages and disadvantages. The method provides for a cost effective approach to analysing microbial communities within both terrestrial and aquatic environments. It enables analysis of both cultivated and uncultivated

microbes using a high throughput automated system. A disadvantage of T-RFLP analysis is that it is PCR based and is thus also subject to PCR bias, mainly linked to non-specific amplification (Blackwood *et al.*, 2003; Marsh, 2005; Nocker *et al.*, 2007). Another major limitation is that an individual peak produced by T-RFLP analysis can correspond to a number of phylogenetic species. This is because one microbial species could have the same restriction site as another non-related species (Marsh, 2005; Schutte *et al.*, 2008)

1.6 Aims and objectives of the study

The aim of this project was to investigate the archaeal, bacterial and cyanobacterial diversity within the Namib Desert salt pans located in two different biogeographical regions (Gobabeb and Swakopmund) within the Namib salt pans. Culture independent techniques including PCR-DGGE, T-RFLP and 16S rRNA gene clone libraries were employed to investigate the diversity composition between the two sites

The objectives were as follows:

- 
- To create a comparative fingerprint of both the archaeal and bacterial communities within the 2 study sites using DGGE
 - Statistical analysis of the fingerprints by the application of the mathematical software program, GelCompar II (cluster analysis and MDS plots)
 - To obtain a quantitative profile of the operation taxonomic units (OTUs) using T-RFLP
 - Statistical analysis of peak profiles by means of *in silico* analysis
 - Investigate the microbial population structure by means of statistical analyses
 - Assign phylogenetic affiliation to peak profiles
 - To construct a 16S rRNA gene clone library for both the Archaeal and Bacterial groups
 - Dereplicate OTUs by means of ARDRA
 - Assess community structure based on statistical analysis
 - Identify phylogenetic groups based on sequence analysis of a clone libraries

Chapter 2: Materials and Methods

2.1 Sampling procedures

Samples were collected from two regions of the Namib Desert, namely Gobabeb and Swakopmund, by a research team led by Professor Don Cowan (formally of the University of the Western Cape). Sediment samples from Gobabeb were collected in April 2010. Samples were collected with sterile spatulas and stored in Whirlpak bags. The Swakopmund samples were collected from two separate locations at a salt pan in Eisfled (Silver Lake Playas) in April 2011. Samples were collected in 50ml sterile falcon tubes, kept on ice during transportation and were stored at 4°C before being processed two weeks later. The conductivity of the Swakopmund samples was measured on site with an electronic conductivity (EC) meter. The conductivity of the pooled Gobabeb samples was measured with an EC meter when processed in 2011. Table 1 details the sampling sites.

Table 1: The three different research sites chosen for this investigation with their respective GPS coordinates.

Site	Date of sample collection	Sample name	Sample description	GPS coordinates
Gobabeb	21 April 2010	GOB1	Mixed surface sample comprising of both orange and green material	S23°30.426' E015°4.305'
		GOB2	Mixed surface sample (close proximity with GOB1)	
		GOB3	Green surface material	
		GOB4	Orange surface	
		GOB5	Salt and musk sediment (green cyano-like material)	
Swakopmund 1	07 April 2011	Sps-01 (A-D)	Soil and water	S 22°28.491' E 014°34.254'
Swakopmund 2	07 April 2011	Sps-02 (A-D)	Soil and water	S 22°29.079' E 014°34.303'

2.1.1 Physio-Chemical Analysis

Sediment analysis of all samples was performed at Bem-Lab, a SANAS accredited testing laboratory (Strand, South Africa). The following chemical analyses were performed: S, C, N, Na, Cl, SO₄, CaCO₃ and pH.

2.2 DNA extraction methods

Two methodologies were used to extract metagenomic DNA from the environmental samples: (i) a commercial DNA isolation kit (UltraClean soil) from MoBio laboratories, Inc. was used for the sediment samples obtained from Swakopmund, and extractions were conducted according to the manufacturer's instructions. ii) All sediment samples obtained from Gobabeb were processed using the modified extraction method from Zhou *et al.* (1999).

2.2.1 Materials used for the modified Zhou *et al.* (1999) DNA extraction method

2.2.1.1 Extraction buffer

The extraction buffer consisted of 100mM NaH₂PO₄ (pH8), 100mM Tris-HCl (pH8), 100mM EDTA (pH8), 1.5M NaCl and 1% (m/v) CTAB.

2.2.1.2 DNA elution buffer/ TE

1x Tris-EDTA (1xTE), pH8 was prepared to a final concentration of 10mM Tris, 1mM EDTA

2.2.1.3 Methodology for the modified Zhou *et al.* (1999) DNA extraction method

Spatulas and weighing boats were cleaned with 70% ethanol before weighing the sediment samples. Aliquots (1g) were placed in sterile 2ml microcentrifuge tubes. Extraction buffer (675µl) containing proteinase K (20mg/ml) was added and the samples were incubated at 37°C for 30 min in a waterbath. After incubation, SDS was added to a final concentration of 1% (v/v). The solution was incubated in a waterbath at 65°C for 2 hours with gentle inversions every 15 min. The samples were removed and centrifuged for 15 min at 16,000 x g. Following centrifugation; the supernatant was carefully removed from samples and placed into a new sterile 2ml microcentrifuge tube. One volume of phenol /chloroform/isoamyl alcohol [24/24/1; v/v/v] was added to the supernatant. Samples were mixed by gentle inversion and subjected to centrifugation at 16,000 x g for 5 min. The aqueous phase was transferred to a new tube and isopropanol (0.6 volumes) was added to the aqueous supernatant and mixed. The solution was incubated at room temperature for 20 min, followed by centrifugation for 10 min at 16,000 x g. The supernatant was discarded and the pellet was

washed twice with 70% (v/v) ice cold ethanol (1ml). The pellet was then air dried in a laminar flow and resuspended in 50µl of 1xTE. DNA samples were stored at -20°C.

2.2.2 Commercial DNA extraction kit: UltraClean Soil DNA Extraction kit (MoBio laboratories, Inc.)

The DNA extraction method was carried out based on the manufacturer's instructions.

2.3 DNA Quantification

The DNA concentrations and purity of the samples was determined using a Nanodrop ND-1000 Spectrophotometer (Thermo Scientific).

2.4 Agarose gel electrophoresis

Agarose gels were prepared according to the method of Sambrook and Russel (2001). Either 1% or 2% (m/v) agarose gels were prepared using SeaKem® LE Agarose (Lonza) in 1xTAE (40mM Tris acetate and 1mM EDTA (pH8)). The 1% gels were used to differentiate between larger fragment and the 2% gel was used for differentiation between smaller fragments. Ethidium bromide (10mg/ml) was added to the molten agarose. Tracking dye (bromophenol blue; 3', 3'', 5', 5''-tetrabromophenolsulfonphthalein) was added to samples and the DNA was separated by electrophoresis at 80-100V for 1 hour. Gels were visualised using the AlphaImager™ HP (AlphaEaseFC (FluorChem8800) [Alpha Inotech]). The size marker λ PstI was used to run alongside both DNA and PCR amplicons to determine individual fragment sizes.

2.5 Denaturing gradient gel electrophoresis

2.5.1 Bacterial 16S rRNA PCR amplification for DGGE analysis

The GeneAmp® PCR system 2700 (Applied Biosystems) thermocycler was used for all PCR amplifications. The PCR amplification was done in two rounds. In the first round of PCR amplification a 50µl reaction consisting of 1x PCR buffer, 0.2mM of each dNTP (dATP, dCTP, dGTP and dTTP), 0.5µM each of the universal bacterial primers E9F/U1510R (Table 2), 0.5U of Dream *Taq* (Fermentas), 20ng of metagenomic template DNA and the volume was adjusted to 50µl with ultra-pure H₂O (Purite /System). The PCR cycling conditions were as follows: an initial denaturation at 94°C for 4 min followed by 30 cycles of denaturation at 94°C for 30 seconds, annealing at 52°C for 45 seconds, elongation at 72°C for 85 seconds and a final elongation at 72°C for 10 min.

In the second round a nested PCR amplification was performed using bacterial primers 341F-GC/534R (Table 2). As prescribed by Muyzer *et al.* (1996) the forward primer was labelled with a 30bp GC sequence tag. Reactions (50µl) contained the same PCR reagents as in the first round amplification. One microliter of the amplified PCR product obtained in first round PCR amplification was used as the template in the second round. The PCR cycling conditions were an initial denaturation at 94°C for 4 min, an annealing temperature of 55°C for 45 seconds, elongation at 72°C for 75 seconds for 20 cycles, followed by an additional 20 cycles of denaturation at 94°C for 30 seconds, annealing at 55°C for 30 seconds, elongation at 72°C for 75 seconds, followed by final elongation at 72°C for 10 min. Amplified fragments obtained were analysed as described in section 2.3.2.

2.5.2 Archaeal 16S rRNA gene PCR amplification for DGGE analysis

The archaeal PCR amplification process was carried out as in section 2.4.1 with minor modifications. The universal-archaeal primer pair A3fa-F/Ab927R (Table 2) was used. The PCR cycling conditions were an initial denaturation at 94°C for 4 min, annealing at 55°C for 45s, elongation at 72°C for 75s for 20 cycles, followed by denaturation at 94°C for 30 seconds, annealing at 55°C for 30 seconds, elongation at 72°C for 75 seconds for an additional 20 cycles with a final elongation at 72°C for 10 min.

In the second round nested DGGE PCR amplification process archaeal primers 340F-GC/533R were used. PCR cycling conditions were set at an initial denaturation at 94°C for 4 min followed by 30 cycles of denaturation at 94°C for 45 seconds, annealing at 53.5°C for 45 seconds, elongation at 72°C for 60 seconds, and a final elongation at 72°C for 20 min.

Table 2: Summary of PCR primers used in this study

Primer set	Sequence 5'-3'	Product size (bp)	Specificity	Annealing temperature (T _m)	Reference
A3fa AB927R	TCCGGTTGATCCYGCCGG CCCGCCAATTCCTTTAAGTTTC	927	Universal archaeal primers used for 1st round DGGE amplification	55	Baker <i>et al.</i> (2003) and McInerney <i>et al.</i> (1995)
A340F-GC A533R	*ACGGGGGGCCCTACGGGGYGCASCAG TTACCGCGGCKGCTG	200	Universal archaeal primers used for 2nd round DGGE amplification	53.5	Ovreas <i>et al.</i> (1997)
8Fa 1492R	TCYSGTTGATCCTGCS GGTTACCTTGTTACGACTT	1492	16S rRNA gene universal archaea (T-RFLP)	55	Costello and Schmidt (2006)
E9F/ U1510R	GAGTTTGATCCTGGCTCAG GGTTACCTTGTTACGACTT	1510	16S rRNA gene universal bacteria (1st round 16s PCR for DGGE)	52°C	Hansen <i>et al.</i> (1998)
341F-GC 534R	*ACGGGGGGCCCTACGGGAGGCAGCAG ATTACCGCGGCTGCTGG	200	16S rRNA gene universal bacteria (2nd round 16s PCR for DGGE)	55	Muyzer <i>et al.</i> (1993)
E9F-Fam U1510R	GAGTTTGATCCTGGCTCAG GGTTACCTTGTTACGACTT	1510	16S rRNA gene universal bacteria (TRFLP)	52°C	Hansen <i>et al.</i> (1998)
CYA359 U1510R	GGGGAATYTTCCGCAATGGG GGTTACCTTGTTACGACTT	1200	16SrRNA gene universal Cyanobacteria (1st round PCR primers for T-RFLP)	60°C	Nüebel <i>et al.</i> (1997)
CYA359F CYA781R	GGGGAATYTTCCGCAATGGG GACTACWGGGGTATCTAATCCCWTT	493	16SrRNA gene universal Cyanobacteria(2nd round PCR primers for T-RFLP)	50°C	Nüebel <i>et al.</i> (1997)
M13F M13R	CCCAGTCACGACGTTGTAACACG AGCGGATAACAATTCACACAGG	1650	Vector Vector	55°C	pGEM-T Easy primers

Footnotes

*CGCCC GCCGCGCGCGGGCGGGGCGGGGGC

All primers were synthesised by Inqaba Biotech (South Africa)

2.5.3 DGGE gel assembly

The set-up of the DGGE system was done according to the DCode™ Universal Mutation Detection System's Manual (BIO-RAD laboratories, 1996). Prior to assembly the glass plates were cleaned by sequential washes with 96% ethanol, methanol and Millipore dH₂O. The 0% and 100% stock solutions were prepared as outlined in Table 3.

Table 3: Preparation of 0% and 100% denaturing stock solutions

Reagent	0% Denaturing solution	100% Denaturing solution
40% Acrylamide	112.5ml	112.5ml
50x TAE	10ml	10ml
Urea	----	210g
Formamide	----	200ml
ddH ₂ O	add up to 500ml	add up to 500ml

Nine percent polyacrylamide gels were prepared for the 30/70% denaturing gradients. The denaturing gradient gels were prepared as shown in Table 4. Prior to casting the gels 0.02 % (v/v) TEMED and 0.5% (w/v) APS was added. Gels were polymerized at room temperature for 2 hours. Electrophoresis was performed at 60°C in 1x TAE buffer for 16 hours at 100V. After electrophoresis the gels were stained in 1x TAE, containing 0.5µg/ml ethidium bromide for 15 min and destained in 1x TAE for 30 min before visualising the gel using an AlphaImager™ HP (Alpha Innotech).

Table 4: Denaturing gels prepared from 0% and 100% stock solutions

Solutions	70%	30%
0%	5.4ml	12.6ml
100%	12.6ml	5.4ml

2.5.4 Analysing DGGE banding patterns

The captured DGGE images were analysed using the GelCompar II (version 5.00) software (Applied Maths). The software was used to calculate the clustering of the samples by means of a dendrogram and an MDS plot. DGGE images were used to identify frequently detected and unique bands which were selected for further analysis.

2.5.5 Sequencing of DGGE bands

Selected bands were excised from the gel with a sterile scalpel and placed in individual sterile microcentrifuge tubes containing 50µl ddH₂O. DNA was allowed to diffuse from the gel slices overnight at 4°C. Eluted DNA was used as the template for the archaea/bacteria second round PCR amplification process as described in sections 2.4.1 and 2.4.2. The PCR fragments obtained were separated on a 1% agarose gel and visualised as described in section 2.3.2. The amplicons that were successfully re-amplified were purified with the GFX PCR DNA and Gel Band purification kit (GE Healthcare, UK) according to the manufacturer's instructions. The purified samples were sequenced at the Central Analytical Facility at Stellenbosch University, South Africa.

The chromatograms were edited using the bioinformatics program BioEdit (version 7.2.5). The edited sequences were analysed by BLAST (www.blast.ncbi.nlm.nih.gov/Blast.cgi) to identify the closest phylogenetic affiliation.

2.6 T-RFLP

2.6.1 PCR amplification of the bacterial 16S rRNA gene

PCR amplification reactions were carried out in 50µl reaction volumes. The 50µl reaction volumes contained 1x Dream buffer, 0.2mM dNTP (dATP, dCTP, dGTP and dTTP), and 5µM each of the universal bacterial primers E9F-Fam/U1510R (Table 2), 0.5U Dream *Taq* and 20ng of metagenomic template DNA. The volume was made up to 50µl with ultra-pure H₂O. The PCR cycling conditions were an initial denaturation at 94°C for 4 min, followed by 30 cycles of denaturation at 94°C for 30 seconds, annealing at 52°C for 30 seconds, elongation at 72°C for 85 seconds and a final elongation at 72°C for 10 min. Since 100µl of PCR product was required for analysis, two 50µl PCR reactions were pooled per sample. Amplicons were electrophoresed in a 1% agarose gel as outlined in section 2.3.2. The amplicons were purified with the GFX PCR DNA and Gel Band purification kit (GE Healthcare, UK) according to the manufacturer's instructions. Purified amplicons were subjected to restriction analysis as stipulated in section 2.5.4

2.6.2 PCR amplification of the archaeal 16S rRNA gene

PCR amplification reactions were performed as outlined in section 2.6.1 using universal archaeal primers 8Fa-Fam/1492R (Table 2). The PCR cycling conditions used were an initial

denaturation at 94°C for 5 min, followed by 30 cycles of denaturation at 94°C for 60 seconds, annealing at 55°C for 60 seconds, elongation at 72°C for 90 seconds and a final elongation at 72°C for 20 min.

2.6.3 PCR amplification of the cyanobacterial 16S rRNA gene

For the PCR amplification of the cyanobacterial 16S rRNA gene a semi-nested approach was used. In the first round PCR 25µl reactions were prepared. The 25µl reaction volumes contained 1x PCR buffer, 0.3mM dNTP (dATP, dCTP, dGTP and dTTP), 0.1mM BSA, 1% glycerol (v/v), and 5µM each of the cyanobacterial-specific primers CYA359F/U1510R (Table 2), 0.5U Dream *Taq*, 20ng of metagenomic template DNA. The volume was made up to 50µl with ultra-pure H₂O. The PCR cycling conditions were an initial denaturation at 94°C for 5 min, followed by 35 cycles of denaturation at 95°C for 60 seconds, annealing at 60°C for 60 seconds, elongation at 72°C for 90 seconds and a final elongation at 72°C for 20 min. Amplified fragments obtained were visualized and separated by electrophoresis as described in section 2.3.2.

In the second round PCR the 50µl reaction volumes contained 1x PCR buffer, 0.3mM dNTP (dATP, dCTP, dGTP and dTTP), 0.1mM BSA, 1% glycerol (v/v), 5µM each of the cyanobacterial –specific primers Fam-CYA359F/781R (Table 2), 0.5U of Dream *Taq*, and 1µl of the amplified DNA from round one. The volume was made up to 50ul with ultra-pure H₂O. The PCR cycling conditions were an initial denaturation at 94°C for 5 min, followed by 35 cycles of denaturation at 95°C for 60 seconds, annealing at 50°C for 60 seconds, elongation at 72°C for 90 seconds, and a final elongation at 72°C for 20 min. Amplified fragments were pooled for each sample and separated on a 2% agarose (section 2.3.3). The DNA fragments that were of the expected size of 493bp were excised from the gel and purified with the GFX PCR DNA and Gel Band purification kit (GE Healthcare, UK). Due to DNA loss during purification two 50µl PCR reactions were pooled per sample. The purified amplicons were subjected to restriction analysis (section 2.5.4).

2.6.4 Restriction digestion and T-RF peak analysis

Restriction digestion of the fluorescently labelled 16S rRNA gene amplicons was carried out as follows. Twenty microliter digests contained 7.5µl of restriction buffer, 10µl purified PCR product, 10U/µl of restriction enzyme (Fermentas). The reactions were incubated at 37°C for 16 hours. The digested product was purified using the NucleoSpin® Gel and PCR

purification kit (MACHEREY-NAGEL) prior to T-RFLP analysis which was performed at the Central Analytical Facility at Stellenbosch University.

Terminal restriction fragments (T-RFs) were first analysed using the software program Peak Scanner v.1.0 (Applied Biosystems). Since the digested fragment size was 1.5kb, the size standard ROX 1.1 was utilised as an internal control. A cut-off value of 30bp was assigned for T-RFs since lower fragments are indicative of primers (Singh *et al.*, 2006). Also, the peak height was used to determine the abundance of a T-RF, fragments that differed by three base pairs were binned together and was considered as the same T-RF, thus representing one OTU.

Edited peak profiles were imported into the statistical software program R (v: 2.13.2). The matrix obtained from R was uploaded into the program PRIMER (v6.1.11). Data incorporated into PRIMER v6 was first transformed into its square root, before analysing the T-RFs by means of both univariate (e.g. ANOSIM) and multivariate (e.g. Clustering and MDS plots) analytical applications.

2.7 Clone library construction

Bacterial and cyanobacterial populations were analysed using separate 16S rRNA gene clone libraries.

2.7.1 Media used for cloning

2.7.1.1 Luria Broth (Sambrook and Russel, 2001)

Luria Bertani (LB) broth was prepared by adding 10g NaCl, 10g tryptone powder and 5g yeast extract to 1L dH₂O. The solution was autoclaved for 20 min at 121°C.

2.7.1.2 Luria Agar (Sambrook and Russel, 2001)

10g NaCl, 10g tryptone powder, and 5g yeast extract and 15g bacteriological agar was added to 1L of dH₂O. The solution was autoclaved for 20min at 121°C.

2.7.2 Preparation of chemical competent cells (Li et al., 2010)

All solutions and plasticware required for the preparation of the chemical competent cells were autoclaved and stored at 4°C to chill before use.

A fresh culture of *E. coli* GeneHog (Invitrogen) was prepared from a glycerol stock by streaking onto LB agar to grow overnight at 37°C. A single colony was used to inoculate 5ml

of LB medium. The starter culture was incubated overnight at 37°C with shaking and 1ml of the overnight culture was inoculated into 100ml of LB medium. The culture was incubated at 37°C with shaking at 180rpm for 1.5-3 hours until an OD₆₀₀ between 0.4-0.6 was reached. The flask containing the cells was placed on ice for 15 min with gentle intermittent mixing. The cells were kept cold from this stage onwards. After 15 min, the cells were harvested by centrifugation at 4000 rpm for 10 min in a Beckman Coulter centrifuge (Rotor GA-20). After centrifugation the supernatant was discarded and the cells were resuspended in 10ml 0.1M ice cold CaCl₂, followed by incubation on ice for 30 min. After incubation on ice, the cells were centrifuged as before. After centrifugation the supernatant was discarded and the cells were gently resuspended in 1ml 0.1M CaCl₂, 15% glycerol (v/v) solution. Aliquots (100µl) of the resuspended cells were stored at -80°C.

2.7.3 Ligation

Ligation reactions were performed using the Promega pGEM-T® Easy kit according to the manufacturer's instructions. The ligations were carried out in 15µl reactions. To each reaction tube the following reagents were added: 2x Ligation buffer, 1µl pGEM-T® Easy vector, 1µl PCR product, 1U T4 ligase and the reaction was made up to final volume with dH₂O. The ligation reactions were incubated overnight at 4°C before being transformed.

2.7.4 Transformation of E.coli GeneHog competent cells

Competent cells were transformed by the addition of 1µl ligation mix to 100µl competent cells thawed on ice. The ligation mixture was placed on ice for 30 min. The cells were subjected to heat shock in a 37°C water bath for 1 min. Following heat shock the cells were placed back on ice and 900µl pre-warmed LB medium was added to the cells. The transformed cells were incubated at 37°C for 30 min with shaking (180rpm). After incubation, 100µl aliquots were plated on LB agar plates supplemented with ampicillin (100µg/ml), IPTG (100mM/ml) and X-Gal (50µg/ml). The plates were incubated at 37°C overnight. The recombinant clones were selected based on the blue/white colony selection and only white insert-containing clones were analysed.

2.7.5 Screening of recombinant clones

2.7.5.1 Colony PCR

A small amount of cell mass from a white colony (a putative positive clone) was added to a PCR mixture using a sterile toothpick. The PCR reaction contained 1x Dream buffer, 0.2mM

dNTP (dATP, dCTP, dGTP and dTTP), 2 μ M each of the primer M13R/M13F (Table 2) and 0.25 units of Dream *Taq* and was made up to a volume of 50 μ l with ultra-pure H₂O. The PCR cycling conditions were an initial denaturation at 94°C for 4 min, followed by 30 cycles of denaturation at 94°C for 30 seconds, annealing at 52°C for 30 seconds, elongation at 72°C for 85 seconds, and a final elongation at 72°C for 10 min. The PCR fragments were separated on a 1% agarose gel (section 2.3.2).

2.7.5.2 Amplified ribosomal DNA Restriction Analysis (ARDRA) of clone libraries

ARDRA was used to identify the various phylotypes found within the libraries. Restriction digests contained 1x buffer, 10 μ l of PCR products (obtained from colonies amplified with M13F/M13R primers from section 2.6.6.1.), and 7.5 μ l of dH₂O and 1U of enzyme. The products were digested for 16 hours at 37°C. The digested products were separated on 2% agarose gels and viewed with an AlphaImagerTM HP (Alpha Innotech). Clones were grouped by visual inspection of the banding patterns and one representative clone per restriction pattern was sequenced.

2.7.5.3 Sequence analysis of clones

The preparation of clones for sequencing was done using the Qiaprep®Spin Minprep Kit (Qiagen) according to manufacturer's guidelines.

In silico analysis of clone sequences were done as follows:

Raw sequences obtained were edited with the bioinformatics tool Bioedit (version 7.1.3). Vector sequences were removed from the sequences with VecScreen (<http://www.ncbi.nlm.nih.gov/VecScreen/>). The sequences were checked for chimeras with the online program nBLAST (Altschul *et al.*, 1990) (<http://blast.ncbi.nlm.nih.gov/>) from NCBI and Bellerophon (Huber *et al.*, 2004) (<http://compbio.anu.edu.au/bellerophon/bellerophon.pl>). The orientations of sequences were also checked with the on-line program nBLAST (Altschul *et al.*, 1990) (<http://blast.ncbi.nlm.nih.gov/>) and OrientationChecker (version1.0) (Ashelford *et al.*, 2006). CD-HIT Suite webserver (Li and Godzik, 2006) (<http://weizhong-lab.ucsd.edu/cd-hit/>) was used to cluster the sequences which had a 97% similarity (homology). Furthermore, one sequence per cluster and the respective reference sequences (obtained from NCBI) were used to construct the phylogenetic trees. The maximum-likelihood (Felsenstein, 1981) and Kimura-2 parameter (Kimura, 1980) methods were used for constructing the phylogenetic trees in MEGA (version 5.05) (Tamura *et al.*,

2011). The maximum likelihood method calculates the highest probability or likelihood of an evolutionary relationship existing among organisms (Felsenstein, 1981) while the Kimura-2 parameter model calculates the mutational rate (transitions and transversion) that occurs at sequence level among taxa (Kimura, 1980). Clones were further identified and assigned phylotypes based on the analysis tool Classifier (Wang *et al.*, 2007), in the known reference 16S rRNA database system, Ribosomal Database project (RDP) (Maidak *et al.*, 1995) (<http://rdp.cme.msu.edu/classifier/classifier.jsp>).

The T-RFs obtained from T-RFLP analysis were further assigned phylogenetic identities by matching the T-RFs to sequences obtained from 16S rRNA clone libraries. This was done by using an *in silico* restriction digestion software program Sequence Manipulation Suite (http://www.bioinformatics.org/sms2/rest_digest.html).

2.7.5.4 Statistical analysis of clones

To assess if the number of clones analysed in libraries were sufficient to cover the overall diversity present in the environmental samples, the library richness estimates S_{Chao1} and S_{ACE} were calculated (Table 5). The online program from the Association for the Science and Limnology and Oceanography (www.aslo.org) (Kemp *et al.*, 2004) was used to calculate S_{Chao1} and S_{ACE} (Table 5).

Table 5: Summary of the diversity indices

Library richness estimates	Calculation	Reference
S_{Chao1} -define as a non-parametric estimator	$S_{\text{Chao1}} = S_{\text{obs}} + \frac{F_1^2}{2(F_2+1)} - \frac{F_1 F_2}{2(F_2+1)^2},$ <p> S_{obs} = number of phylotypes F_1 and F_2 are the number of phylotypes occurring either once or twice </p>	Chao <i>et al.</i> , 1987
S_{ACE} -define as a coverage based estimator	$S_{\text{ACE}} = S_{\text{abund}} + \frac{S_{\text{rare}}}{C_{\text{ACE}}} + \frac{F_1}{C_{\text{ACE}}} \gamma_{\text{ACE}}^2$ <p> F_1 = number of phylotypes that appear only once in the library, S_{rare} = number of phylotypes that occur less than 10 times, S_{abund} = number of phylotypes that occurs more than 10 times </p>	Chao <i>et al.</i> , 1993

Chapter 3: Bacterial Diversity

3.1 Introduction

Differences in soil chemistry and biogeography account for the varying distribution and composition of microbial communities in extreme saline habitats, such as salt pans (Lopzupone and Knight, 2007). For instance, low G+C bacteria, Firmicutes and Betaproteobacteria were isolated from sulphate rich athalossohaline environs of Lake Chaka (China) (Jiang *et al.*, 2006); whereas sulphate reducing bacteria (*Desulfobacteraceae* and *Peptococcaceae*) and methanogens (*Methanosarcinaceae*) were detected in salt pan sediments from Tirez lagoon, which contain mostly carbonate salts (Montoya *et al.*, 2011). In other studies conducted in crystallizer salt pans of the Peruvian Andes, extreme salt dependant bacterial species including *Salinibacter ruber*, *Rhodospirillum salinarum* and *Marinococcus halophilus* were isolated, along with various strains of *Pseudomonas* (Maturrano *et al.*, 2006). Other investigations into athalassohaline regions isolated various novel species of bacteria including *Halomonas koreensis* (Lim *et al.*, 2004), *Halomonas taeanensis* (Lee *et al.*, 2005), *Desulfosalsimonas propionica* (Kjeldsen *et al.*, 2010), *Caenispirillum salinarum* (Ritika *et al.*, 2012) and *Virgibacillus natechei* (Amzaine *et al.*, 2013). All these studies highlighted that microbial diversity between salt pans may vary and that the degree of salinity is a major contributing factor shaping bacterial diversity within athalossohaline environs.

The aim of the current study was to investigate the bacterial diversity of three physiochemically and geomorphologically diverse athalassohaline habitats in the Namib Desert. Culture-independent techniques including DGGE, T-RFLP and clone libraries were used to determine the phylogenetic groups present in the Gobabeb and Swakopmund salt pans.

3.2 Results and discussion

3.2.1 Description of the sampling sites

Five separate soil samples were collected from a 200cmx200cm area in a salt pan at the Gobabeb site (Figure 6) and were labelled GOB1-5. At the Swakopmund study areas, site 1 and site 2 (Figure 6) were identified. Four soil samples were collected at each of the

individual sites and were labelled as Sps01 for Swakopmund site 1 and Sps02 for Swakopmund site 2.



Figure 6: The two sampling sites. ● Gobabeb (near the Gobabeb Research Centre) and ● Swakopmund (near the coast) in the Namib Desert. Gobabeb and Swakopmund sampling sites are approximately 127km apart. (Adapted from Eckardt and Drake, 2011).

Although the five Gobabeb soil samples were collected within a 200cmX200cm area, and within to the same saline spring, they represented different micro-niches within the stream, differing in physical appearance and also in chemical composition (Table 1). For instance, GOB1 was recorded as consisting of mixed orange and green filamentous mats, whereas GOB2, which was taken in relatively close proximity to GOB1, was found to consist of only the orange mats mixed with soil. Sample GOB3 was found to contain predominantly green microbial growth, while the surface of GOB4 was orange. The physical appearance of the soil collected at GOB5 was recorded as having a salt precipitated on its surface containing green cyanobacterial-type material.

All samples collected at Swakopmund site 1 and 2 were composed of soil and water, with the exception of Swakopmund site 2 samples which also contained part of the salt crust layer and

green material. Furthermore, as seen in Figure 7, the geomorphology of all three sampling sites was similar - consisting of ephemeral streams with salt-like precipitations on the soil surface.



Figure 7: The sampling sites included in this study Gobabeb site (1, 2), Swakopmund site 1 (3, 4) and Swakopmund site 2 (5, 6), with their respective conductivity readings. Conductivity was measured in milliSiemens per centimetre (mS/cm), with $1\mu\text{s/cm}=0.6\text{mg/kg}$ of NaCl. The pictures of Gobabeb sampling site depict the soil with a layer of salt precipitates on its surfaces together with green material, while Swakopmund site 1 represents the epidermal rivers. The soil of Swakopmund site 2 sampling site is surrounded by gypsum containing water with the crust containing distinct microbial stratification layers of orange, and green material. (Photos taken by the investigating team from IMBM).

The electrical conductivity of Swakopmund samples were measured *in situ* in the stream when the samples were collected, and were found to be 150mS/cm for Sps01 and 180mS/cm for Sps02. The electrical conductivity of the pooled Gobabeb samples was measured in the laboratory and found to be 103mS/cm. Electrical conductivity measurements relate to the salinity of a sample and provide a collective measurement of the number of unbound inorganic solutes such as Na^{2+} , Cl^- , Mg^{2+} , SO_4^{2-} , and CO_3^{2-} present within a sample. However, it does not provide a detailed account of the anions and cations present (Hershey

and Sand, 1993). To further analyse the chemical composition accounting for this salinity gradient, further physiochemical analysis was done on the pooled samples from each site. Ideally, chemical analysis should be done on each individual sample; however, due to the small sample volumes collected for analysis, pooling of samples collected at each site was necessitated.

Table 6: Physiochemical evaluation of the Gobabeb (GOB) and Swakopmund (Sps01 and Sps02) sediment samples

Sampling Sites	Samples pooled	pH (KCl)	Conductivity (mS/cm)	S ²⁻ % (w/w)	C (%)	N ³⁻ (%)	SO ₄ ²⁻ % (w/w)	Na ⁺ (%)	Cl ⁻ (%)	CaCO ₃ ²⁻ Equivalent
Gobabeb	GOB1-5	8.3	103	0.41	0.88	0.15	0.017	1.38	1.38	24.3
Swakopmund site 1	Sps01A-D	8.1	150	0.31	0.64	0.12	2.76	1.49	1.49	17.27
Swakopmund site 2	Sps02A-D	8.2	180	0.32	2.48	0.29	1.96	*	1.51	21.59

Footnotes: CaCO₃ calculates the water alkalinity and hardness

CaCO₃ is measured in mg/L

S and SO₄ is measured in mg/kg

*Insufficient sample obtained to do analysis

The results from the physiochemical analysis of the soils are presented in Table 6. All sites examined were alkaline (pH range 8.1-8.3). Further evaluation of the chemical composition of the sediment samples clearly shows that Na⁺, Cl⁻ and S²⁻ ion levels were high at all three sites, with almost no significant inter-site variation observed. Interestingly, in previous investigations into the mineral composition of the Namib saline pools at Eisfeld in Swakopmund and Hosbabes in Gobabeb, researchers detected high concentrations of CaCO₃²⁻ (<3%) and SO₄²⁻ (<1%) in these areas which would favour the formation of gypsum (Eckardt *et al.*, 2010). In the present study, the concentration of SO₄²⁻, CaCO₃²⁻ and C were found to be higher at the Swakopmund sites (Table 6) than at the Gobabeb site, which was evident by the formation of thick salt crust (Figure 7 and Table 6) visible at Swakopmund site 2 (Sps02). The elevated level of CaCO₃²⁻, and not SO₄²⁻ and C in the Gobabeb region likely contributed to the slightly higher alkalinity level compared to the Swakopmund sites. Furthermore, the results obtained from the electrical conductivity measurements and physiochemical analysis (Table 6), as well as the geomorphology of each site indicated that ions other than Na⁺, Cl⁻ and S²⁻ contributed to the mineral composition of the sampling sites. Since the principle component analysis (PCA) (not shown) analysis of the data presented in Table 6 and the physical properties indicated that the sampling sites were highly diverse, it was decided that they should be analysed separately as to highlight each sites unique microbial diversity.

3.2.2 Analysis of Metagenomic DNA extraction procedures

Studies have shown that both the quantity and quality of metagenomic DNA extracted from environmental samples is influenced by the chemical composition of the soil or sediment (Lipthay *et al.*, 2004) and that DNA extraction methodologies used should be adapted to suit the physiochemical properties of the soil, as well as the soil type (Martin-Laurent *et al.*, 2001; Robe *et al.*, 2003; Lipthay *et al.*, 2004). In the present study two direct DNA extraction methods were employed to extract metagenomic DNA from soil samples. The modified Zhou *et al.* (1996) method was used for the less saline Gobabeb samples (which were higher in CaCO_3^{2-}) and the UltraClean Soil DNA Extraction kit (MoBio laboratories, Inc.) was used on the Swakopmund samples due to its higher salinity (Table 6 and Figure 7).

While two different DNA extractions would introduce bias due to preferential lysis, and therefore representation, between Gram positive and negative bacteria, it was found that the Zhou method was better suited to extracting DNA from the Gobabeb samples even though it favoured the extraction of Gram negative bacteria. This is likely due to the Gobabeb samples containing more organic material, which was evident from the samples physical appearances (green and orange material) and therefore it is highly probable they contain more humic acids and/or polysaccharides. Since the Zhou kit has been shown in a previous investigation to be more effective in the removal of humic acids from terrestrial soils (Zhou *et al.*, 1996), it was found to be more suitable to extract DNA from the Gobabeb samples than the commercial kit. Also, while the commercial DNA extraction kit from MoBio (UltraClean DNA extraction) is reputed to lyse Gram positive and Gram negative bacteria equally it was found to be more suited to extract DNA from the extreme saline environment of Swakopmund since it incorporates more stringent lysis methods to extract DNA from salt embedded soils (chemical and mechanical) (Braid *et al.*, 1999).

3.2.3 DGGE analysis

The first part of the investigation was to obtain a microbial community profile for each of the individual sites (Gobabeb, Swakopmund site 1 and Swakopmund site 2) by means of DGGE analysis. Metagenomic DNA (section 3.2.2) was used in the first round PCR amplification with universal 16S rRNA gene bacterial primers E9F/U1510R (Table 2). This amplification yielded a PCR amplicon of approximately 1,5kb in size (Figure 8).

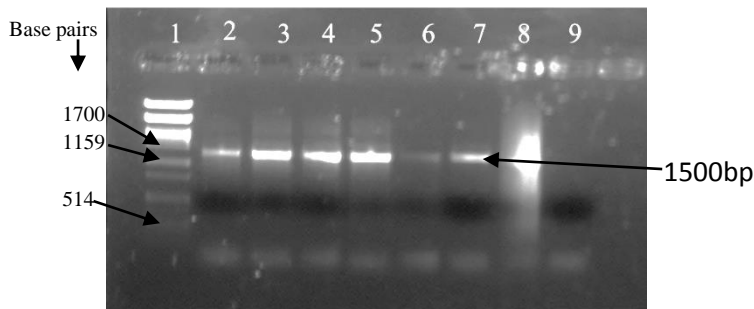


Figure 8: The amplified bacterial 16S rRNA gene fragments separated on a 1% agarose gel. Lane 1: $\lambda PstI$ marker, Lane 2-7 Gobabeb samples, Lane 8: positive control *E. coli* DNA, Lane 9: No template control.

The PCR amplicons obtained in the first PCR were used as the template in the second round of nested PCR using the nested GC clamp primers 341F-GC/534R (Table 2). The PCR fragments were separated on a 1% agarose gel and yielded fragments of the expected size of approximately 200bp. The fragments generated by nested PCR were separated on a 30-70 gradient DGGE gel and were analysed using GelCompar II (version5) software.

3.2.4 Statistical analysis of DGGE

3.2.4.1 Gobabeb site

The dendrogram (Figure 7) reveals the rich species diversity present within the Gobabeb salt pan. Samples GOB1, GOB2 and GOB3 were found to cluster, while both GOB4 and GOB5 did not. Based on the number of distinct bands obtained for the samples, 19 OTUs were present in GOB1, 17 for GOB2, 20 for GOB3, 18 for GOB4 and 16 for GOB5. The unique fingerprints of GOB4 and GOB5 were confirmed by cluster analysis, showing they shared 40% similarity with the other samples. The clustering patterns observed within the dendrogram were further differentiated by using the cophentic correlation. The cophentic correlation, like bootstrap analysis, measures the reproducibility of pairwise distances observed between clusters (Holmes, 2003). The correlation coefficient between GOB1, GOB2 and GOB3 was ≤ 98 which indicated that the observed clustering was highly confident. These samples were found to share 55% similarity between each other. Samples GOB4 and GOB5 were found to share a similarity of 40% with the GOB1, GOB2 and GOB3 cluster (Figure 9).

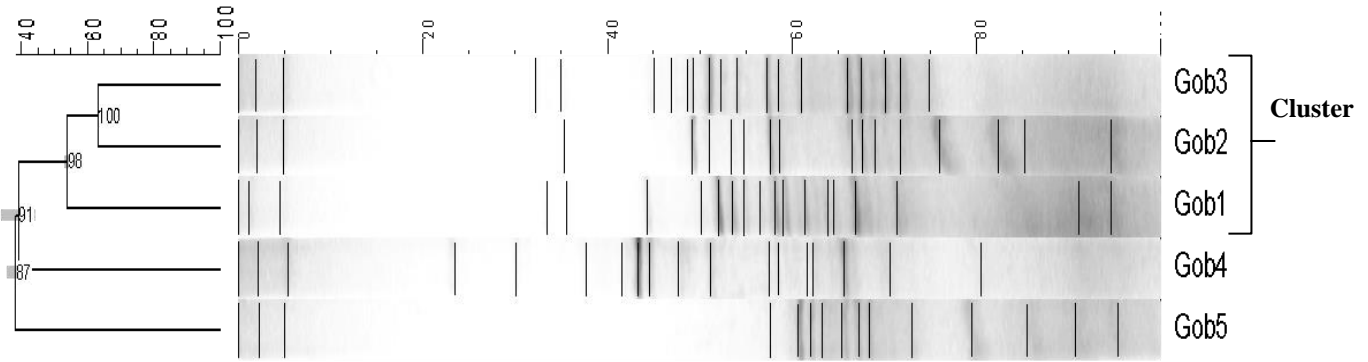


Figure 9: The similarity dendrogram constructed for Gobabeb site. The software GelCompar (version5) was used with the similarity matrix DICE coefficient and the UPGMA cluster method. The similarity ruler is represented above the diagram. Sample GOB1, 2 and 3 formed a cluster, while GOB4 and GOB5 were found to cluster separately.

The results obtained from the similarity dendrogram (Figure 9) were further supported by MDS analysis (Figure 10). As for the dendrogram, the plot indicated weak clustering of GOB1 with GOB2 and GOB3, while GOB4 and GOB5 clustered separately.

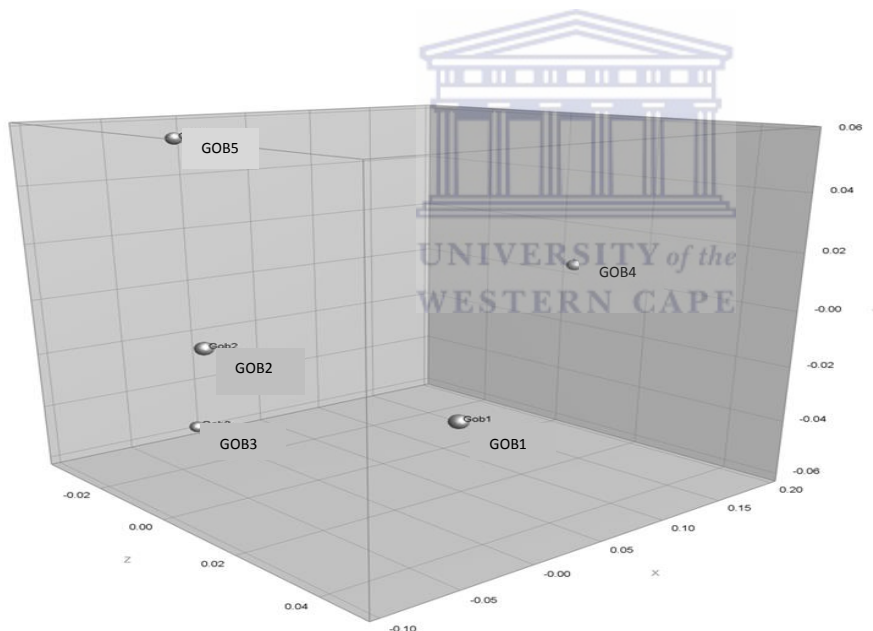


Figure 10: The MDS plot constructed from DGGE data for the five samples collected at the Gobabeb site from (GOB1-5) using GelCompar II (version5). The plot was constructed using the similarity matrix Pearson coefficient and the UPGMA cluster method. The MDS plot scale separates the samples at 0.02 intervals at the Z-axis and 0.05 intervals at both the X and Y-axis.

3.2.4.2 Swakopmund site 1

Due to their different physiochemical properties the two Swakopmund sites were analysed separately. From the similarity dendrogram (Figure 11) for Swakopmund site 1, it can be seen that samples Sps01C and Sp01D both contain 19 OTUs, while Sps01A contain the fewest OTUs (17), and sample Sps01B contained the most OTUs (24). Also, Sp01A and Sp01D

were found to cluster (60% similarity), while samples Sp01B and Sp01C clustered separately sharing less than 50% similarity (confidence interval of 87).

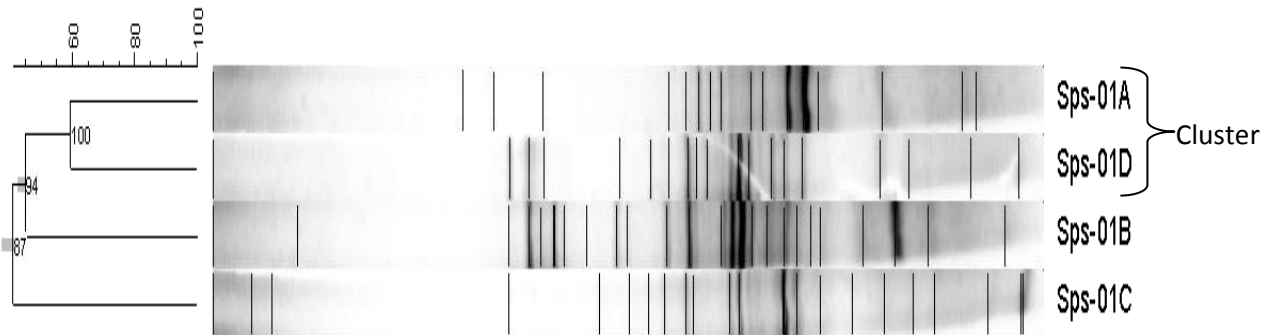


Figure 11: Similarity dendrogram constructed for Swakopmund site 1 samples. The software GelCompar II (version5) was used in combination with the similarity matrix DICE coefficient and the UPGMA cluster method. The dendrogram illustrates that Sp01A and Sp01D forms a cluster, whereas Sp01B and Sp01C do not cluster

The similarity dendrogram (Figure 11) clustering pattern was supported by the MDS analysis (Figure 12). Again Sp01A and Sp01D were found too cluster tightly together, while Sp01B and Sp01C did not cluster.

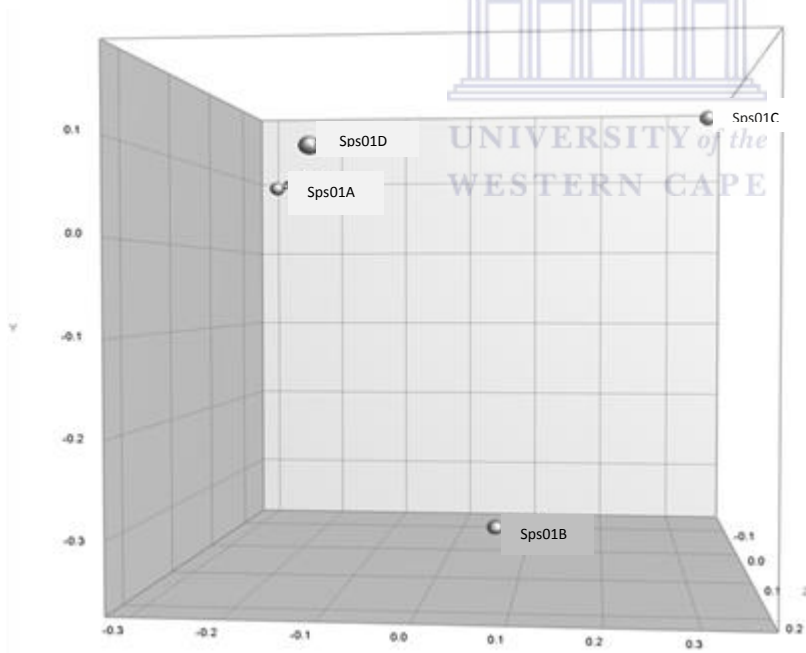


Figure 12: The MDS plot constructed from DGGE data for Swakopmund site 1 for the four samples (Sp01A-D) collected using GelCompar II (version5. Samples Sp01A and Sp01D cluster while Sp01C and Sp01B did not cluster. The MDS plot scale is scored at 0.1 intervals on all three axes (X, Y and Z)

3.2.4.3 Swakopmund site 2

The results obtained from the similarity dendrogram (Figure 13) illustrates that all the samples collected from Swakopmund site 2 were similar and clustered together at a 66% similarity. Furthermore, DGGE analysis indicated that all samples contained approximately the same number of OTUs (Sp02A=27 OTUs, Sp02B=26 OTUs, Sp02D=26 OTUs), except for sample Sp02C which only contained 19 OTUs. The fragments were electrophoresed over a 70-30 gel gradient and separated out over a narrow range with all samples sharing at least two common dominant bands. When bands are separated over such a narrow range more than one band could possible represent the same species. The cophentic coefficient illustrates that the relationships between the samples (Sp02A-Sp02D) were reproducible with a confidence value (bootstrap) of ≤ 90 .

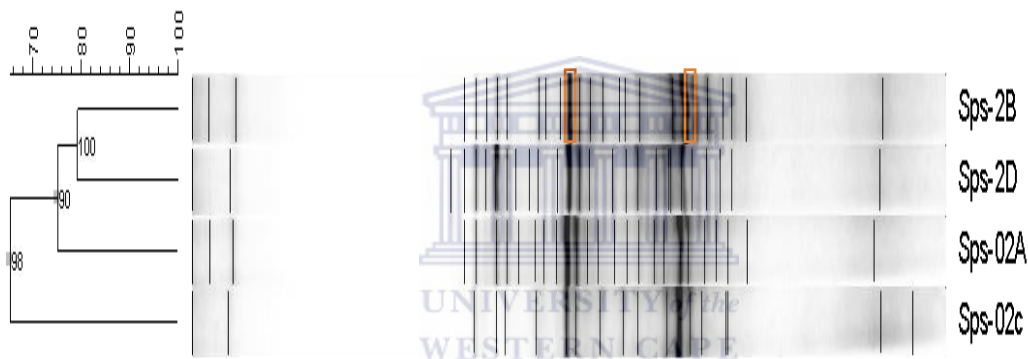


Figure 13: Similarity dendrogram constructed for Swakopmund site 2. The software GelComparII (version5) was used in combination with the similarity matrix DICE coefficient and the UPGMA cluster method in the analysis. The similarity dendrogram shows how samples Sp02B and Sp02D were cluster while Sp02A and Sp02C did not. The dominant band present in all samples is highlighted in orange.

The results obtained from the MDS plot (Figure 14) support the similarity dendrogram (Figure 13). The MDS plot confirmed that samples Sps02B and Sp02D cluster more closely, while Sp02A and Sp02C do not cluster.

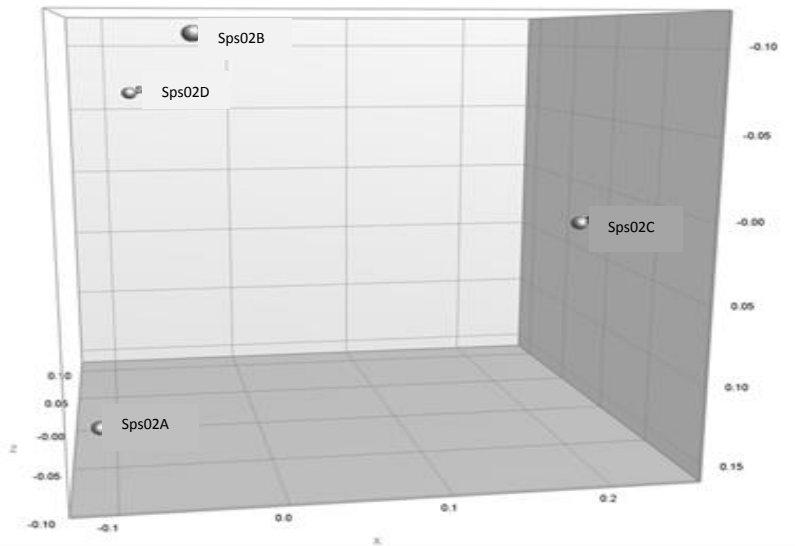


Figure 14: The MDS plot constructed from DGGE data for the four samples collected from Swakopmund site 2 using GelCompar II (version5). Samples Sp02B and Sp02D cluster, while Sp02A and Sp02C do not. The MDS plot scale separates the samples at 0.05 intervals at the Y-axis and 0.1 intervals at both the X and Z-axis.

3.2.5 T-RFLP analysis

Although both DGGE and T-RFLP analysis are PCR based and provide a genotypic fingerprint of the bacterial communities within environmental settings, T-RFLP analysis was employed since it uses an automated method in which a DNA sequencer generates an electropherogram to separate and assess different terminal fragment lengths compared to DGGE analysis which is a more laborious and less sensitive technique (Zhang *et al.*, 2004; Harmann *et al.*, 2005). For T-RFLP analysis all other samples from Gobabeb (GOB1-GOB5), Swakopmund site 1 (Sps01A and Sps01B) and Swakopmund site2 (Sps02A-D) yielded an amplicon of the expected size (1.5kb) and were digested singly with the enzymes *HpaII* and *HaeIII* (section 2.6.4). Based on the Peak Scanner results the two GC-recognising enzymes (*HpaII* and *HaeIII*) used generated a diverse range of OTU's and therefore it was deemed unnecessary to utilise more than two restriction enzymes for the analysis. As with DGGE analysis the T-RFLPs derived for the individual sampling sites were all analysed separately.

3.2.6 Comparison of OTUs obtained by restriction analysis for the different sampling sites

Figures 13-17 compare OTU diversity based on T-RFLP patterns at each sampling site. Restriction enzymes (*HpaII* and *HaeIII*) were utilised for this analysis. Also, T-RFs were binned based on the method outlined in section 2.6.4

3.2.6.1 Analysis of Gobabeb site OTUs

In Figure 15, it can be observed that the majority of the OTUs obtained for the five samples collected at Gobabeb site differ from one another. Eleven OTUs were obtained with *HaeIII*, and 16 OTUs with *HpaII*. The graph (Figure 15) shows that only one T-RF (77) was found to be common in all samples for *HpaII* and two T-RFs for *HaeIII* (76 and 120). The graph (Figure 13) also shows that sample GOB4 contained the highest number of unique OTUs, five (464, 483, 280, 322, 220) generated from both restriction enzymes respectively, compared to GOB1 (253 and 476) and GOB2 (455 and 590) which both had two unique OTUs generated from *HpaII*. GOB3 contained three unique OTUs (890, 401 and 515) generated with *HaeIII* and GOB5 had five unique OTUs (126, 136, 201, 211 and 499) generated from both restriction enzymes respectively. OTUs 76 and 77 were found to be the most frequently detected T-RFs at all sites. Due to the similar recognition sites (C[^]CGG and GG[^]CC) it is possible that T-RF 76 (generated with *HaeIII*) and T-RF 77 (generated with *HpaII*) represent the same out, and the same applies for T-RF 120 with each enzyme. Overall, the venn-diagram shows that of the 29 T-RFs generated from the two restriction enzymes collectively, only three T-RFs were found to be common in all five samples. The venn-diagram (Figure 16) further shows GOB1 and GOB4 to share two T-RFs, GOB3 and GOB2 share two T-RFs, and GOB3 and GOB1 share one T-RF.

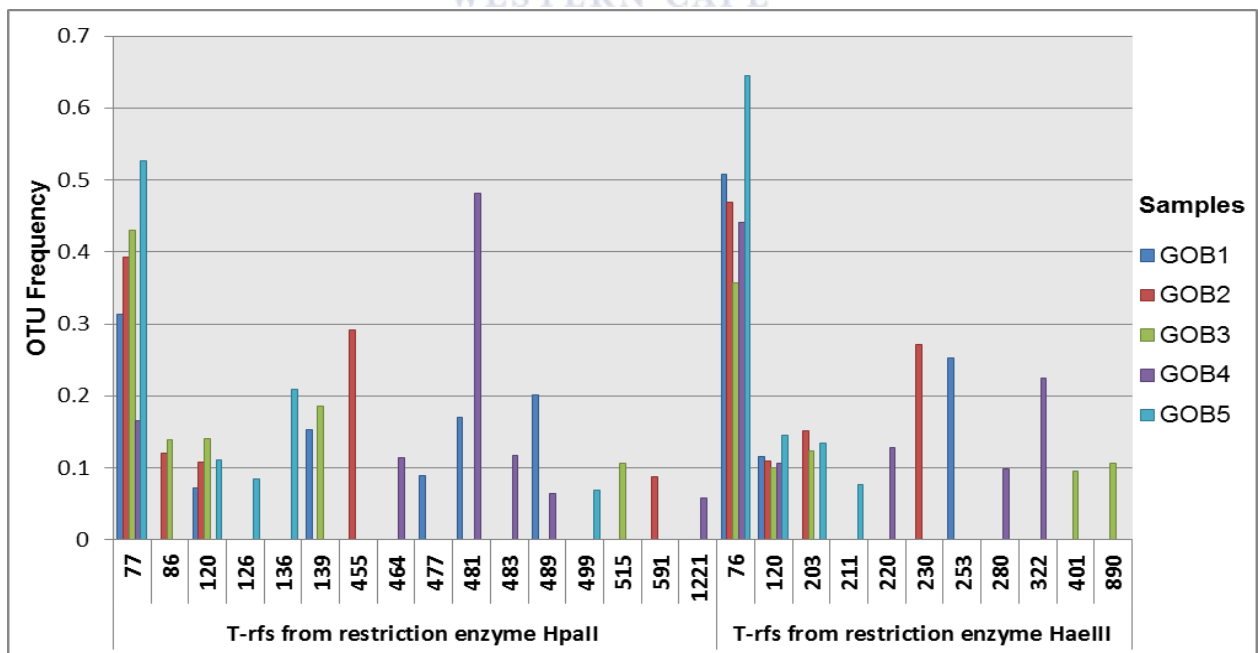


Figure 15: Distribution of OTUs within Gobabeb site. The graph represents the number of T-RFs generated from the restriction enzymes *HaeIII* and *HpaII* between the five samples (GOB1-GOB5). Three of the OTUs (76, 77, and 120) were found to be shared among the five samples.

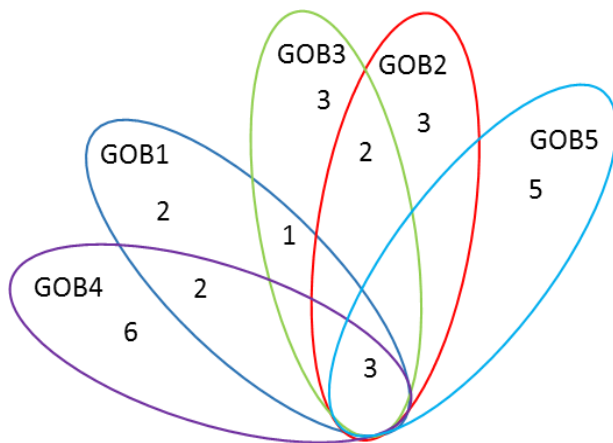


Figure 16: Venn-diagram illustrating the number of T-RFs shared between the samples obtained at Gobabeb site.

3.2.6.2 Analysis of Swakopmund site 1 OTUs

The microbial communities detected in Swakopmund site 1 Sps01A and Sps01B were found to differ. Four T-RFs (58, 77, 120 and 489) were obtained with *Hpa*II and four T-RFs (58, 76, 120, and 405) with *Hae*III (Figure 17). Two of the T-RFs (77 and 120) generated from *Hpa*II and two of the T-RFs (76 and 120) generated from *Hae*III were found to be common between the two samples. Also only Sps01B was found to contain three (58, 405, and 489) unique T-RFs while Sp01A did not contain any unique T-RFs. Also, T-RFs 58, 77, 76 and 120 prevalent in sample Sps01B was found to be common for both restriction enzyme digests. The venn-diagram (Figure 18) further shows that the two samples analysed for the site share four T-RFs. Overall, the OTUs generated at Swakopmund site 1, revealed the site to be diverse even though only two samples were successfully analysed. However, while an attempt has been made to analyse the data generated, the number of T-RFs obtained was unexpectedly low, considering the number of OTUs obtained through DGGE analysis (Figure 11). Given the relatively higher OTU frequency for some of the T-RFs observed (Figure 17), it is possible that these represent multiple species, and highlights one of the well-known limitations associated with the T-RFLP tool.

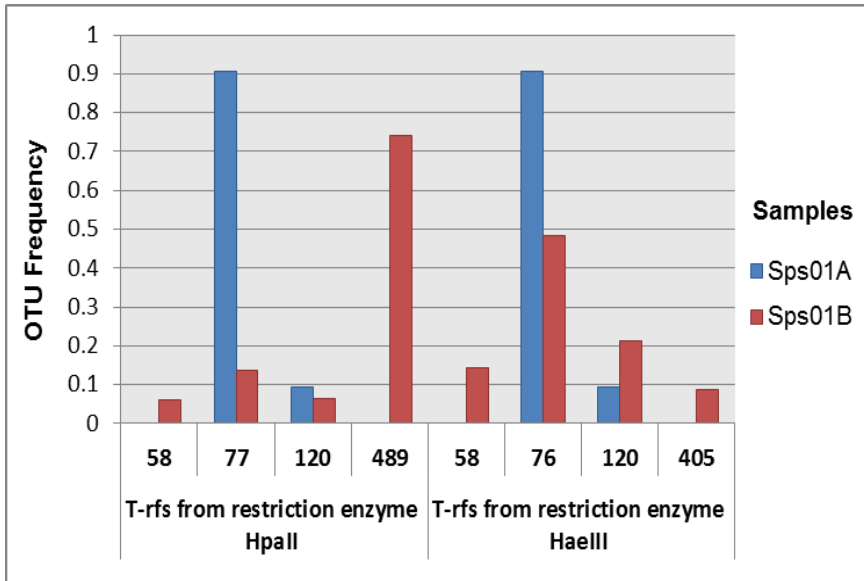


Figure 17: Distribution of OTUs within Swakopmund site 1. The graph represents the number of T-RFs obtained with restriction enzymes *HaeIII* and *HpaII* within Swakopmund site 1.

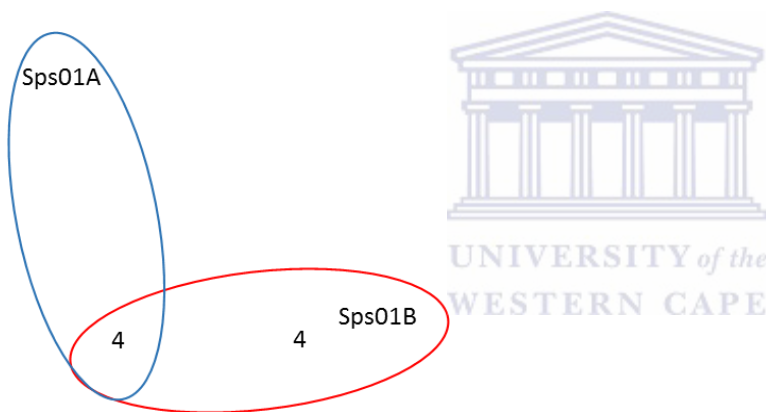


Figure 18: Venn-diagram illustrating the number of T-RFs shared between samples Sps01A and Sps01B obtained at Swakopmund site 1.

3.2.6.3 Swakopmund site 2 OTUs

The T-RF patterns obtained for the four samples at Swakopmund site 2 were found to be dissimilar. Six T-RFs were generated with *HaeIII* and nine T-RFs were generated with *HpaII* (Figure 19). As shown on the graph (Figure 19), T-RF 76 and 77 were present in all the samples; while T-RF 120 was detected in all the samples except for Sp02B. Similarly, T-RF 877 was found to be common in all the samples except for Sp02C. Sample Sp02D did not contain any unique OTUs, while the remaining samples contained between two and three unique T-RFs each. The venn-diagram (Figure 20) further shows that the samples only share three OTUs, while Sps02A and Sps02B share two T-RFs. Overall, the OTUs generated from

the two restriction enzymes indicated Swakopmund site 2 to be somewhat diverse, although the four samples collected at the site shared some common OTUs.

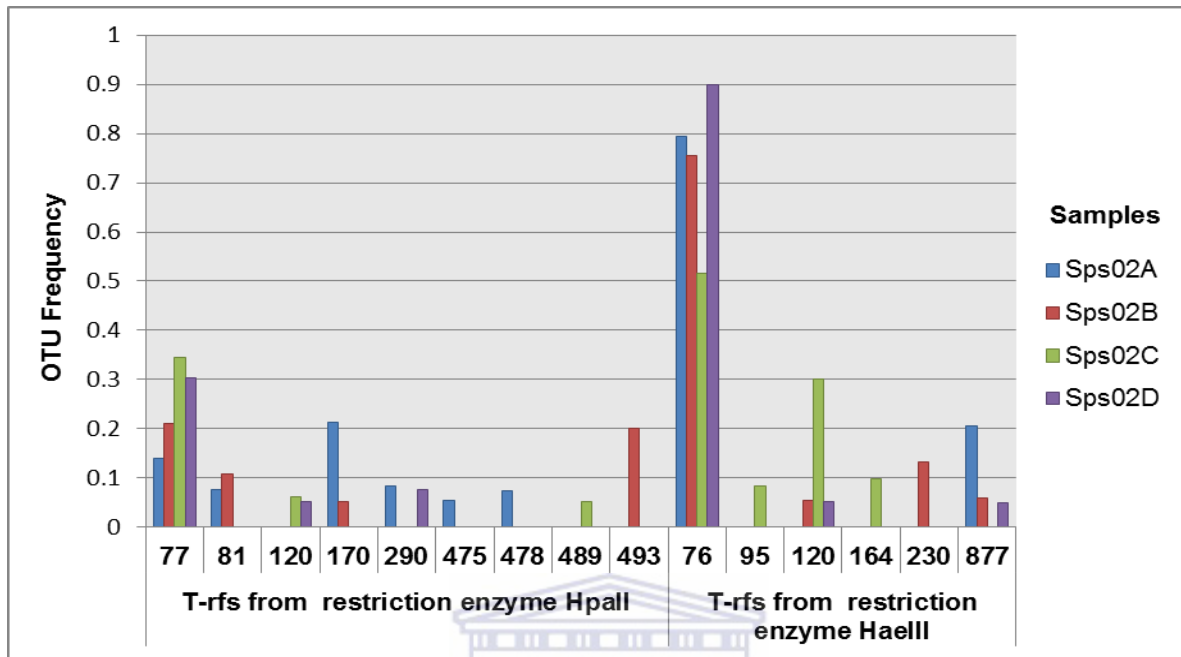


Figure 19: Distribution of OTUs within Swakopmund site 2. The restriction enzymes (*HaeIII* and *HpaII*) utilised generated 16 OTUs collectively. Only two of the T-RFs (76 and 77) were shared while the majority of the T-RFs were found to separately between the four samples, Sps02A-Sps02D obtained at this site.

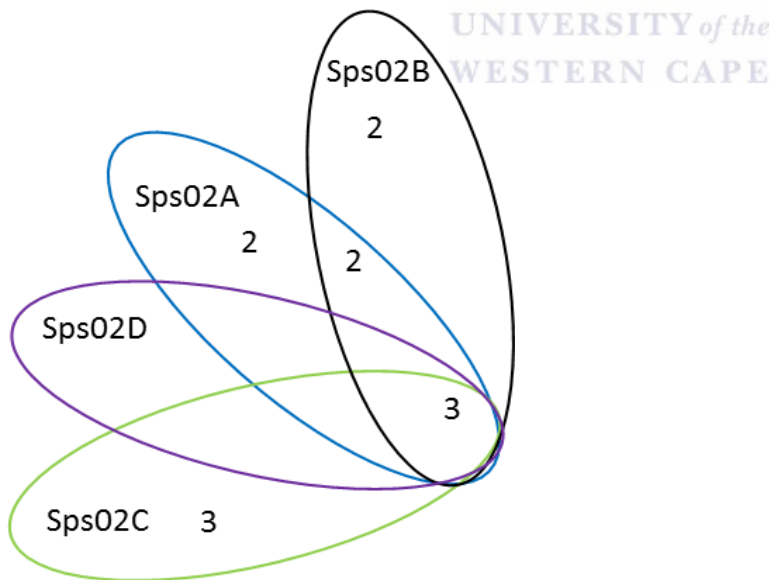


Figure 20: Venn-diagram illustrating the number of T-RFs shared between the samples obtained at Swakopmund site 2

3.2.7 Statistical analysis of T-RFs

The Bray-Curtis similarity index (also known as the Czekanowski's Quantitative Index) was used to evaluate intra-site variability between sites, since it provides a true measurement of

similarity to quantify dissimilarities between groups (Bloom, 1981). Also, the 2D (low dimensional space) stress value was used to determine the confidence interval between samples in high dimensional space. A stress value defines the confidence between sample relationships, with a smaller stress value (less than 0.20) being desired (Clarke and Gorley, 2006).

3.2.7.1 Gobabeb site OTUs

The MDS plot (Figure 21) generated by T-RFLP analysis for the Gobabeb sites indicated that samples GOB1, GOB2, GOB3 and GOB5, were found to cluster at 40% similarity, while GOB4 was found to cluster separately, sharing only 20% similarity with the other samples. Also, GOB1 and GOB5 were found to cluster less closely within the MDS plot sharing 40% similarity with GOB2 and GOB3, which cluster more closely. The MDS plot generated by T-RFLP analysis for the Gobabeb sites indicated that the similarity between the samples was low (Figure 21), even though they were collected within relatively close proximity. The 2D stress value generated for the Gobabeb site was 0, thus indicating a strong confidence relationship between the samples (Clarke and Gorley, 2006). From this, one could conclude that samples GOB2 and GOB3 share more similar bacterial communities than samples GOB1 and GOB5, and GOB4 to harbour several unique (relative) microbial taxa.

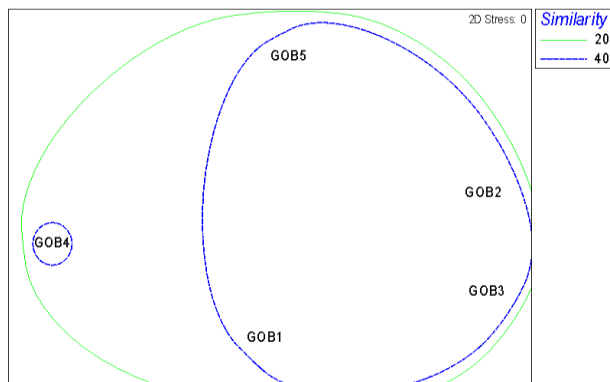


Figure 21: The MDS plot constructed from T-RFLP data for Gobabeb site. Samples GOB1-GOB3 and GOB5 cluster at 40% similarity while GOB4 clusters separately, sharing only 20% similarity with the other samples.

3.2.7.2 Swakopmund site 1 OTUs

Samples Sps01C and Sps01D were excluded from the study since the samples failed to amplify after several attempts to optimise the PCR and DNA extractions processes. The failed amplifications could be due to the presence of salt that was not efficiently eliminated in

the DNA extraction process. Even though only two samples (Sps01A and Sps01B) were analysed for this site, the samples were found to share half (four) of the eight T-RFs obtained at this site. This finding, of low similarity between samples, was also observed for the Gobabeb site.

3.2.7.3 Swakopmund site 2 OTUs

The MDS plot obtained for Swakopmund site 2 (Figure 22), indicated that all the samples cluster together at 40% similarity. The plot also showed that Sp02A and Sp02B were more similar, and cluster at 60% similarity. The same trend was observed for samples Sp02C and Sp02D. The 2D stress value obtained for the MDS plot was equal to zero, thus indicating a strong confidence interval between the samples. Also, samples Sps02A and Sps02B were found to cluster more closely (60% similarity) compared to samples Sps02C and Sps02D. While these samples (Sps02C and Sps02D) cluster less, they do share 60% similarity (Figure 22). The close clustering of samples Sps02C and Sps02D could be that they share more similar communities than sample Sps02A and Sps02B. To conclude, all four samples obtained at the Swakopmund site 2 were found to share 40% similarity.

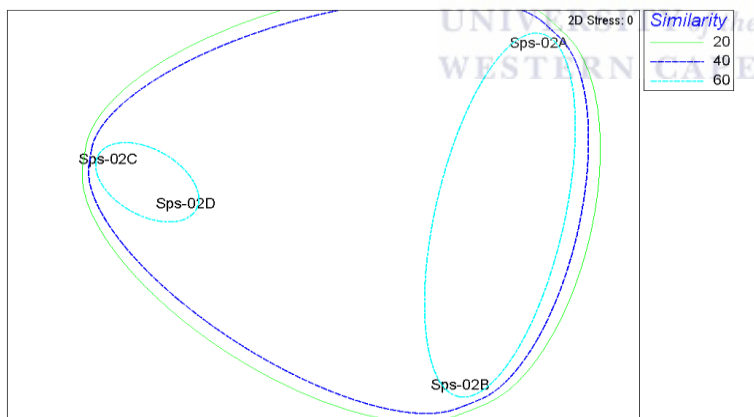


Figure 22: The MDS plot constructed from T-RFLP data for Swakopmund site 2. The samples clustered in two groups (Sps02A and Sps02B; Sps02C and Sps02D) at the 60% similarity level. All four samples obtained from this site share 40 similarity.

3.2.8 Construction of bacterial 16S rRNA gene clone libraries

3.2.8.1 Clone library construction

T-RFLP analysis was used to guide construction of the clone libraries (Table 7). In general, a similarity value of less than 40% obtained from T-RFLP cluster analysis was used as the cut-off for pooling samples for library construction. Since four (GOB1, 2, 3 and 5) of the five

Gobabeb samples clustered at 40% similarity (Figure 19) these samples were pooled. As GOB4 clustered separately at 20% similarity a separate library was constructed for this sample. Similarly, Swakopmund site 2 samples (Sps02A-D) were also pooled since samples were found to cluster at 40% similarity (Figure 20). As only two samples were analysed for Swakopmund site 1 (Sps01A and Sps01B) these were also pooled. Overall four 16S rRNA clone libraries (GOB, GOB4, Sps01 and Sps02) were constructed to represent the microbial communities present within their respective sites.

Table 7: Origins of the bacterial 16S rRNA gene clone libraries

Origin	Libraries	Pooled DNA
Gobabeb	Library 1	GOB1,GOB2, GOB3, GOB5
Gobabeb	Library 2	GOB4
Swakopmund site1	Library 3	Sps01A, Sps01B
Swakopmund site 2	Library 5	Sps02A-D

3.2.8.2 ARDRA analysis of clone libraries

Clone libraries were constructed and recombinant clones were screened with M13F/M13R primers (section 2.7.5.2). As several clones failed to re-amplify; only 81 clones each were screened from libraries Sps01A and Sps01B, 92 from GOB, 82 from GOB4 and 84 clones from library Sps02.

Clones containing the correct sized insert (1.5kb) were subjected to ARDRA analysis. As the enzyme *HpaII* yielded the most diverse OTU's in the T-RFLP analysis it was initially utilised for ARDRA. Figure 18 is a representation of 40 recombinant clones digested with *HpaII* for library GOB4. As ARDRA analysis with *HpaII* digestion identified a large number of OTU's in all five libraries examined (Figure 23) analysis with a second restriction enzyme was deemed unnecessary.

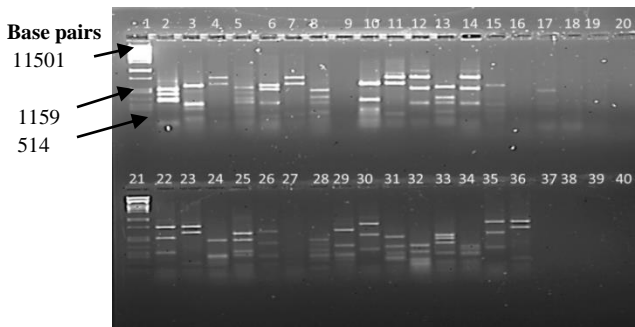


Figure 23: Restriction digests of amplicons of library 2 (GOB4) digested with enzyme *HpaII*. The amplicons were viewed on 2% agarose gel. Lane 1 and 21: ladder $\lambda PstI$, Lane: 2-20 and lane 22-36 digested amplicons

3.2.8.3 Analysis of 16S rRNA gene clone libraries

Several methods were used to analyse the species abundance of the samples including the non-parametric abundance-based richness estimators S_{Choa} and S_{ACE} . The richness estimators, S_{Choa} and S_{ACE} should be approximately equal when determining the phylotype abundance within a sampling site (Kemp and Aller, 2004). This is because the richness estimators take into consideration both the rare and abundant phylotypes present within a sample; and when the two are equal it shows that both the rare and abundant phylotypes within the sample have been detected. In addition, the results obtained from the richness estimators should be corroborated with the rarefaction curve reaching the asymptote. The rarefaction curve is represented by the Good Cs value which is a coverage estimate that compares the number of ribotypes observed to the number of sequences analysed (Choa *et al.*, 1993).

The results obtained from the predicated S_{ACE} and S_{Choa1} for library Sps02 were found to be equal (Table 8), thus indicating that the number of clones utilised were sufficient to characterise the bacterial diversity encompassing these sites. This result was supported by the rarefaction curve obtained from the Good C's value which had reached a stable asymptote (Figure 24).

For libraries Sps01, GOB4 and GOB both the richness estimators S_{choa1} and S_{ACE} were found not to be equal. The rarefaction curves created by the Good C's value had not yet reached a plateau which further supported this finding. Even though more than 80 clones were analysed for the libraries the richness estimators revealed that sampling sites of Gobabeb (GOB and GOB4) and Swakopmund site 1 (Sps01) had not been sufficiently sampled (Table 8 and Figure 24). Despite the low species diversity detected at GOB and Sps01 sites, as these

libraries were from pooled samples the finding that these libraries had not been sufficiently analysed is not unexpected.

Table 8: Summary of results obtained from library richness estimates: S_{Chao1} and S_{ACE}

Library	Nr of clones	Nr of phylotypes	Predicted S_{Chao1}	Predicted S_{ACE}
Sps01	81	29	190.62	204.47
Sps02	84	11	11.01	11.03
GOB4	82	34	56.16	74.27
GOB	92	50	370.37	191.72

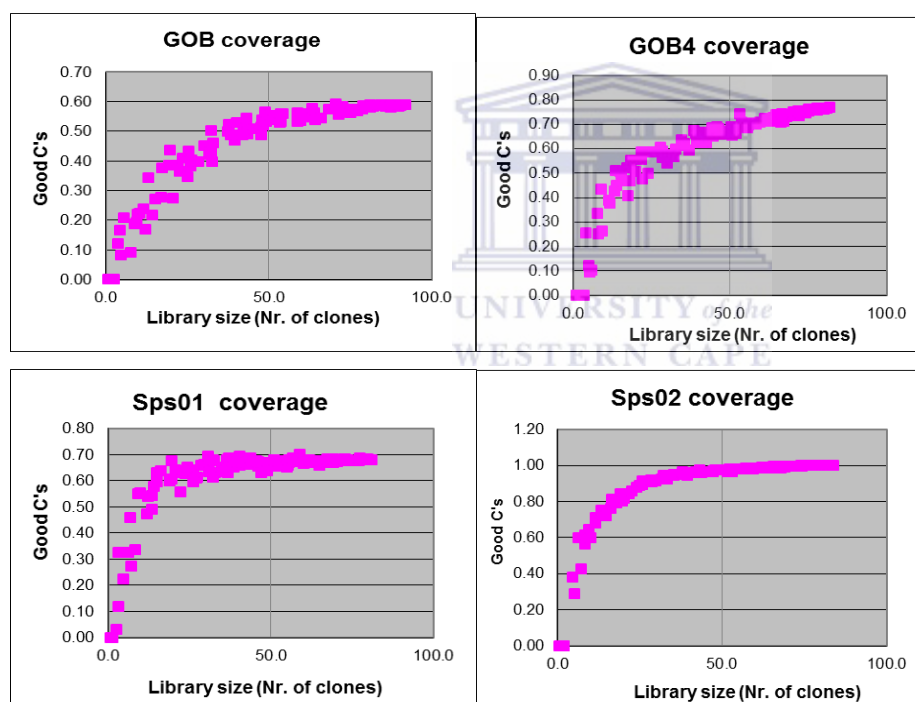


Figure 24: The coverage estimates obtained from both S_{Chao1} and S_{ACE} for libraries GOB, GOB4, Sps01 and Sps02

3.2.9 Sequence analysis of 16S rRNA gene clones

One hundred and forty clones were selected for sequencing based on their frequency (occurred more than twice) and uniqueness (only occurred once) in the generated ARDRA profiles. Phylogenetic analysis was performed (method outlined in section 2.7.5.3) for the sequenced clones. A chimera check was done and nine clones were subsequently removed from the analysis. A total of 131 clones were screened with an average sequence length of

approximately 600bp. A nucleotide BLAST search against GenBank database identified the closest phylogenetic neighbours of the clones (Appendix A). Furthermore, the sequences obtained were related to their nearest phylogenetic ancestors based on the RDP database (Appendix E) in a histogram (Figure 25). To further identify the presence of novel phylotypes in libraries, a cut off value of 94% sequence homology to RDP database assignments was used. This threshold was adopted because DNA-DNA hybridisation studies have shown that 94% homology can be used to distinguish strains at the genus level even if they share more than 70% DNA-DNA homology (Stackebrandt and Goebel, 1994; Konstantinidis and Tiedje, 2005). To construct the phylogenetic trees, clone sequences were grouped and analysed based on the method outline in section 2.7.5.3. Finally, T-RFs were assigned phylogenetic identifications based on their affiliation with the clone libraries.

3.2.9.1 Phylogenetic analysis of Gobabeb site

Of the 131 clones sequenced 63 of the sequences came from the Gobabeb sites (GOB+GOB4). The 63 sequences were grouped into 47 clusters based on their sequence homology in the clustering program CD-HIT Suite (Appendix A). Thirteen of the sequences (GOB43, GOB103, GOB26, GOB46, GOB111, GOB108, GOB39, GOB17, GOB134, GOB4-101, GOB4-60, GOB4-127, and GOB4-46) were found to share less than 95% homology to uncultured sequences in GenBank (Appendix B). At least four phylotypes identified from Gobabeb library were found to share more than 98% homology to sequences in GenBank at the genus level. These sequences affiliated to halophilic organisms such as *Microscilla sericea* (AB078081.1, cluster 2), *Marvivirga tractuosa* (NR 0409181), *Leptolyngbya* sp. (JF 703676.1) and *Spingomonas* sp. (AY749436.1) (Appendix A).

Furthermore, the histogram constructed (Figure 25) further illustrated the distribution of at least eight different phylotypic groups, *Nitrospira*, Planctomyces, Verrucomicrobia, Bacteroidetes, Firmicutes, Cyanobacteria, Alpha- and Gammaproteobacteria) obtained at the Gobabeb site. The Bacteroidetes were found to be the most dominant (30%) in both libraries (GOB and GOB4). Of the remaining seven phylotypes isolated from Gobabeb site, the Firmicutes (10%) and Alphaproteobacteria (13.3%) were only isolated from library GOB4. Similarly, *Nitrospira* (2.3%) and Cyanobacteria (2.3%) were only detected in library GOB. but at a relatively low abundance. The number of unclassified bacteria obtained, were similar

for both libraries (22.7% and 20%). Based on this finding there is a strong probability that these represent novel bacterial species.

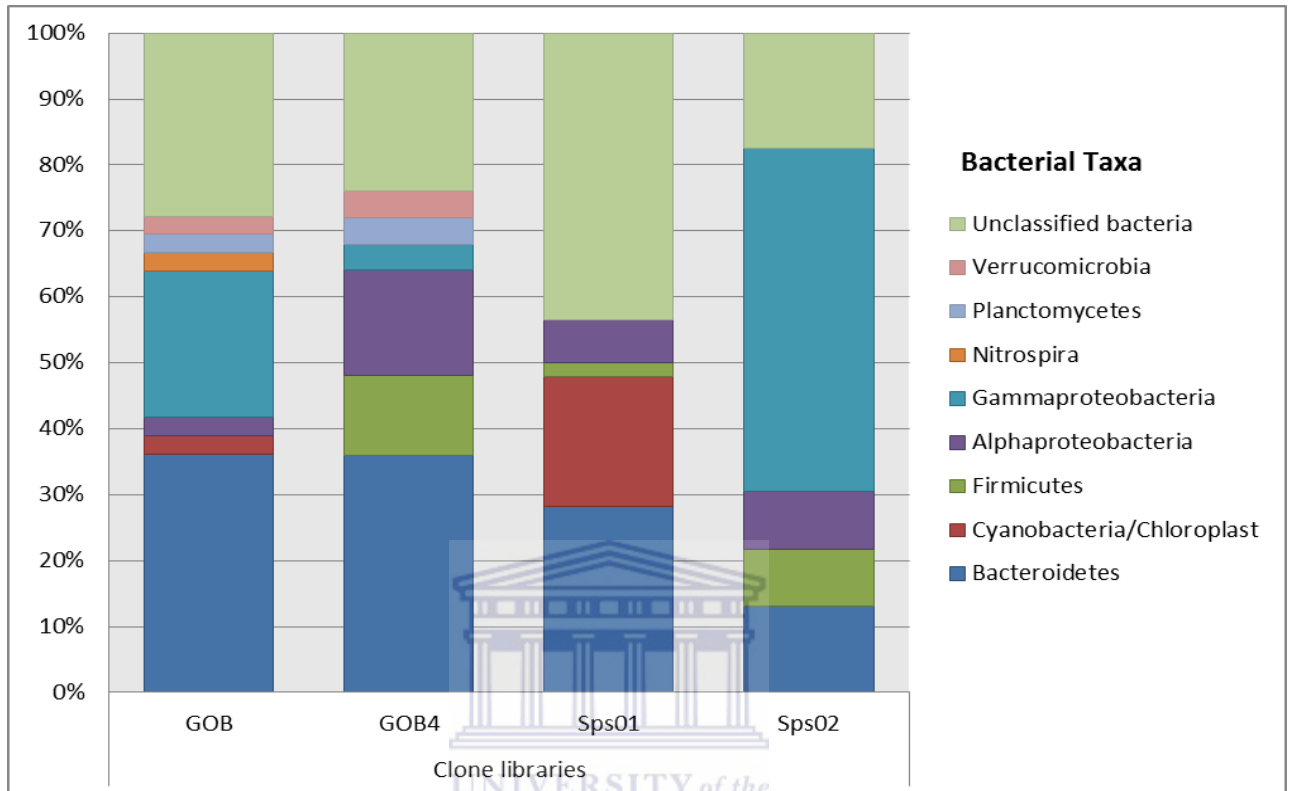


Figure 25: Histogram representing the different phylotypes identified from the clone libraries GOB, GOB4, Sps01A, Sps01B and Sps02. The clones were assigned phylogenetic affiliation based on the RDP database.

The three phylogenetic trees created for the bacteria identified in the Gobabeb samples (Figure 24-26) further indicated the clustering of these sequences within their respective clades. Because of the diverse range of sequences included in each phylogenetic tree, outgroups could not be included. The phylogenetic trees were categorised into their respective phylogenetic communities based on their associations in Classifier (RDP). From the phylogenetic tree (Figure 26) the sequences affiliating to the Proteobacteria clades (Gamma- and Alphaproteobacteria) were found to cluster. Similarly, sequences affiliating within the phylum Bacteroidetes (e.g. *Microscilla sericea* and *Flexibacteraceae* bacterium) (Figure 27), Verrucomicrobia, Firmicutes and Cyanobacteria were also found to cluster within their respective clades (Figure 28). The sequences affiliating to *Nitrospira* were removed from the phylogenetic trees since they did not cluster. Furthermore, the unclassified bacteria were found to form weak affiliations (bootstrap value less than 50) with their

assigned phylogenetic ancestor. Although, these weak affiliations is not unexpected since the unclassified bacteria could represent novel bacterial strains.

The sequences obtained from the Gobabeb clone libraries (GOB and GOB4) were further used to assign phylogenetic identities to the T-RFs obtained from T-RFLP analysis (Figure 15). The results obtained from *in silico* analysis showed that six of the T-RFs (76, 86, 120, 121, 126, 464) generated by restriction enzyme *HpaII* and five T-RFs (76, 202, 203, 230, 280) from *HaeIII* were found to be affiliated with sequences from 16S rRNA clone libraries. Also, T-RF 120 (common in both restriction enzymes) was found to be affiliated with three sequence clusters (3, 8, and 39) (Appendix B). These sequences were affiliated to uncultured bacteria (HQ9166101.1, JN418887.1 and AB247829.1) identified in terrestrial or saline environments. Several T-RFs obtained from the two different restriction enzymes were found to be affiliated to the same sequences. For example T-RF 203 (*HaeIII*) and T-RF 464 (*HpaII*) were affiliated with uncultured bacterium (FJ973579.1), while T-RF 76 and T-RF 126 were affiliated to an uncultured organism (JN436310.1).

To conclude, the distribution of phylotypes detected in the two libraries constructed for Gobabeb site indicate the presence of a diverse group of bacteria present at the site, dominated by halophilic bacteria. Also, the presence of the large number of unclassified bacteria detected at the site could be a representative of novel phyla that are prevalent within the Gobabeb site.

3.2.9.2 Phylogenetic analysis of Swakopmund site 1

The 47 sequences analysed for Swakopmund site 1 were clustered into 21 clusters with the CD-HIT program (Appendix B). Of the 21 sequence clusters, six of the clusters (1, 2, 12, 14, 18, and 21) were found to share less than 95% sequence identity to sequences in GenBank. Even though the majority of the sequences were found to be most related to uncultured bacteria, two of the clusters (7 and 16) were found to affiliate to *Sphingobacteriaceae* (DQ490464.1) and *Caulobacter* sp. (KC160785.1) (Appendix B). Also, most clones obtained in Swakopmund site 1 were similar to microbes originally isolated or detected (metagenomic studies) in soil and sediment samples obtained from marine habitats.

The histogram (Figure 25) constructed identified four phylogenetic groups (Alphaproteobacteria, Firmicutes, Cyanobacteria and Bacteroidetes) isolated at Swakopmund site 1. Unlike for the Gobabeb site, the majority of the phyla isolated at Swakopmund site 1 affiliated to unclassified bacteria (43%), thus indicating a high possibility of finding novel phylotypes at this site. Phylogenetic analysis revealed that phylotypes affiliated to Proteobacteria all clustered except for sample Sps01-81 (related to a *Caulobacter* species) which were found to cluster with Sps01-74, an uncultured Cyanobacterium. (Figure 29). Also, all of the members of *Rhodothermaceae* family were found to cluster. Like Gobabeb, the unclassified bacteria were found to form weak affiliations (bootstrap value less than 50) with their assigned phylogenetic ancestor.

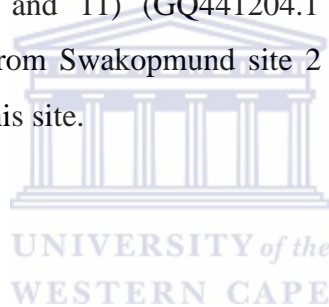
The sequences obtained from the Swakopmund site 1 clone libraries were further used to assign phylogenetic identities to the T-RFs obtained from T-RFLP analysis (Figure 17). The results obtained from *in silico* analysis showed that only two (120 and 489) of the ten T-RFs obtained with restriction enzymes *HpaII* and *HaeIII* was found to affiliate with sequences from 16S rRNA clone libraries. Of the shared T-RFs (obtained from both restriction enzymes), T-RF 120 was found to affiliate to cluster 2, (uncultured bacteria, EU869403.1) from a marine environment, while T-RF 489 affiliated to two different clusters (4 and 5). Both clusters (4 and 5) were found to affiliate to uncultured bacteria (AB533936.1 and AB533966.1) and originated from the same terrestrial environment of California (Appendix B). The overall phylogenetic analysis obtained from Swakopmund site 1 indicated a small halophilic bacterial community colonising this site, with the majority of the phylotypes being mostly closely related to unclassified taxa.

3.2.9.3 Phylogenetic analysis of Swakopmund site 2

The 25 sequences obtained for Swakopmund sites 2 were found to cluster into 12 groups (Appendix C) based on the CD-HIT clustering program. All of the sequences analysed were found to share more than 94% similarity to sequences within GenBank that were isolated in both terrestrial and marine environments. Even though the majority of the sequences affiliated to uncultured bacteria, two of the sequence clusters (1 and 5) were found to group with a known phylogenetic ancestor, *Idomarina* species (EF409427.1 and FJ404759.1). Also, the histogram (Figure 25) constructed identified four phylogenetic groups (Firmicutes, Bacteroidetes, Alpha- and Gammaproteobacteria) at Swakopmund site 2. Unlike Gobabeb and Swakopmund site 1, the majority of the phyla isolated at this site affiliated to

Gammaproteobacteria (52%), clustering in one phylogenetic tree (Figure 30). Phylotypes affiliating to Gammaproteobacteria were all found to cluster except for sample Sps02-68 (*Idomarina* sp.) which clustered with Sps02-11, a Firmicute (*Closteridaeeceae* bacterium).

The sequences obtained from the Swakopmund site 2 clone libraries (Appendix C) were further used to assign phylogenetic identities to the T-RFs obtained from T-RFLP analysis (Figure 19). The results obtained from *in silico* analysis showed that only three (81, 120 and 170) T-RFs obtained from restriction enzymes (*HpaII* and *HaeIII*) were found to affiliate with sequences from the 16S rRNA clone libraries. The shared T-RF (120) obtained from both restriction enzymes was found to affiliate to two sequence clusters (1 and 7). Sequence cluster 1 affiliated to *Idomarina* sp (EF409427.1), while sequence cluster 7 affiliated to uncultured bacteria (GQ441204.1). Both isolates obtained from cluster 1 and 7 originated from a marine environment. Also, T-RF 81 and T-RF 170 were found to affiliate to uncultured bacteria (Cluster 6 and 11) (GQ441204.1 and EU245110.1). The overall phylogenetic analysis obtained from Swakopmund site 2 indicated a specialised halophilic bacterial community inhabiting this site.



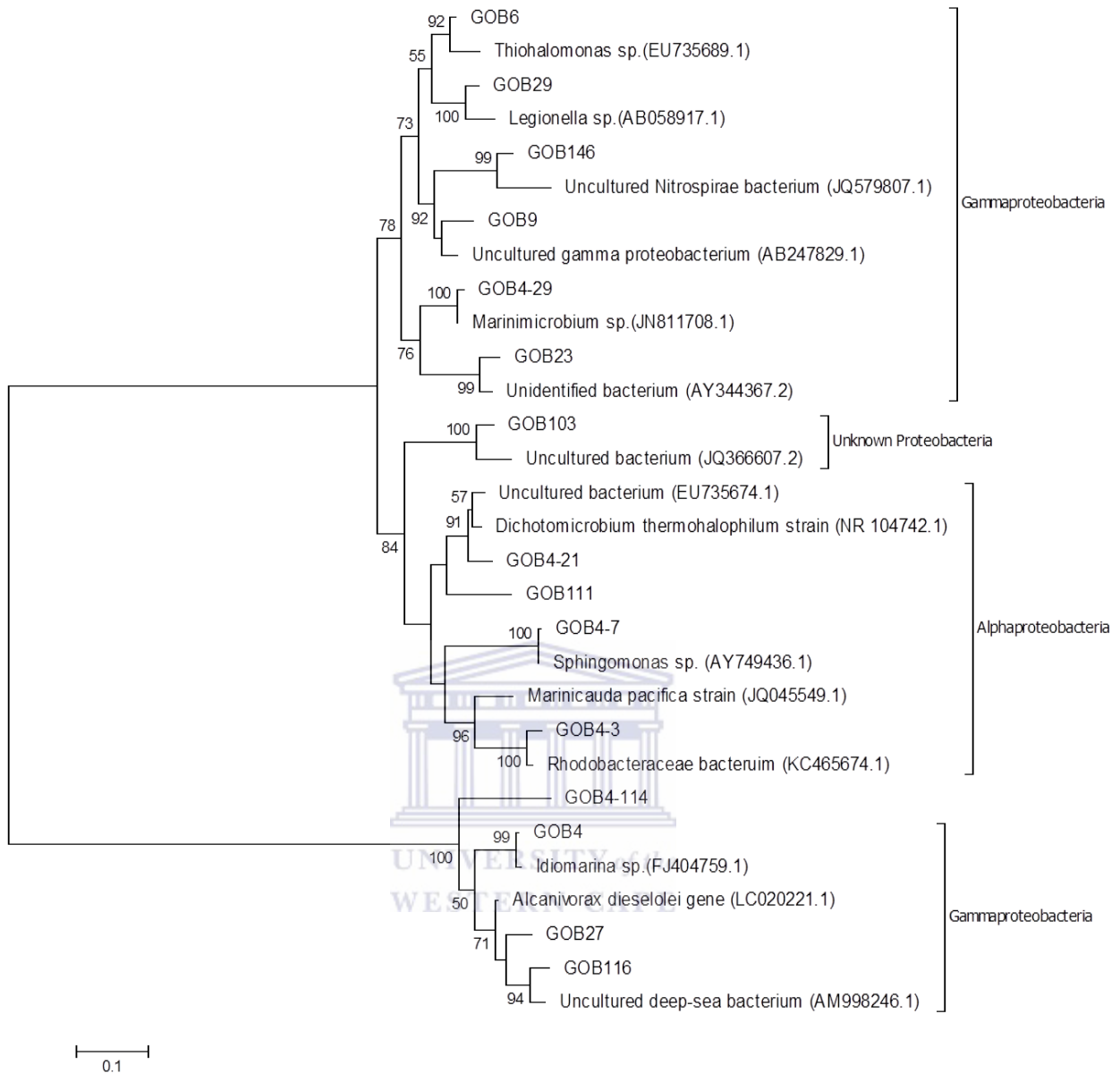


Figure 26: Phylogenetic tree of 16S rRNA gene sequences that affiliated to Proteobacteria. One sequence per cluster was used in constructing the phylogenetic tree with the Mega 6 software. The evolutionary relationship between taxa was assessed using the maximum likelihood method and the Kimura 2-parameter model. A 1000 replicates were inferred based on the bootstrap consensus to analyse the evolutionary relationship between taxa. The sequences of Proteobacteria were clustered into their respective classes: Alphaproteobacteria and Gammaproteobacteria. Bootstrap values less than 50 were excluded from the tree.

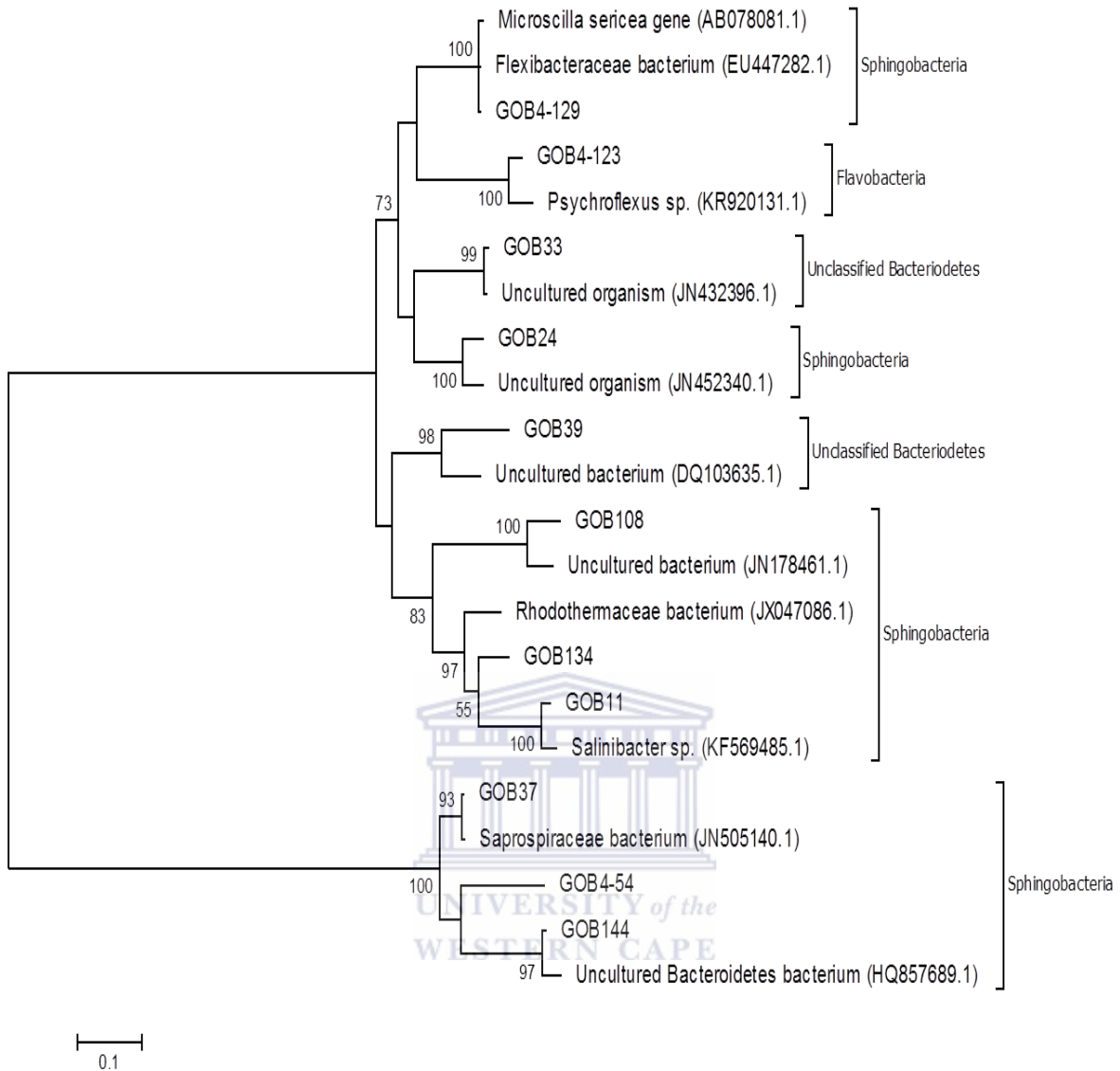


Figure 27: Phylogenetic trees of 16S rRNA gene sequences that affiliated to Bacteroidetes. One sequence per cluster was used in constructing the phylogenetic tree with the Mega 6 software. The evolutionary relationship between taxa was assessed using the maximum likelihood method and the Kimura 2-parameter model (Kimura, 1980). A 1000 replicates were inferred based on the bootstrap consensus to analyse the evolutionary relationship between taxa.

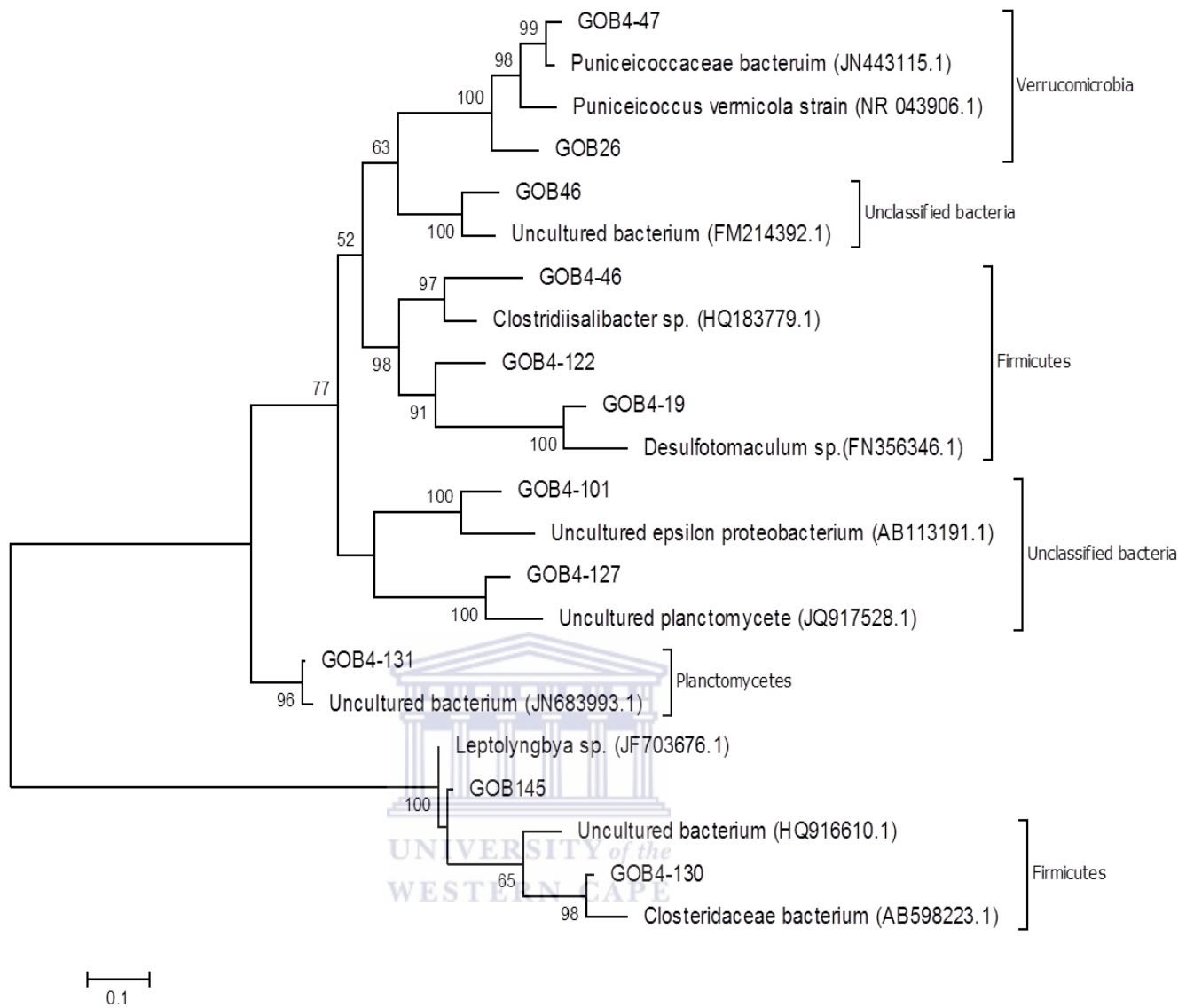


Figure 28: Phylogenetic trees of 16S rRNA gene sequences that affiliated to the minority groups: Firmicutes, Verrucomicrobia, Planctomycetes, *Nitrospira* and Cyanobacteria. One sequence per cluster was used in constructing the phylogenetic tree with the Mega 6 software. The evolutionary relationship between taxa was assessed using the maximum likelihood method and the Kimura 2-parameter model (Kimura, 1980). A 1000 replicates were inferred based on the bootstrap consensus to analyse the evolutionary relationship between taxa.

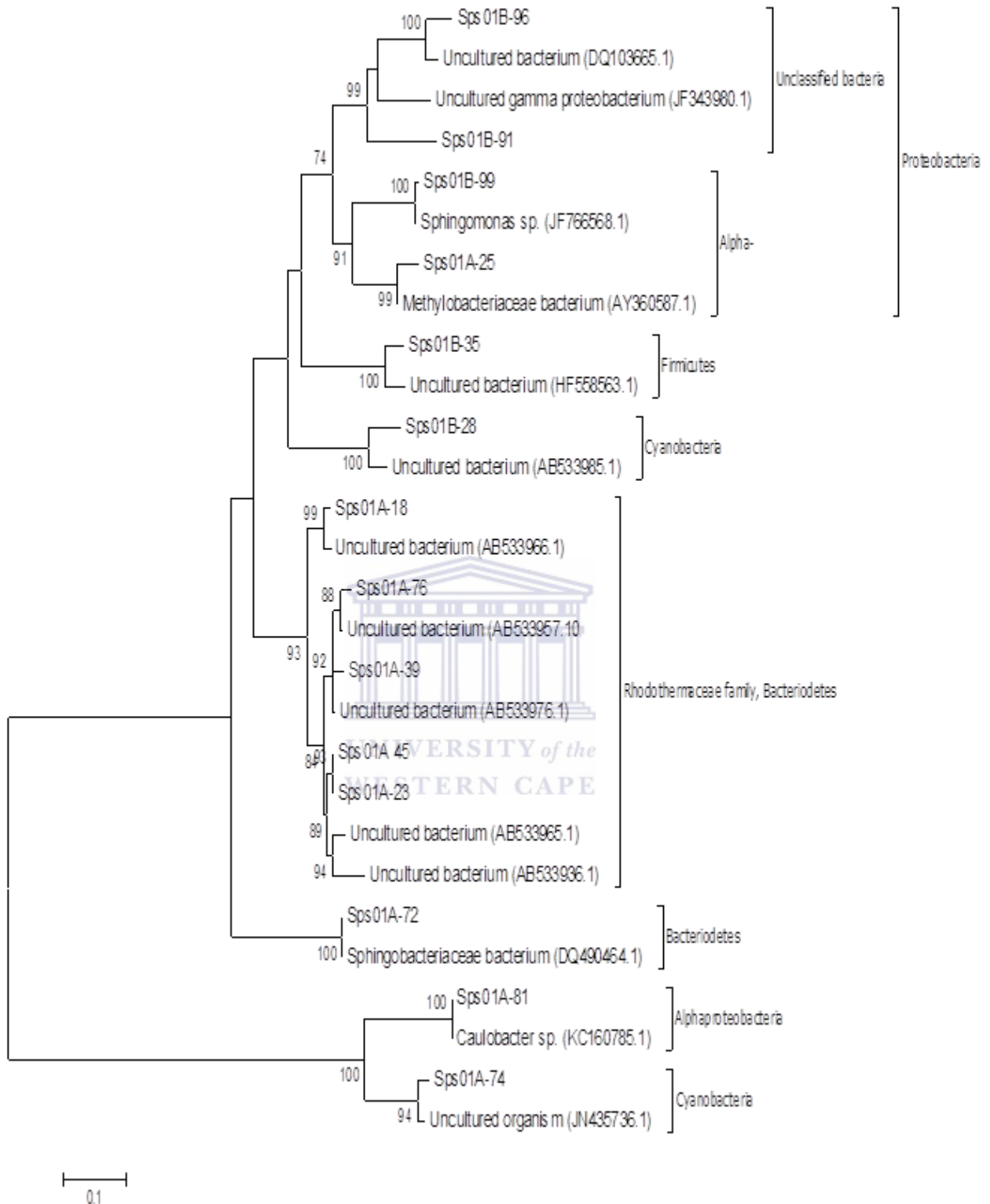


Figure 29: Phylogenetic tree of 16S rRNA gene sequences that were isolated at Swakopmund site 1. One sequence per cluster was used in constructing the phylogenetic tree with the Mega 6 software. The evolutionary relationship between taxa was assessed using the maximum likelihood method and the Kimura 2-parameter model. A 1000 replicates were inferred based on the bootstrap consensus to analyse the evolutionary relationship between taxa. The sequences were clustered into their respective phyla of *Proteobacteria* (Alphaproteobacteria), Bacteroidetes, Cyanobacteria, Firmicutes and unclassified bacteria. Bootstrap values less than 50 were excluded from the tree.

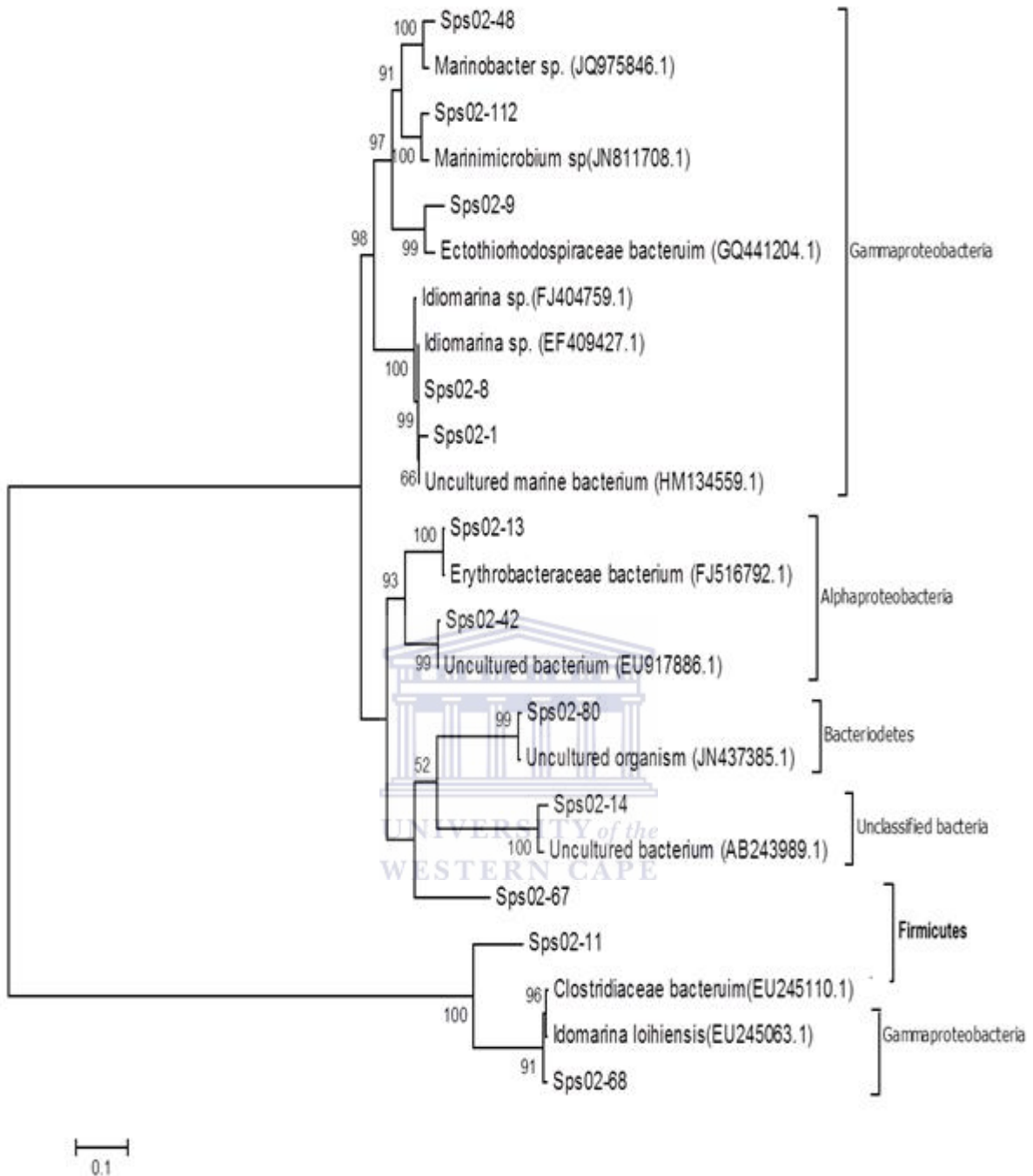


Figure 30: Phylogenetic tree of 16S rRNA gene sequences that were isolated at Swakopmund site 2. One sequence per cluster was used in constructing the phylogenetic tree with the Mega 6 software. The evolutionary relationship between taxa was assessed using the maximum likelihood method and the Kimura 2-parameter model. A 1000 replicates were inferred based on the bootstrap consensus to analyse the evolutionary relationship between taxa. The sequences were clustered into their respective phyla of *Proteobacteria* (Alphaproteobacteria), Bacteroidetes, Cyanobacteria, Firmicutes and unclassified bacteria. Bootstrap values less than 50 were excluded from the tree.

3.3 Summary of bacterial diversity findings

The molecular methods (DGGE, T-RFLP and 16S rRNA gene clone library analysis) used in this study to analyse bacterial diversity of the saline habitats of Gobabeb and Swakopmund revealed that unique and diverse bacterial communities were present. In general, the findings from the three methods employed did agree.

It should be noted, that as only a few samples were analysed for each sampling site, the program GelComparII automatically adjusted the MDS plot's scale to represent the samples evenly in three dimensional space by using a smaller scale (0.1 to 0.05). Therefore, while the samples may appear to cluster relatively far apart this is a reflection of the scale used to construct the plots. Despite two different DNA extraction methodologies being utilised to assess the diversity within the sites, two OTUs (76 and 119) were found to be common among the sites. Also, the two GC-recognising enzymes (*HpaII* and *HaeIII*) utilised for T-RFLP analysis were found to generate the same OTUs for different sequences even though it was found to give a diverse number of OTUs based on Peak scanner results. This result is not surprising since Stomeo *et al* (2013) also used the same two GC rich enzymes and found that it gave the same OTUs for both enzymes. One of the limitations of T-RFLP analysis is that one individual peak produced by T-RFLP analysis can correspond to a number of phylogenetic species; or one microbial population could also be represented by more than one terminal fragment (Marsh, 2005; Svhatte *et al*, 2008). Due to these shortcomings of T-RFLP analysis the data analysis of terminal fragments such as the binning of the peaks are important factors in analysing the T-RFLP data.

Ultimately the study is in agreement with other studies showing that the diversity pattern between sites with different chemical compositions differs (Hackl *et al.*, 2004; Canfora *et al.*, 2014).

3.3.1 Summary of the Gobabeb microbial diversity

Both the fingerprinting techniques (DGGE and T-RFLP) used to analyse the microbial diversity at the Gobabeb sites indicated that the distribution of microbial taxa differed between samples collected. Firstly, the similarity dendrogram (Figure 9) generated for the Gobabeb site indicated that the majority of the samples (GOB1, GOB2 and GOB3) shared at least 55% similarity in microbial communities, while GOB4 and GOB5 shared 40% similarity. This result correlated with T-RFLP clustering analysis (Figure 21) indicating again

that the majority of the samples shared at least 40% common microbial communities, while GOB4 shared only 20% similarity. From the two restriction enzymes used to assess microbial diversity within the Gobabeb site, 27 collective OTUs were detected within the Gobabeb site of which two OTUs (76 and 120) were found to be common to all samples (Figure 15). In addition, sample GOB4 was found to contain the majority of the unique OTUs (five), and based on MDS analysis was distinctly different for the other samples at this site. The OTUs were compared to phylotypes obtained from clone libraries (GOB and GOB4) in which the two T-RFs common to all samples (T-RF 120 and 76) were found to be related to different uncultured phylotypes. The phylogenetic analysis of Gobabeb samples also corroborated the fingerprinting (T-RFLP) results showing that Alphaproteobacteria and Firmicutes were only isolated from library GOB4, while *Nitrospira* and Cyanobacteria were only isolated in the GOB library. The Gobabeb site was found to be moderately saline (103mS/cm) with the physical properties (Figure 7) of the samples potentially indicating the presence of carotenoids (orange material) and cyanobacteria (green material) in the soil samples, which was confirmed by 16S rRNA gene clone libraries analysis which detected Cyanobacteria (*Leptolyngbya* sp). Several moderate halophilic organisms such as *Microscilla sericea*, *Marivirga tractuosa* and *Spingomonas* species were identified at the Gobabeb site. The orange material found in samples (GOB2 and GOB4) is likely due to the formation of carotenoids which acts as a protection barrier for moderate halophiles during the photo-oxidation process (Ventosa *et al.*, 1998). These organisms are linked to the production of the orange pigmentations which have been affiliated to phyla of Gammaproteobacteria (detected only in GOB library), Firmicutes (isolated only from library GOB4), and Flavobacteria (isolated in both libraries). In conclusion the bacterial diversity obtained at the Gobabeb site agreed with other studies showing bacterial diversity at moderate saline sites to be diverse and comprised of both specialised and terrestrial phyla (Ghai *et al.*, 2011; Meliani *et al.*, 2012).

3.3.2 Summary of the Swakopmund site 1 microbial diversity

For Swakopmund site 1, DGGE analysis was found also to concur with T-RFLP analysis showing that the microbial communities did not cluster. Unfortunately, due to difficulties with PCR amplification only two samples, Sps01A and Sps01B were analysed by T-RFLP. Clustering analysis obtained by T-RFLP indicated that the two samples analysed shared four T-RFs. Also, only two of the T-RFs (120, 489) were found to be most closely related to uncultured sequences (EU869403.1, AB533936.1 and AB533966.1) through clone library

analysis. Interestingly, these three sequences obtained were found to be either from a hypersaline environment or a terrestrial environment. This is not surprising since the collected samples contained both water and soil in which terrestrial organism could have easily been mixed with the extreme organisms due to environmental factors such as wind or water currents. Phylogenetic analysis of the Swakopmund site 1 further indicated that the site was dominated by six phyla of which the majority (43%) were related to unclassified bacteria (Figure 25). The phylogenetic analysis further indicated the presence of extreme halophiles such as *Spingobacteriaceae*, *Caulobacter* species and members of the *Rhodothermaceae* family being the most dominant phyla isolated at the site, which is to be expected since this was an extreme saline (150mS/cm) environment (Figure 7). The microbial diversity at this site corresponds to previous investigations showing that as salinity increases the bacterial diversity present within a site becomes more specialised. The detection of a large number (29) of halophilic phylotypes isolated at this site confirms this hypothesis.

3.3.3 Summary of Swakopmund site 2 microbial diversity

As with the other sites investigated, Swakopmund site 2 fingerprinting results (DGGE and T-RFLP analysis) were in agreement showing that the samples collected at the site differ. The similarity dendrogram (Figure 13) constructed from the DGGE analysis indicated that the majority of the samples contained the same number of OTUs. DGGE analysis also indicated that the similarity between bacterial communities was 66%. In T-RFLP cluster analysis (Figure 22), Sps02A and Sps02B were found to cluster more closely and share at least 60% similar bacterial communities. Sps02C and Sps02D were found to cluster less closely but also shared 60% of bacterial communities. The T-RFs (81, 120, and 170) were linked to sequences obtained from clone libraries with T-RF 120 affiliating to *Idomarina* sp. (EF409427.1). The phylogenetic analysis further indicated that the majority of phylotypes identified were affiliated with Gammaproteobacteria (55%) and unclassified bacteria formed only 15% of the phylotypes detected. Swakopmund site 2 has been found to be an extreme saline site (180 mS/cm) which corresponded to the phylotypes found at the site. In general the microbial diversity at this site was found to be low. These results correspond to previous investigations showing that as salinity increases the bacterial diversity present within the site becomes restricted to more specialised phyla and this can be seen by the low number of phylotypes (Table 8) identified at this site.

Chapter 4: Cyanobacteria

4.1 Introduction

Cyanobacteria are photosynthetic organisms which are often referred to as blue green algae. Both filamentous and unicellular cyanobacteria are common in the microbial mats found in hypersaline lakes and salt pans. Microbial mats are typically stratified in microbial communities. The top brown layer is often colonised by the cyanobacteria *Aphanothece halophytica*. A second green layer typically harbours members of the genus *Oscillatoria* (*O. salina* and *O. neglecta* species) while the two bottom layers (purple and black) are comprised of *Chromatium*-like anoxygenic phototrophs and precipitated metal ions. These cyanobacterial species thrive in salinity concentrations up to 3.5M (Ventosa, 2006). Although cyanobacteria are found to be relatively diverse and abundant in saline environs, communities are ultimately structured by the chemical composition of the environment.

The aim of the present study was to characterise the diversity of cyanobacteria in the salt pans of the Namib Desert. This study formed part of a parallel culture-dependent study where researchers at IMBM isolated several cyanobacterial species (*Leptolyngbya Pseudanabaena*, *Chroococcus* and *Halothece* species) from sediment samples collected from Swakopmund site 2 (Ramond and Benkaddour, unpublished). Based on these preliminary findings it was decided that a culture-independent investigation into the cyanobacteria community colonising the Gobabeb and Swakopmund salt pans was warranted.

4.2 Results and discussion

4.2.1 Community profile of Cyanobacteria

A microbial fingerprint of the cyanobacteria present at the three sites was obtained using T-RFLP analysis. The PCR amplification consisted of two rounds of PCR in which the products obtained from the first round of PCR were used as the template for the second round of amplification. The primer pair CYA359/U1510R was used in the first round of amplification which yielded a DNA fragment of 1200bp. In the second amplification the cyanobacterial-specific primers Fam-CYA359/781R were used, which yielded amplicons of 493bp. Using this semi-nested PCR approach a greater number of phylotypes were tagged since the cyanobacterial specific degenerate primers used in the second round of amplification are able to tag both dominant and rare cyanobacterial species which were enriched for during the first amplification (Keyster M, 2007).

PCR products that were of the expected size (493bp) after the second round of amplification were excised from the gel and purified. The purified products were digested with the enzymes *RsaI* and *AluI*, followed by analysis on an automated DNA sequencer.

4.2.2 OTU Analysis of T-RFs

Initially enzyme selection was based on MICAIII (ISPaR) virtual digest analysis and the two enzymes selected yielded the largest number of OTUs with the subset of primers utilised in this study. MICAIII (ISPaR) uses a general bacterial database and is therefore not specific to cyanobacteria. Despite this, the results obtained from MICAIII indicate that a larger number of T-RFs would be obtained for Cyanobacteria phyla using the two restriction enzymes, *AluI* and *RsaI*. The two restriction enzymes chosen had different recognition sites (*AluI* recognises AG[^]CT; *RsaI* recognises GT[^]AC) thus making it possible to detect a broad range of taxa. Also, T-RFs were binned based on the method outlined in section 2.6.4.

4.2.2.1 Gobabeb site OTUs

Although two different enzymes were used to analyse the OTU composition between samples, it was found that enzyme *AluI* gave limited resolution and only produced 4 T-RFs compared to *RsaI* with 14 T-RFs (Figure 31). GOB5 was found to contain the majority of the unique T-RFs (6), GOB2 had four (52, 88, 417, 444), GOB3 with one (382) and GOB4 with one (385), while GOB1 contained no unique OTUs. GOB4 was found to be dominated by T-RF 101 while T-RF 421 was the dominant T-RF at GOB3 (Figure 31). The venn-diagram (Figure 32) further shows that there is no T-RF which is common to all the GOB sites. Also, only GOB1 and GOB3 were found to share two common T-RFs (274, 421) while GOB5 shares one T-RF (417) with GOB4 and two T-RFs (88 and 124) with GOB2 respectively. Overall, the diversity of Cyanobacteria within the Gobabeb site tends to be low with samples sharing less than 40% of the Cyanobacteria OTUs amongst one another.

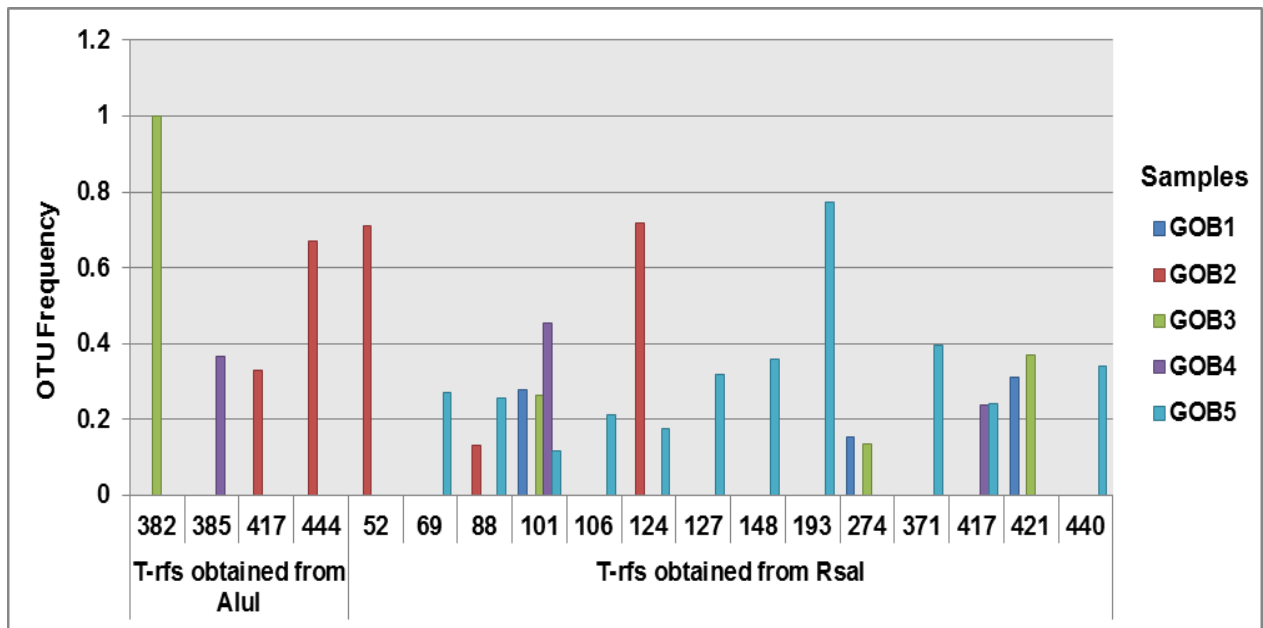


Figure 31: The graph represents the OTU distribution between all the samples obtained at Gobabeb site. The asterisks (*) represents the OTU at its highest frequency.

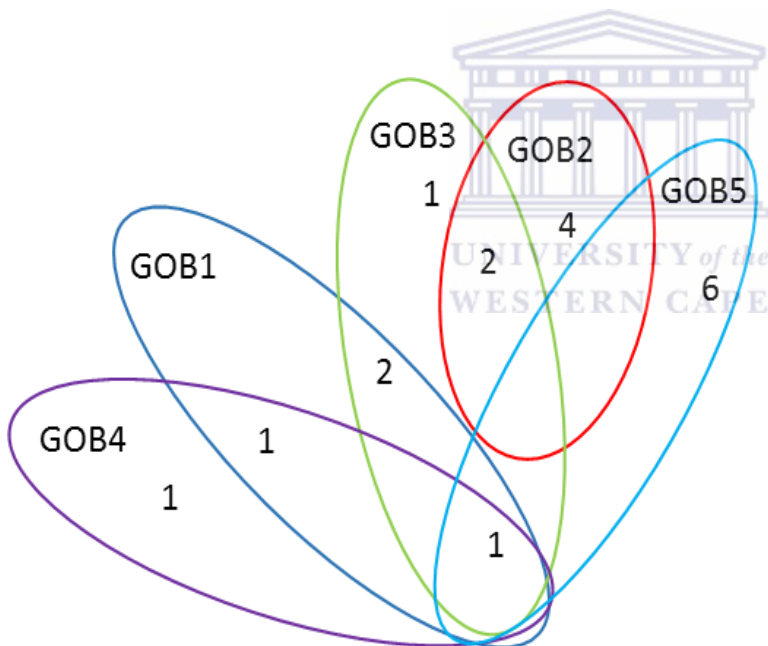


Figure 32: The Venn-diagram shows the distribution of OTUs between the samples collected at the Gobabeb site

4.2.2.2 Swakopmund site 1 OTUs

Relatively few T-RFs were detected with both restriction enzymes *AluI* and *RsaI* for Swakopmund site 1. Only three T-RFs (90, 233, and 419) were detected with *AluI* in which one T-RF (90) was common to Sps01A and Sps01B, T-RF 233 were common in Sps01B, Sps01C and Sps01D, and T-RF 419 was found to be unique to Sps01B. In addition, the four

T-RFs (101, 118, 419 and 437) detected with *RsaI* were unique to sample Sps01D (Figure 33). Also, sample Sps01D is the only sample containing any unique OTUs compared to the other samples (Sps01A-Sps01C). The venn-diagram (Figure 34) illustrates that none of the OTUs identified at the Swakopmund site 1 were found to be common to all four samples collected at the site. Furthermore, only one T-RF (233) was found to be common in three of the samples (Sps01B, Sps01C and Sps01D) (Figure 33 and Figure 34). The low number of T-RFs obtained for samples Sps01A-Sps01C could be that the majority of the DNA was lost during the purification process since the PCR products are purified twice, once before digestion and once post digestion, prior to analysis. Based on the possibility that the DNA yield was compromised during the purification processes the assumption that the number of cyanobacteria is low at this site, should be made with caution.

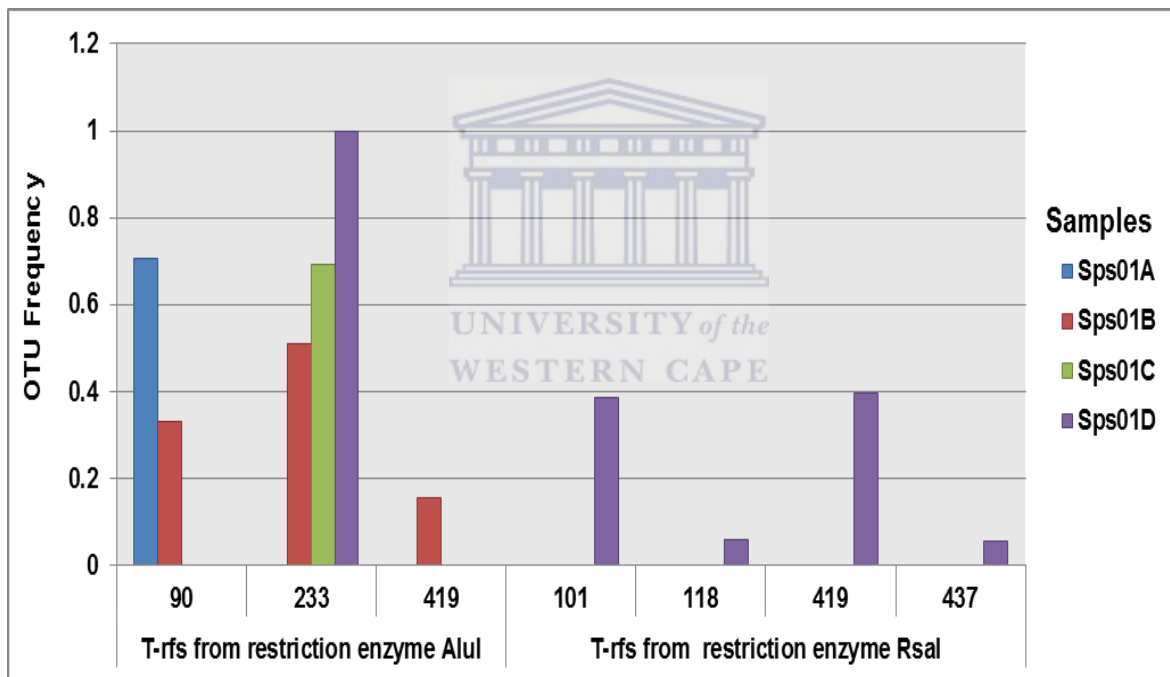


Figure 33: The graph represents the number of OTUs obtained from the different T-RFs between the samples obtained at Swakopmund site 1.

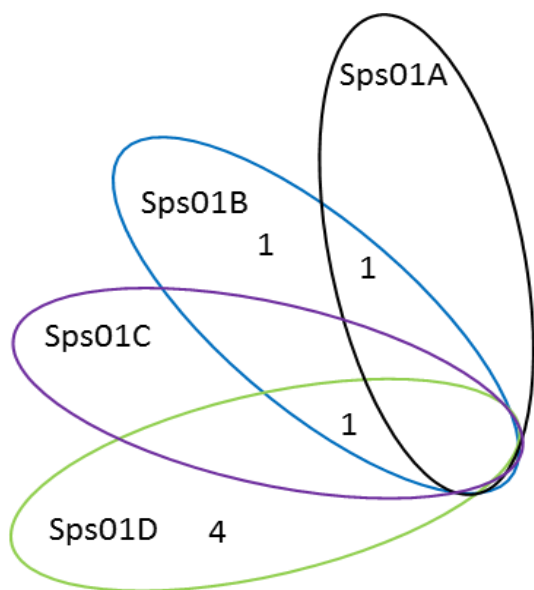


Figure 34: The Venn-diagram shows the distribution of OTUs between the samples collected at the Swakopmund site

4.2.2.3 Swakopmund site 2 OTUs

Of the two enzymes utilised only two T-RFs (137, and 348) were obtained from restriction enzyme *AluI* of which T-RF 137 was detected only in sample Sps02B (Figure 35). Also, T-RF 348 was detected in all three samples analysed. Using restriction enzyme *RsaI* only four T-RFs (99, 124, 419, 445) were obtained of which only T-RF 445 was found to be present in Sps02D (Figure 35). Furthermore, both samples Sps02B and Sps02D were found to contain one unique OTU (137 and 445, respectively) compared to Sps02C which did not contain any OTUs. From the venn-diagram (Figure 36), only one T-RF (348) was found to be common in four samples while samples Sps02B and Sps02D were found to share two T-RFs and, samples Sps02C and Sps02D shared only one T-RF (99). Regardless of the use of cyano-specific primers and the stringent PCR conditions applied Cyanobacteria diversity detected at Swakopmund site 2 was generally low. It has been documented that as salinity increases the prevalence of Cyanobacteria decreases (Nagasathya and Thajuddin, 2008), and this can be seen at this mineral rich site of Swakopmund site 2.

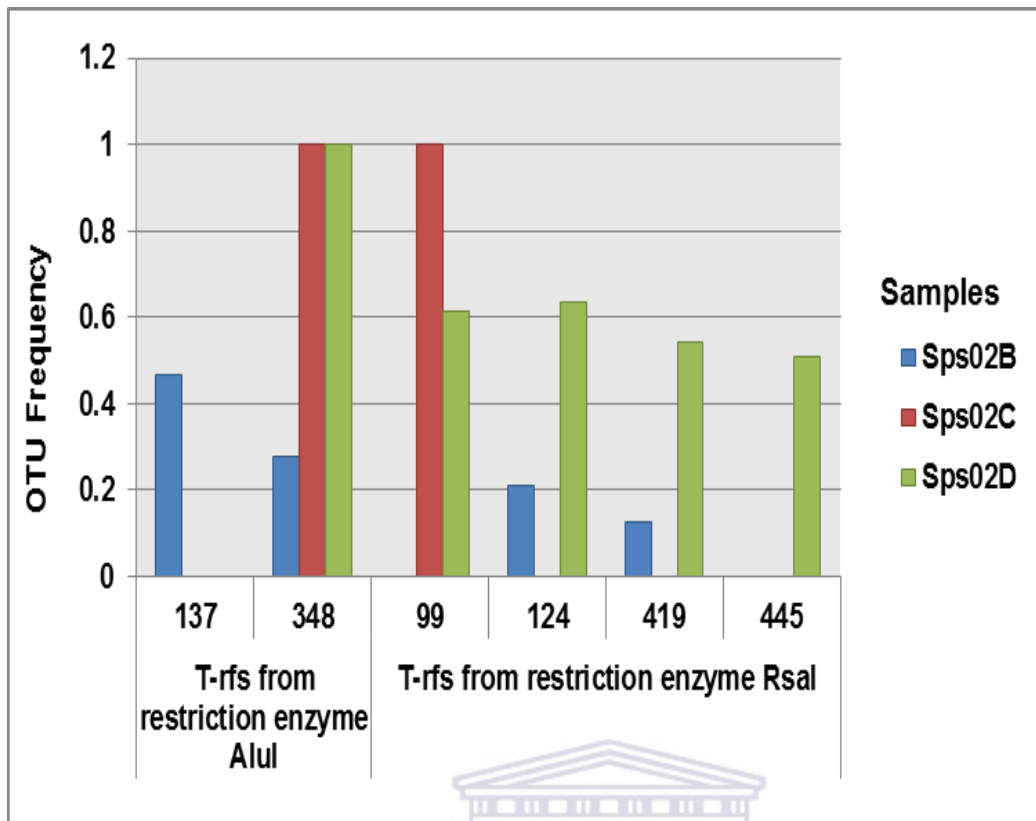


Figure 35: The graph represents the OTU distribution between all the samples obtained at Swakopmund site 2.

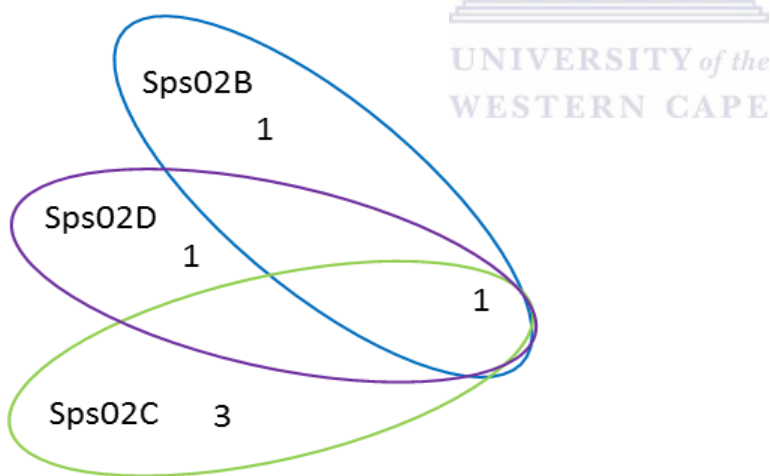


Figure 36: The Venn-diagram shows the distribution of OTUs between the samples collected at Swakopmund site 2

4.2.3 T-RF cluster analysis

4.2.3.1 Gobabeb site cluster analysis

A T-RFLP based MDS plot (Figure 37) indicated that the Gobabeb samples (GOB1-5) differ. The Gobabeb samples GOB2, GOB4 and GOB5 were found to share 20% similarity, while

GOB1 and GOB3 were found to be more closely related and shared 60% similarity. A 2D stress value of 0 indicates a strong confidence interval between samples. These results differed from the bacterial analysis, where only sample GOB4 was found to be dissimilar (20% similarity) and clustered separately, while in this investigation GOB4, GOB5 and GOB2 was found to be dissimilar sharing only 20% similarity with the rest of the samples.

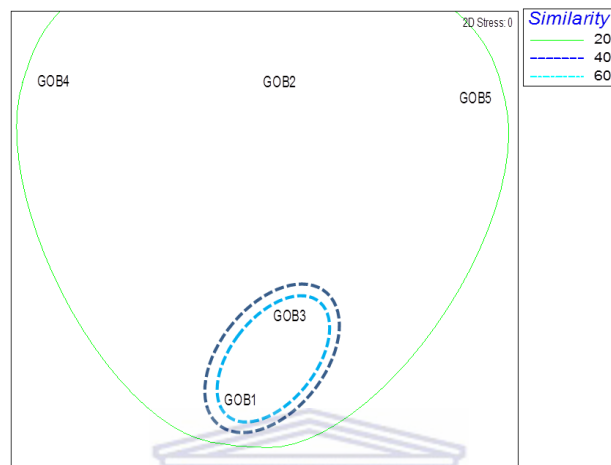


Figure 37: MDS plot created for Gobabeb. The Gobabeb samples, GOB1 and GOB3 cluster at 60% while GOB4, GOB5 and GOB2 cluster separately sharing 20% similarity.

4.2.3.2 Swakopmund site 1 sampling site cluster analysis

As with Gobabeb samples, all samples collected at Swakopmund site 1 (Sps01A-Sps01D) were found to differ. The samples were found to be very different and only samples Sps01B and Sps01C shared 40% similarity. The 2D stress value of 0 indicates a strong confidence interval between samples (Figure 38).

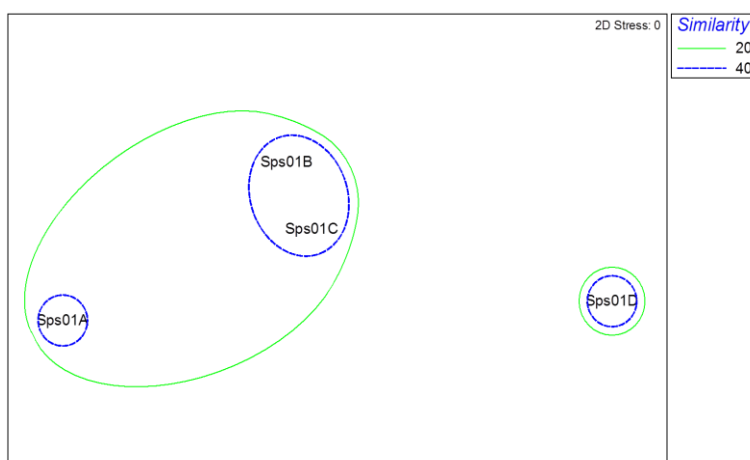


Figure 38: MDS plot created for Swakopmund site 1. Samples were found to share 20% similarity with one another while Sps01B and Sps01C cluster at 40% while Sps01A and Sps01C cluster separately at 20%.

4.2.3.3 Swakopmund site 2 cluster analysis

After several unsuccessful attempts to extract and amplify DNA from sample Sps02A it was decided to exclude it from the study. One possible explanation for the failed amplification is that the number of cyanobacteria within sample Sps02A was too low to detect. T-RFLP analysis showed that the samples differed (20% similarity) with Sps02B and Sps02C clustering at 40% similarity. Again, the 2D stress value of 0 indicates a strong confidence interval between samples (Figure 39).

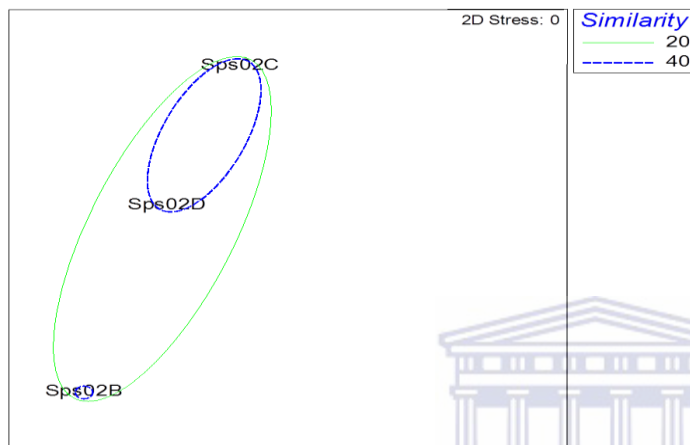


Figure 39: MDS plot created for Swakopmund site 2. The samples collected at Swakopmund, Sps02C and Sps02D cluster at 40% while Sps02B clustered at 20% similarity.

4.2.4 Cyanobacteria 16S rRNA gene clone libraries

As with bacterial clone library construction, T-RFLP analysis was also used as a guide to construction clone libraries (Table 9). Based on the low diversity obtained in T-RFLP analysis for individual samples collected at the different sampling sites [Gobabeb (Figure 31); Swakopmund site 1 (Figure 33); Swakopmund site 2 (Figure 35)], it was decided to pool all of the samples per site. This was done as to create an overview of the diversity present within the different sites. To conclude three 16S rRNA gene clone libraries GOB, Sps01 and Sps02) were constructed to represent the three individual sampling sites.

4.2.4.1 ARDRA analysis of clones

The same PCR conditions and primers used in the T-RFLP analysis were used to construct the 16S rRNA gene libraries. Recombinant clones were amplified using the primer pair M13F/M13R (Table 2). One hundred clones per library were screened, of which 80 positive clones from library Sps02, 62 from GOB and 70 from Sps01 contained the correct insert.

Plasmids were digested with *HpaII* (Figure 40) and grouped into phylotypes based on digestion patterns. One representative sample per restriction pattern was sequenced.

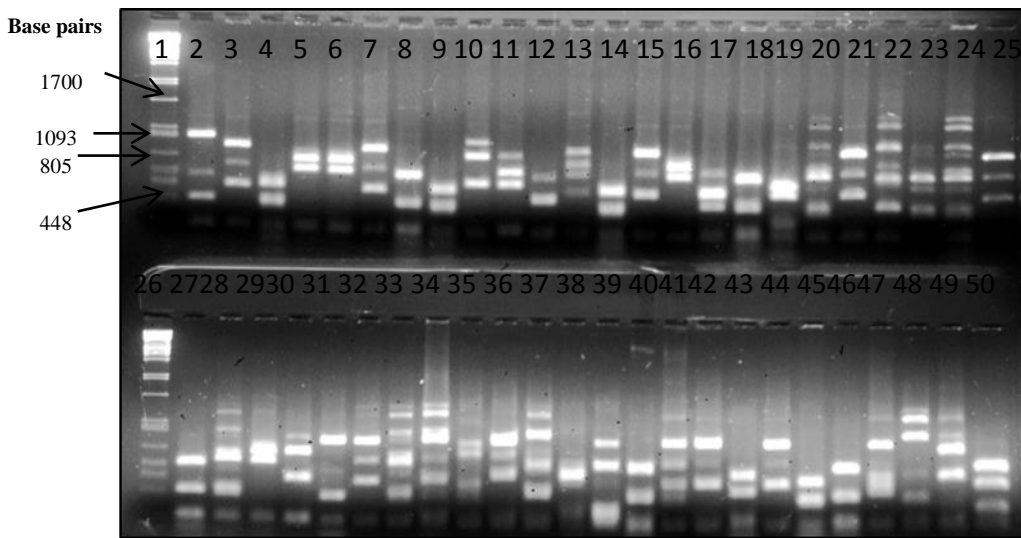


Figure 40: ARDRA analysis of the GOB cyanobacterial 16S rRNA gene clone library. Clones were digested with *HpaII*. Samples were separated on a 2% agarose gel. Lane 1 & 26: ladder λ PstI, Lane 2-25, 27-50: digested clones.

4.2.4.2 Statistical analysis of 16S rRNA gene clone libraries

To determine whether a sufficient number of clones had been sequenced to represent the libraries analysed the library richness estimates, S_{Chao1} and S_{ACE} were calculated for the libraries (section 2.7.5.4). The results indicated that the number of clones analysed for library GOB did not represent the majority of the phylotypes present within the sampling sites (Table 9). This can be seen with the predicated richness estimator, S_{Chao1} (55.26) being half the value of S_{ACE} (100.76). Although, this is not surprising since the entire GOB samples were pooled to create library GOB and based on the T-RFLP analysis Gobabeb site was colonised by a relatively diverse cyanobacterial population. For library Sps01 the predicated S_{Chao1} and S_{ACE} were found to be equal, thus indicating that the number of clones analysed was sufficient to represent most of the phyla present within the sampling sites. This result was corroborated with rarefaction curves reaching an asymptote (Figure 41). Since library Sps02 is a pooled a sample, it is not surprising to note that the two richness estimators were found not to be equal. This result indicates that the number of clones analysed for this site did not represent all the phyla present within this site; this can be seen with the rarefaction curve not entirely reaching the asymptote (Figure 41).

Table 9: Summary of the results obtained from both richness estimators S_{Chao1} and S_{ACE} and

Library	Nr of clones	Nr of Phylotypes observed	Predicated S_{ACE}	Predicated S_{Chao1}
Sps01	70	8	8	8
Sps02	80	17	93.5	84.29
GOB	62	16	55.26	100.76

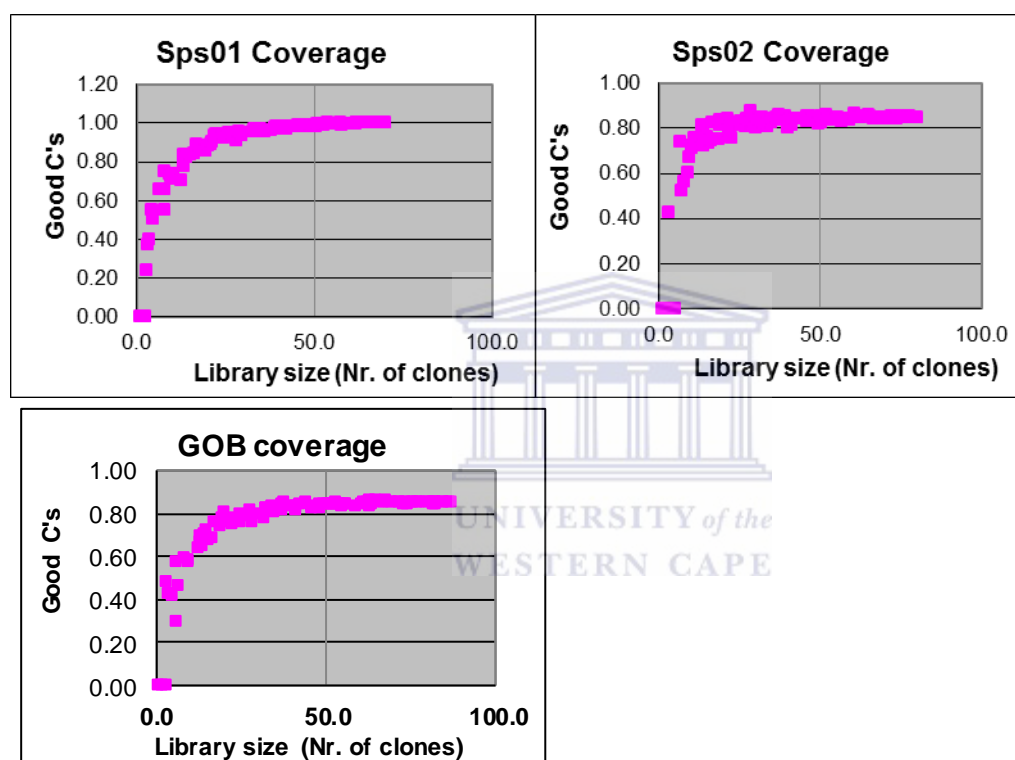


Figure 41: The coverage (Good's C) of the cyanobacterial 16S rRNA gene clone libraries (Sps01, Sps02 and GOB). The overall coverage is shown in the Y- axis and the number of clones per library in the x-axis.

4.2.5 Phylogenetic analysis of clones

Gobabeb, Swakopmund site 1 and Swakopmund site 2 Cyanobacterial 16S rRNA gene clone libraries was analysed separately using the methodology outlined in section 2.7.5.3.

4.2.5.1 Gobabeb site

Since many of the clones from the Gobabeb library displayed the same ARDRA pattern only 32 clones were analysed. The sequenced clones were clustered into 16 groups based on CD-HIT Suite program (Appendix E). The BLAST results of clones revealed that six of clusters (1, 4, 9, 11, 12 and 15) displayed less than 95% sequence identity to sequences within the

database. Also, all of the sequences were found to be affiliated to uncultured bacteria, except for cluster 7, which was affiliated to *Leptolyngbya* species (EU249119.1) (Appendix E). The clones were further affiliated to four different phylogenetic groups based on their phylogenetic assignment in the RDP database (Classifier). Also, to discern between novel phylotypes, a cut off value of 95% was assigned. Based on this cut off value half of the sequences analysed for GOB library contained novel phylotypes (Figure 42). However, the remaining taxa were comprised of Cyanobacteria constituting 38% of the total ribotypes, while Planctomycetes (9%) and Firmicutes (3%) accounted for the minor phyla detected at this site (Figure 42 and Appendix H).

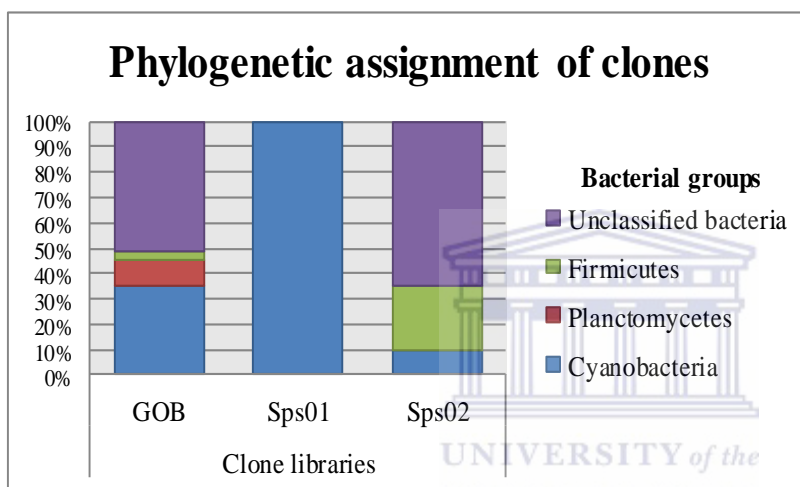


Figure 42: Histogram representing the distribution of ribotypes found in sampling sites GOB, Sps01 and Sps02. Clones were matched and grouped based on the data obtained from the RDP database.

The T-RFs obtained from T-RFLP analysis (Figure 31) were assigned to a phylogenetic ancestor based on the method outlined in section 2.7.5.3. The results obtained showed that five of the T-RFs (69, 124, 274, 371, 421) obtained from restriction enzyme *RsaI* and one T-RF (417) from restriction enzyme *AluI* were affiliated to uncultured Planctomycetales bacteria (JN881628.1) and a uncultured Halanerobiaceae bacterium (DQ647099) (Appendix E). Also, three pairs of T-RFs were found to affiliate with the same clones; T-RF 124 and 417 affiliated to cluster 4 uncultured Halanerobiaceae bacterium (DQ647099.1), T-RF 69 and 274 affiliated to cluster 10 uncultured Gammaproteobacteria (JF948429.1). Also, T-RF 421 obtained from *RsaI* were found to affiliate to uncultured Planctomycetales bacterium (cluster 13, JN881628.1). To conclude, the results obtained from 16S rRNA gene clone library indicated that the Cyanobacteria bacteria diversity within this site to be low, consisting of only one phylogenetic group. Although present, the cyanobacterial community was found to constitute only one third of the bacterial population group detected with cyanobacterial

primers. However, since half of the ribotypes were found to be related to unclassified bacteria the possibility of finding perhaps novel cyanobacteria within this site is high.

4.2.5.2 *Swakopmund site 1*

From ARDRA analysis, 17 clones were selected since some of them displayed similar or unique patterns from one another. Sequences obtained from these clusters were separated into two groups based on the CD-HIT Suite program. BLAST results revealed that none of the sequences shared less than 95% sequence homology with uncultured sequences within the BLAST database. Also, all of the sequences obtained were found to affiliate to ribotypes isolated from extreme saline environments (Appendix F). The result obtained from the program Classifier (RDP database) related all of the 20 sequences analysed for Swakopmund site 1 to the same phylogenetic ancestor, Cyanobacteria (Family IV) (Figure 42 and Appendix H).

Furthermore, the T-RFs obtained from T-RFLP analysis (Figure 33) were assigned to a ribotype based on the method outlined in section 2.7.5.4. The results obtained showed that of the seven T-RFs obtained (three T-RFs from *AluI* and four T-RFs from *RsaI*) for this site; only two T-RFs (118 and 419) could be assigned to a phylogenetic group (Appendix H). Since all of the phylotypes identified at this site were uncultured bacteria, the T-RFs were also assigned to uncultured bacteria (FJ175512.1 and FJ536482.1). Overall the phylogenetic results obtained showed that even though cyanobacteria species were dominant and the only organisms found at Swakopmund site 1, they were present at low numbers (Figure 33 and Figure 42). This low diversity of Cyanobacteria and the low number of taxa detected from this group may suggest that cyanobacteria have formed specialised communities adapted for the environment.

4.2.5.3 *Swakopmund site 2*

The sequences obtained from ARDRA analysis were clustered into seven clusters based on the clustering program CD-HIT Suite. Furthermore, BLAST results revealed that all of the sequences analysed affiliated to uncultured bacteria previously identified from extreme saline environments (Appendix G). Also, the sequences obtained from BLAST results revealed that all of the sequences, except for cluster 1 (88%) (AM930333.1), shared less than 95% sequence homology with sequences within the BLAST database. Since the cut off value of 94% is recommended to assign sequences to genus level based on the 70% DNA-DNA

homology being shared between species, it can be considered that values lower than 94% is indicative of novel species (Konstantinidis and Tiedje, 2005). The result obtained from the program Classifier (RDP database) found that all of the 17 sequences analysed belonged to two phylogenetic groups (Cyanobacteria and Firmicutes) (Figure 42) and Appendix H). Even though cyano-specific primers were used, Cyanobacteria were found to only comprise 10% of the total phyla isolated at the site, while the majority of the isolates affiliated to unclassified bacteria (65%), although, it is possible the unclassified bacteria identified could include novel cyanobacteria genera.

Of the six T-RFs (137, 348, 99, 124, 419 and 445) obtained from T-RFLP analysis (Figure 35) only T-RF 419 was found to affiliate to uncultured Verrucomicrobia sequences in cluster 3 (FJ844124.1). Overall, the results obtained showed that the Cyanobacterial diversity present within Swakopmund site 2 was low. As had been observed at the other sites, since the majority of the phyla were found to relate to unclassified bacteria (65%), the chances of finding novel cyanobacteria or more specialised halophiles as this site is high. The results obtained for this extreme saline (conductivity =180mS/cm) site correlated with other studies showing that as salinity gradient increases the number of phylotypes present within the site decreases and become more specialised (Benlloch *et al.*, 2002; Baati *et al.*, 2008; Wang *et al.*, 2011).

4.2.6 Phylogenetic tree construction

Even though the three sampling sites were analysed separately, as relatively few phylotypes were found to be present within libraries, one phylogenetic tree (Figure 43) was constructed. The phylogenetic tree was constructed based on the method outline in section 2.7.5.3 and *Haloquadratum walsbyi* (NR_028207.1) was used as an outgroup.

The results obtained from the phylogenetic tree showed that all of the phylotypes cluster within their respective clades (Cyanobacteria, Firmicutes and Planctomycetes). Also, the majority of Swakopmund and Gobabeb samples were found to cluster within their respective sites. However, within the Cyanobacteria clade samples obtained from Gobabeb (GOB19, GOB7, GOB60) and Swakopmund site 1 (Sps01-105) were found to cluster with Swakopmund site 2 samples (Sps02-63, Sps02-69) because they are affiliated to the same Cyanobacteria phylotype (Family VII). Similarly, samples Sps02-17, GOB59, and Sps01-105

were also found to cluster within the same Firmicutes (*Halanerobiaceae*) clade even though these sites were found to be geographically and physio-chemically different.



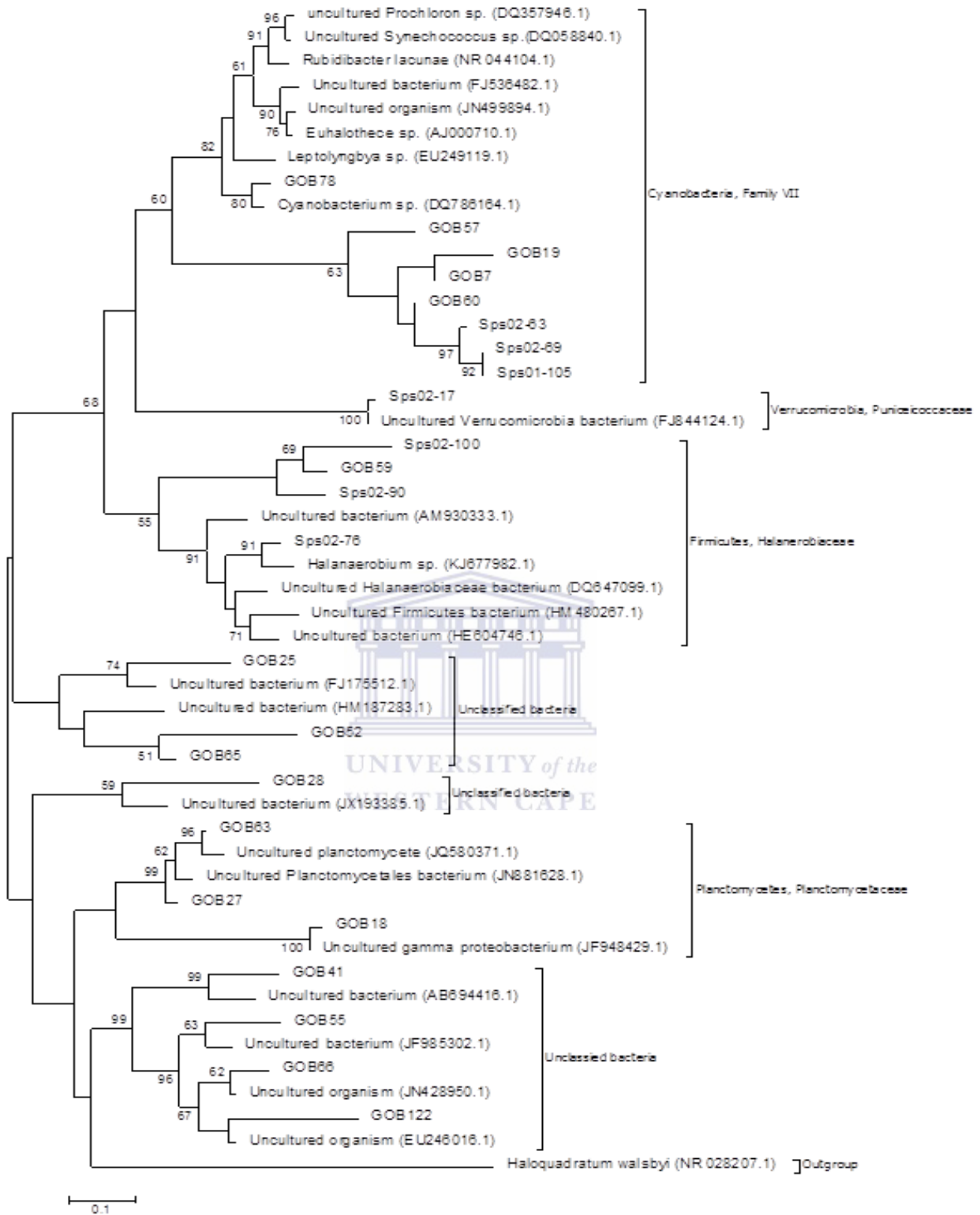


Figure 43: Phylogenetic tree representing the evolutionary relationships between Cyanobacterial clone sequences for libraries constructed for Gobabeb, Swakopmund site 1 and Swakopmund site 2. Mega 6 software was used to construct the phylogenetic tree with the Maximum Likelihood method and the Kimura 2_{parameter} model. Bootstrap values were set at a 1000 replicates. One cluster per group was used to construct the tree, with the outgroup being *Haloquadratum walsbyi* (NR_028207.1). Bootstrap values less than 50 are not indicated on the tree.

4.3 Summary of cyanobacterial diversity findings

The previous culture-based study identified strains related to *Leptolyngbya*, *Pseudanabaena*, *Chroococcus* and *Halotheces* species in the Swakopmund site (Sps02) samples. However, only relatively few representatives of these taxa were detected in the current study.

4.3.1 Cyanobacteria diversity findings of Gobabeb site

Both T-RFLP analysis and 16S rRNA gene clone libraries showed the cyanobacterial diversity within the Gobabeb site to be low, and representing only 38% of the phyla resident within the site. Even though the T-RFLP analysis (Figure 31 and Figure 37) indicated that the different samples (GOB1-GOB5) used to assess the cyanobacterial diversity within the site differed, it did however show the collective number of OTUs within the Gobabeb site to be low. BLAST sequence analysis of Gobabeb clones identified several cyanobacterial genera including *Leptolyngbya* species, uncultured *Synechococcus* and *Prochloron* species (Appendix E) were present, although the majority of the sequences affiliated to uncultured bacteria. Compared to findings from the bacterial analysis where 2.3% of the ribotypes were related to cyanobacteria a far greater number of cyanobacterial (38%) was detected in this investigation. Even though the frequency of cyanobacteria detected was high; the diversity was found to be low. This is because all of the cyanobacteria taxa detected were found to belong to the same family (Family VII, Grp VII).

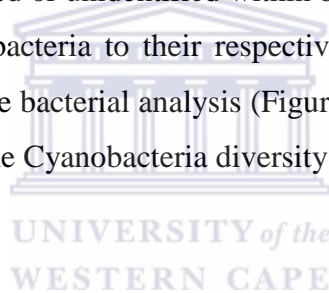
4.3.2 Cyanobacteria diversity findings of Swakopmund site 1

Results obtained from T-RFLP analysis (Figure 33) and 16S rRNA gene clone libraries (Figure 42) were in agreement showing the diversity of cyanobacteria within the Swakopmund site 1 to be low. Only seven T-RFs were obtained from the two restriction enzymes utilised, and all of 17 clones were found to affiliate to two phylogenetic groups (FJ536482.1 and GU229750.1), with both groups linked to uncultured bacterium (Appendix F). The results obtained from Classier (RDP database) (Appendix H) further identified the two phylogenetic groups being affiliated to Cyanobacteria. These results correlate with the Cyanobacteria detected from the bacterial analysis section (Figure 25) both showing that the Cyanobacteria resident within this site to be low and possibly specialised.

4.3.3 Cyanobacteria diversity findings of Swakopmund site 2

The results obtained from T-RFLP analysis (Figure 35) correlated with 16S rRNA gene clone libraries (Figure 42), which both indicated that the prevalence of Cyanobacteria within

Swakopmund site 2 was low. In T-RFLP analysis only six T-RFs were obtained collectively from the two restriction enzymes utilised (*AluI* and *RsaI*), with Sps02D having the highest number of ribotypes. Also, despite the fact that cyano-specific primers were used, the majority of clones analysed for the Sps02 library were associated with the uncultured *Verrucomicrobia* clade with a very high homology value of 99% (Appendix G). However, in the RDP Classifier database (Appendix H) the clones were found to show similarity values of below 30% to the *Verrucomicrobia* phylum. Although the majority of the clones analysed in Swakopmund site 2 were not related to cyanobacteria, potentially novel bacterial taxa such as *Verrucomicrobia* species were identified. Although Cyanobacteria were found in the culture-based microscopy analysis of samples obtained from Sps02, the same Cyanobacteria genera could not be identified in the molecular study. This is not surprising since studies have shown that identifying Cyanobacteria with morphological methods to species level to be more precise than using genotyping methods (Bukuwasku *et al.*, 2014). This is because a large number of phyla remain uncultured or unidentified within bacterial nucleotide databases, thus making it difficult to associate bacteria to their respective taxa (Bukuwasku *et al.*, 2014). Taking into consideration both the bacterial analysis (Figure 25) and the current investigation (Appendix G), it is evident that the Cyanobacteria diversity within this site is limited.



4.4 Concluding remarks

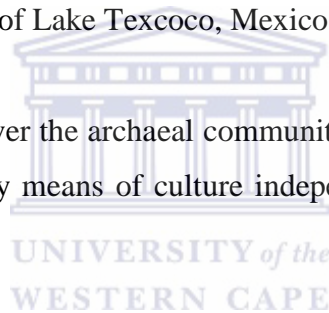
A nested PCR approach was adopted to increase the specificity of the PCR used in the generation of amplicons for T-RFLP analysis and the creation of 16S rRNA gene clone libraries. Despite using the nested PCR approach with cyanobacterial specific primers, the number of sequences that represented non-cyanobacteria was still found to be high. Although a large group of possible novel cyanobacteria were tagged; the sequences found to affiliate to cyanobacteria were all found to be associated to one phylogenetic group, chloroplast/cyanobacteria which were detected in all three sampling sites. It is possible that the combination of primers used in the study preferentially amplified 16S rRNA gene sequences from this bacterial group. While a diverse group of cyanobacteria thrive in salt pans (Abed *et al.*, 2011), some researchers have found that the diversity of cyanobacteria in salt pans was generally low, and dominated by one or two phyla (Nedumaran and Perumal, 2012; Luo *et al.*, 2014). The findings from this study indicate that the cyanobacterial diversity is relatively low in these salt pans and is therefore in agreement with previous investigations.

Chapter 5: Archaeal diversity

5.1 Introduction

Early microbial diversity studies claimed that archaea thrived only in extreme habitats (as cited in Ventosa, 2006), but subsequent studies have shown that archaea are found in all environments, but at varying population sizes. Studies have shown that they contribute to at least a third of the 16S rRNA genes detected in soil (Kemnitz *et al.*, 2007) and in marine habitats (Stoica and Herndi, 2007). In saline environments the archaeal phylum *Euryarchaeota* (which includes the family *Halobacteriaceae*) are dominant, with *Crenarchaeota* (predominately methanogens) forming the minority of the archaeal groups (McGenity and Oren, 2010). Walsh and colleagues (2005) isolated several members of the *Methanosarcinales* family in the saline soils of Saltspring in British Columbia, (Canada), whereas Valenzuela-Encinas and colleagues (2008) isolated several members of *Halobacteriales* in the salty soils of Lake Texcoco, Mexico.

The present study aimed to uncover the archaeal communities residing within the saline soils of the Namib Desert salt pans by means of culture independent techniques (DGGE and T-RFLP).



5.2 Results and discussion

5.2.1 DGGE analysis

DGGE was used to obtain a phylogenetic fingerprint of the archaeal diversity inhabiting the Namib salt pans. Metagenomic DNA (sections 2.3.1 and 2.3.2) was used as the template for the first round of DGGE amplification with primers A3Fa/Ab927R (Table 2). This generated a PCR amplicon of the expected size of ~900bp for samples from Sps01 and GOB, while for Sps02 an amplicon of ~1kb was generated.

In the second round nested PCR amplification, the PCR products obtained in the first round of DGGE amplification was used as the template. The primer pair 340GC/A533R (Table 2) was used with the forward primer tagged with a GC clamp. This yielded a 200bp fragment for Sps01 and GOB samples. Sample GOB4 from the Gobabeb salt pan was removed from the analysis as it failed to amplify after several attempts to optimise the PCR. The 200bp PCR fragments were obtained for the remaining samples. These amplicons were separated on a 30-

70% denaturing gel and statistical analysis was performed using the software GelComparII (version5) (Applied Maths) (section 2.4.4).

5.2.2 Statistical analysis of DGGE

A dendrogram was constructed using the similarity matrixes DICE coefficient and Unweighted Pair Group Method and Arithmetic Averages (UPGMA).

5.2.2.1 Gobabeb site

The results obtained from the dendrogram (Figure 44) constructed for the Gobabeb site indicated that all of the samples (GOB1, GOB2, GOB3 and GOB5) analysed were dissimilar. The banding pattern observed between samples showed that sample GOB3 had the highest number of OTUs (15), while samples GOB1 and GOB2 had nine OTUs each. Despite the differences in the number of OTUs samples GOB2 and GOB3 were found to share 35% (bootstrap value of 100). Overall, all of the Gobabeb samples analysed were found to share a very low similarity (15%).

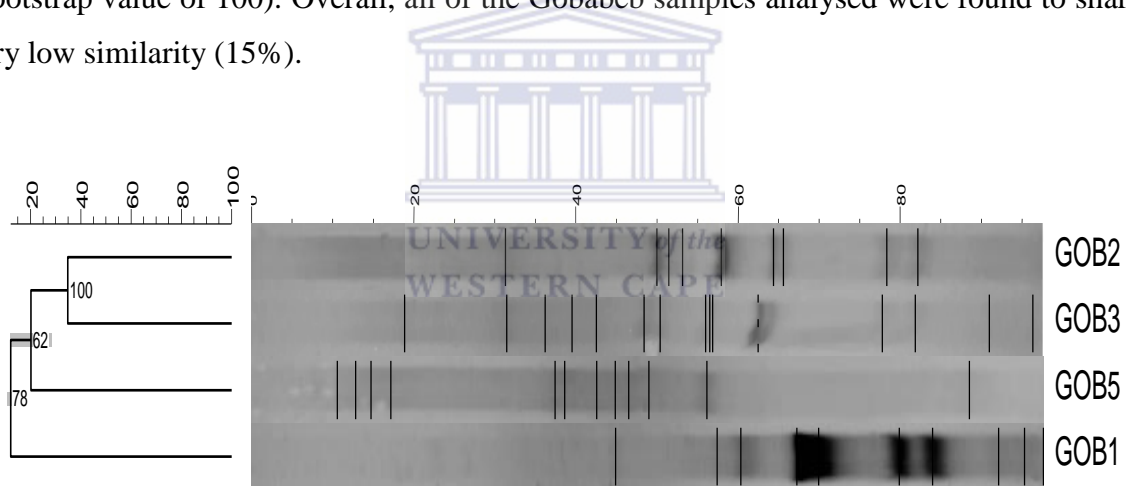


Figure 44: Similarity analysis for the Gobabeb samples. The dendrogram was constructed using the GelComparII (version 5) software, the similarity matrix DICE coefficient and the UPGMA cluster method. The four samples were found to be highly dissimilar, with the similarity between the samples being 15%..

The MDS plot (Figure 45) confirmed the DGGE results. The MDS plot and the similarity analysis indicated that GOB2 and GOB3 were more similar, with the other samples clustering separately.

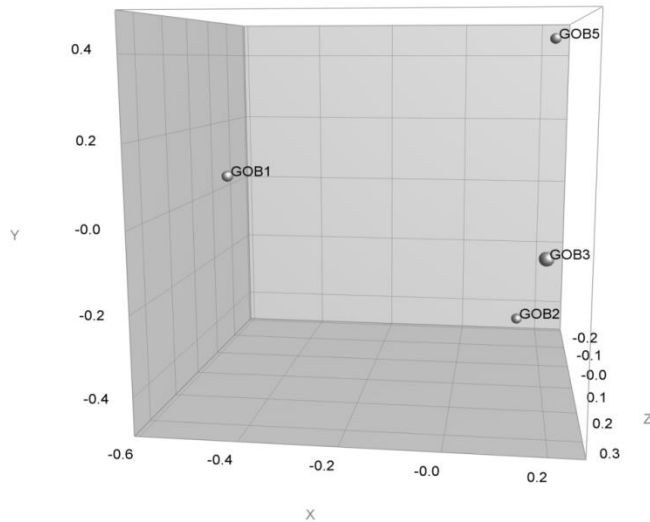


Figure 45: MDS plot was constructed for Gobabeb site using GelComparII (version5) software. The four Gobabeb samples (GOB1, 2, 3 and 5) were found not to cluster. The scale for MDS plot separates the samples on the X, Y and Z plane at 0.2 intervals.

5.2.2.2 Swakopmund site 1

The clustering analysis (Figure 46) for Swakopmund site 1 also indicated that all samples were dissimilar. Sample Sps01A and Sps01C both contained 17 OTUs each while Sps01D only had five OTUs. Furthermore, sample Sps01A and Sps01B were found to cluster at 40% similarity (bootstrap value of a 100). Overall the cluster analysis of Swakopmund site 1 showed low similarity (20%) between samples which was similar to the level of similarity observed for the Gobabeb site.

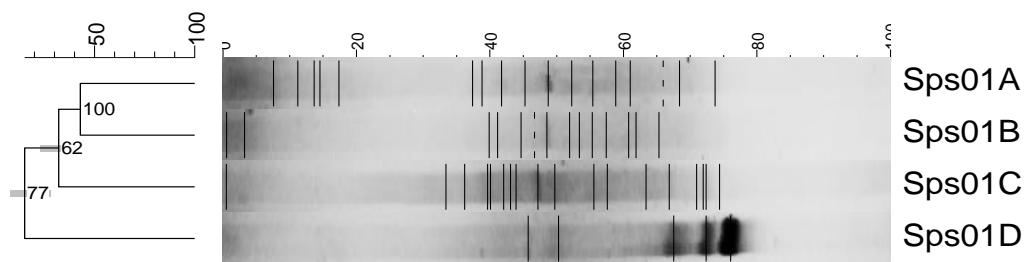


Figure 46: Similarity analysis for Swakopmund site 1. The dendrogram was constructed using the GelComparII (version 5) software, the similarity matrix DICE coefficient and the UPGMA cluster method. The four samples were found to contain different banding patterns with both Sps01A and Sps01C with 17 bands, Sps01B with 14 bands and Sps01D with five bands.

The MDS plot (Figure 47) constructed from the dendrogram confirmed the close clustering of Sps01A with Sps01B, while the rest of the samples clustered separately.

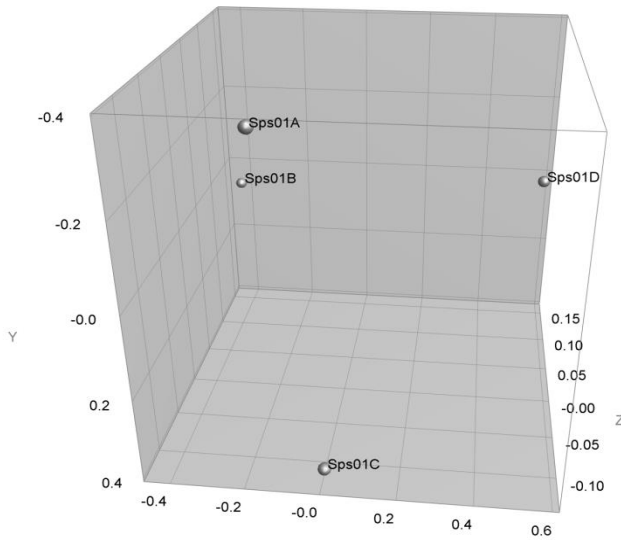


Figure 47: MDS plot construct for Swakopmund site 1 using GelComparII (version5) software. Samples Sps01A and Sps01B clustered separately from Sps01C and Sps01D. The scale of MDS plot is set at 0.2 intervals for both the X and Y plane while at the Z plane intervals are set at 0.05 intervals.

5.2.2.3 Swakopmund site 2

Cluster analysis for Swakopmund site 2 (Figure 48) indicated that all of the samples collected for the site were dissimilar. Sample Sps02B was found to contain the most OTUs (19), while Sps02A and Sps02D were both found to have five and nine OTUs, respectively. Samples Sps02A and Sps02B are found to share 20% similarity (bootstrap value of 100). Overall, the four samples (Sps02A-Sps02D) collected at Swakopmund site 2 were found to be dissimilar, sharing less than 20% similarity.

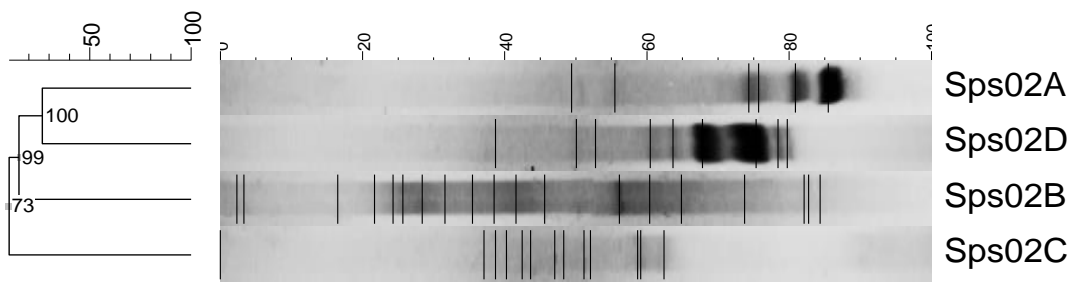


Figure 48: Similarity analysis for Swakopmund site 1. The dendrogram was constructed using the GelComparII (version 5) software, the similarity matrix DICE coefficient and the UPGMA cluster method. The four samples were found to contain different banding patterns with Sps02A with six bands, Sps02B with 19 bands, Sps02C with 11 bands and Sps02D with nine bands

Furthermore, the MDS plot (Figure 49) constructed from the dendrogram confirmed the clustering of Sps02D and Sps02A with one another, while the other samples (Sps02B and Sps2C) did not cluster.

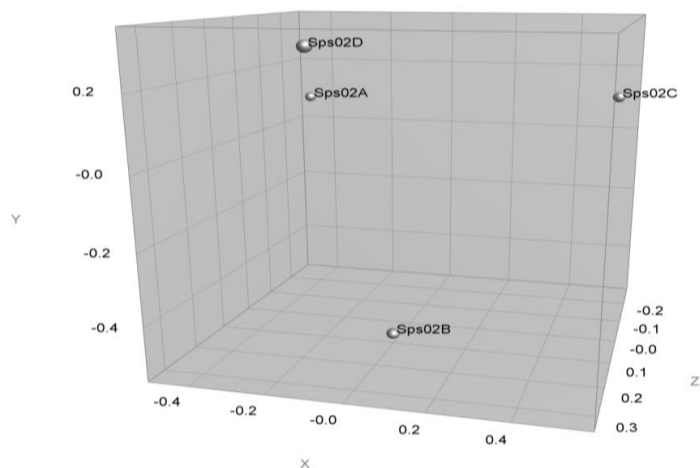


Figure 49: MDS plot constructed for Swakopmund site 2 using GelComparII (version5) software. Sample Sps02D and Sps02D clustered while Sps02B and Sps02C did not. The MDS plot scale separates the samples at 0.2 intervals for both the X and Y plane, while the Z plane separating samples at 0.1 intervals.

5.2.3 Profiling of DGGE bands

To further identify the phylogenetic groups present within the environmental samples several bands (Figure 50, bands 1-6) were excised from the DGGE gel. Bands with sufficient intensity were selected based on either their frequency (present in more than one sample) or uniqueness (present in a single sample only) (Figure 50).

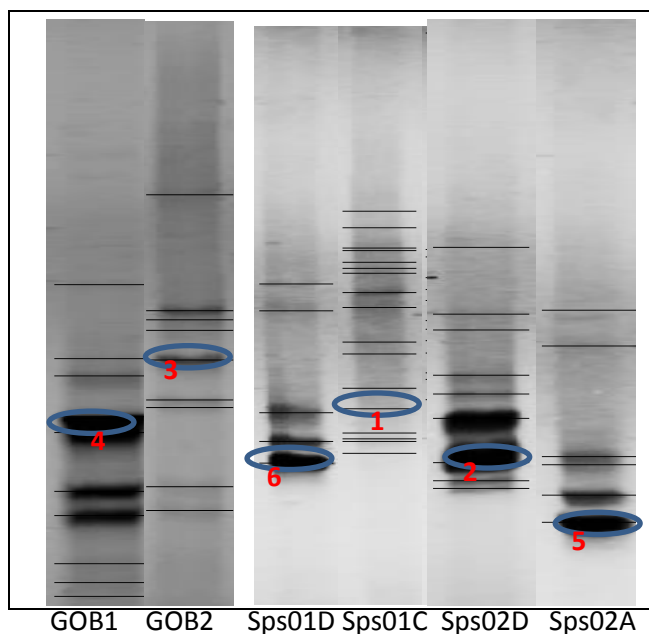


Figure 50: DGGE analysis from all three sites for community profiling. The six bands excised from the gel are marked

Although the amplicons were ~200bp in length, when the amplicons were sequenced using the reverse primer only 120bp of useable sequence was obtained for all the amplicons. Sequence analysis revealed that the shorter 120bp sequences obtained from sequencing could be due to the formation of secondary structures caused by a string of G/C nucleotides present in the sequences. The shorter sequences were edited and blasted against reference sequences in GenBank (BLASTn) to obtain their closest phylogenetic neighbours (Table 10).

All six excised bands obtained from sequence analysis were related to uncultured archaeal clones (Table 10). Interestingly, as found for the general bacterial analysis, all the clones identified were isolated from either marine or a mineral rich environment (Table 10).

To conclude, although relatively few archaea were identified in this study they were all related to uncultured archaea. In addition, this is one of the first studies to positively identify archaeal ribotypes by DGGE analysis. Several researchers investigating archaea present in other terrestrial environments were unable to detect any archaea within their samples using molecular-methods (Warren-Rhodes *et al.*, 2006; Pointing *et al.*, 2007).

Table 10: Sequence identification of DGGE bands obtained from BLASTn, NCBI database

Band	Sample site	Accession nr.	Strain (partial 16S RNA sequence)	Max indent	Origin of clones
1	Sps01D	JN825281.1	Uncultured archaeon clone MA18	91%	Acidic lakes (Northern Russia)
2	Sps02D	AB573140.1	Uncultured archaeon gene: clonehusua-a2	91%	Coastal marine sediment (Hiroshima Bay)
3	GOB2	EU377213.1	Uncultured marine archaeon clone Au-Fg10-Arch8	95%	Collected from the surfaces of corals
4	GOB1	AJ969917.1	Uncultured archaeon 16S rRNA gene, clone ss111	87%	Salt spring (Canada)
5	Sps02A	AF505695.1	Uncultured haloarchaeon clone ZB-A39	88%	Zabuye Lake (Tibet)
6	Sps01C	EF598908.1	Uncultured archaeon clone arcsalE08	81%	Hypersaline lagoon (Brazil)

5.2.4 T-RFLP analysis

T-RFLP analysis was performed to obtain a quantitative profile of the archaeal communities and to observe the differences in the diversity present in the research sites. T-RFLP analysis was carried out using the archaeal universal primer pair 8fa/1492R (Table 2) (Figure 51). Since it proved difficult to amplify most of the samples with the archaeal primers, even after repeated DNA extraction and PCR amplifications, it was decided to choose one sample per site to serve as a representative sample (GOB2, Sps01B and Sps02A).

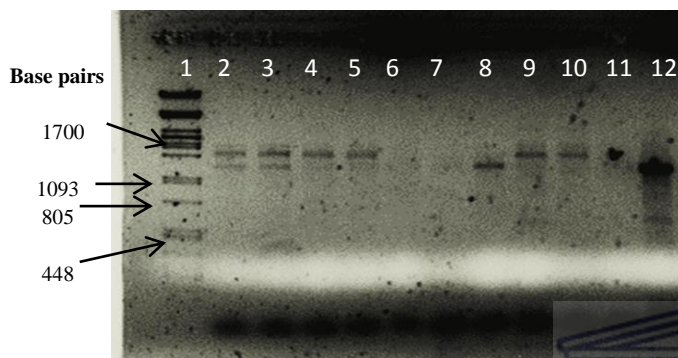


Figure 51: PCR amplicons of metagenomic DNA generated using the universal archaeal primer pair 8fa/1492R. Lane1: λ PstI ladder, Lane 2 and 3: GOB2, 4 and 5: GOB3, 6: Sps01A, 7: Sps01C, 8: Sps01B, 9 and 10: open soil, 11: Negative control, 12: Positive control: *S. sulfolobus*.

The resultant PCR fragments obtained were between 1492bp and 1800bp in size with the expected size being ~1492bp. According to Costello and Schmidt (2006) the band size at ~1492bp represents the archaeal small subunit (ssu) and the band at ~1800bp represents the eukaryotic ssu. In the present study, both fragment sizes were obtained after amplification of the Gobabeb metagenomic DNA, and only the expected 1492bp archaeal fragment from the Swakopmund site (Sps01). Since both fragments were present in the Gobabeb sample, the 1492bp fragment was excised from the gel and purified. Also, as only the 1800bp PCR fragment was detected for the Sps02 sample it was included in further downstream analysis.

5.2.4.1 OTU analysis of T-RFs

Enzyme selection was based on MiCAIII (ISPaR) virtual digest analysis in which the selected enzymes (*AluI* and *HaeIII*) yielded the largest number of OTUs with the subset of primers utilised. The two enzyme utilised *AluI* and *HaeIII* ultimately gave limited resolution, with sample Sps02 generating three T-RFs (77, 90,159) from *AluI*, Sps01 only generated one T-RF (77) and GOB was found not to generate any T-RFs. With *HaeIII*, Sps02 generated three T-

RFs (117, 443 and 489); one T-RF (443) with GOB, while Sps01 did not generated any T-RFs. Since both *AluI* and *HaeIII* gave limited resolution two additional restriction enzymes *RsaI* and *HpaII* was also selected from MiCA (ISPaR) virtual digest analysis, since it too yielded a large number of OTUs. From *RsaI*, Sps02 yielded four T-RFs (117, 279,284 and 516) and both GOB and Sps01 generated one T-RF (259). From *HpaII* only Sps02 generated two T-RFs while GOB and Sps01 did not generated any. The restriction enzymes utilised was also based on the different recognitions sites it tagged with both *HaeIII* and *HpaII* recognising GC rich ribotypes while *AluI* recognises AG[^]CT and *RsaI* recognises GT[^]AC. Finally, the assignment of T-RFs in the program MiCA III is based on the combination of the restriction enzymes and primers used, which can influence the diversity detected. Therefore, it is recommended that more than one enzyme should be employed (Schutte *et al.*, 2008). Despite using a combination of restriction enzymes in this study no more than ten OTU's per restriction digest were identified and because of this the results can therefore be viewed with some degree of confidence.



5.2.5 Assessment of Archaeal primers

In this study two culture independent techniques (using two different primer sets) were used to provide a quantitative profile of the archaeal diversity inhabiting the three salt pans. Since previous investigations have shown that the combination of primer pairs used in fingerprinting techniques can alter diversity profiles (de Liphay *et al.*, 2004; Baker and Cowan, 2004) the degenerative primer pairs utilised in this study were reviewed using the bioinformatics program Silva (Table 11). The program was set as to allow for the maximum mismatches between 0, 3 and 5 base pairs for both primer pairs. The specificities for both primer pairs increase as the number of mismatches increase (Table 11). However, as the number of mismatches increases the primers tag a greater number of eukaryotic species (Table 12). This is not surprising since the eukaryote domain lineages were derived from the archaeal domain and share homogeneity amongst certain genes (Williams *et al.*, 2012). For this reason, the PCR conditions used in this study were stringent (section 2.5.2 and section 2.6.2) and optimised to amplify only archaeal phylotypes, which was successful as sequencing analysis confirmed that only archaea were identified.

Archaea are considered as extremophiles and hence the diversity of these microorganisms in salt rich environments can consist of Euryarchaeata, Crenarchaeata and even the most

recently identified Nanoarchaeata and Korarchaeata phyla. Studies have identified phylotypes from the Euryarchaeota phylum such as halophiles (Halobacteria), methanogens (Methobacteria) (Montoya *et al.*, 2011; Yuan *et al.*, 2014) and even thermophiles (Thermococci) (Karthikeyan *et al.*, 2013) (Table 11) within salt pans. Phylotypes from the Crenarchaeata phyla are also found in salt pans but to a lesser degree than the Euryarchaeata (McGenity and Oren, 2010).

Table 11: Evaluation of the archaeal primer pairs A3Fa/Ab927R and 8Fa/1492R using Silva. Numerical values are given in percentages. Archaea phylotypes frequently isolated in saline environments are highlighted in yellow.

Primer pair	A3Fa/Ab927R			8Fa/1492R		
	0	3	5	0	3	5
Maximum nr of mismatches	0	3	5	0	3	5
Domain: Archaea	49.9	81.4	84.5	15.7	54.0	54.6
Phylum: Crenarchaeota	66.5	87.2	89	3.8	85.1	88.3
<i>Thermoprotei</i>	66.5	87.2	89	3.8	85.1	88.3
Phylum: Euryarchaeota	41.5	83.6	86.8	12.6	46.1	47.0
<i>Archaeoglobi</i>	45.3	100	100	22.2	90.9	90.9
<i>Halobacteria</i>	18.4	31.2	33.2	3.5	23.7	24.1
<i>Methanobacteria</i>	31.8	67.1	76.8	2.5	64.7	64.7
<i>Methanococci</i>	76.7	96.8	96.8	11.1	95.5	95.5
<i>Methanomicrobia</i>	28.1	85.6	92.6	29.9	80.6	81.4
<i>Methanopyri</i>	100	100	100	0	100	100
<i>pCIRA-13</i>	0	100	100	0	0	0
<i>Thermococci</i>	84.1	93.5	93.5	11.1	82.6	84.8
<i>Thermoplasmata</i>	64.2	87.5	89.5	22.7	66.1	66.9
Phylum: Korarchaeota	0	88.9	100	0	66.7	66.7
Phylum: MHVG-1	45.5	62.5	87.5	0	100	100
Phylum: Nanoarchaeota	0	100	100	0	50	50
Phylum: Thaumarchaeota	58.2	79.8	84	43.6	76.9	77.2
Other domains						
Bacteria	0	0	0	0	0	0
Eukaryota	66.9	88.9	88.9	0.2	54.9	54.9

5.2.6 Phylogenetic assignment of T-RFs

The T-RFs were assigned phylogenetic affiliations using the program MiCA III (PAT+) (Table 12). The results obtained from the samples compared to the reference database (MiCA III) found that the majority of the T-RFs obtained were associated with reference sequences

which were identified in saline environments (Table 12). The phylogenetic assignment of the T-RFs further showed the GOB sample shared one T-RF (443) with the Sps02 sample; however this T-RF had no phylogenetic affiliation in the database. Similarly, the same GOB sample shared one OTU (259) with Swakopmund site 1 (Sps01), which was found to be related to an uncultured archaean clone from mine sediment (Table 12). Lastly, Sps01 and Sps02 were also found to share one T-RF (77), and it too was found not to affiliate to any of the phylogenetic ancestor within the database. Overall, the diversity of archaea within the salt pans (Gobabeb, Swakopmund site 1 and Swakopmund site 2) was found to be low, with T-RFs associating to archaean ribotypes isolated from mostly extreme environs.

Table 12: Phylotypic assignment of the OTU's obtained from T-RFs generated from enzymes *AluI*, *RsaI*, *HaeIII* and *HpaII* using MiCA III (PAT+)

Site	Enzyme	T-RF (bp)	Accession nr	Affiliation	Origin of clones
Sps02, Sps01	<i>AluI</i>	77		no affiliation	
Sps02	<i>AluI</i>	90	EU662680	Uncultured archaean S7	Cold sludge
Sps02	<i>HaeIII</i> , <i>HpaII</i> , <i>RsaI</i>	117	AF419644	Uncultured archaean CIR048	Marine sediment from the Guaymas Basin
Sps02	<i>AluI</i>	159	AF419644	Uncultured archaean CIR048	Marine sediment from the Guaymas Basin
GOB/Sps01	<i>RsaI</i>	259	FJ718924	Uncultured archaean 36	Mine pit (South Dakota)
Sps02	<i>RsaI</i>	279		no affiliation	
Sps02	<i>HpaII</i>	282	EF069338	Uncultured Marine Group I Crenarchaeote	Sediments collect from bathypelagic region in Antarctica
Sps02	<i>RsaI</i>	284		no affiliation	
GOB/Sps02	<i>HaeIII</i>	443		no affiliation	
Sps02	<i>HaeIII</i>	489		no affiliation	
Sps02	<i>RsaI</i>	516	GQ375000	Uncultured Haloarchaean Cry7 clone 54	Crystallised ponds in Australia

5.3 Summary of archaeal diversity findings

The DGGE analyses showed that all sites had low archaeal diversity. The results further showed that both Gobabeb and Swakopmund site 2 contained 45 ribotypes each, while Swakopmund site 1 contained 53 ribotypes. Also, sequencing analysis of selected DGGE

bands indicated the presence of mostly uncultured archaea (Table 12) which could possibly represent novel archaea based on their low sequence identities.

In T-RFLP analysis, tetrameric enzymes *RsaI*, *HaeIII* and *AluI* and the hetero-tetramer enzyme *HpaII* were used to assess OTU composition. Initially two enzymes (*HpaII* and *HaeIII*) were utilised, but because of the low number of OTUs obtained from the enzymes, an additional two (*AluI* and *RsaI*) were utilised. Even though two additional enzymes were utilised these two enzymes were also found to detect low archaeal diversity. Furthermore, all four enzymes were chosen based on their compatibility with the given primer set (8Fa/1492R) and because they have been used frequently in molecular studies to assess the OTU structure of archaea in marine environments (Moesender *et al.*, 2001; Luna *et al.*, 2009). Therefore, it was decided that the low levels of diversity detected was likely to be a true reflection of the diversity present. T-RFLP phylogenetic analysis revealed the archaeal diversity of site Sps02 to be slightly more diverse compared to GOB and Sps01 sites (Table 12). The higher archaeal diversity of Sps02 site may be the result of the more extreme soil chemistry of this site which would favour extremophiles. Also, archaeal diversity in salt pans tends to increase in more mineralised regions, with the *Halobacteria* group occupying the majority of the ribotypes in the more extreme pans (Grant *et al.*, 2001).

It should be noted, that the presence of a second larger 1800bp fragment in certain samples may have skewed the analysis. The 1492bp fragment was the recommended PCR fragment stipulated by the authors Costello and Schmidt (2006) to represent the archaea community, whereas the 1800bp fragment is reported to represent eukaryotes. In this study, although both fragments were amplified for the GOB sample, only the 1492bp fragment was gel purified prior to T-RFLP analysis. This larger fragment was analysed for Sps02 and found to in fact represent archaea. Therefore it is possible that the same diversity could have been missed for GOB. The assignment of T-RFs to sequences within the GenBank based on the MiCA III (PAT+) software affiliated five of the 13 T-RFs obtained with sample Sps02 to uncultured archaea of marine origin (Table 12). However, it is possible that 50% of unaffiliated T-RFs associated to sample Sps02 may represent eukaryotes, since the larger 1800bp fragment was used for downstream applications. Overall, the archaeal diversity for both Swakopmund site 1 and Gobabeb were found to be low, while Swakopmund site 2 was found to be slightly more diverse (Table 12).

Two DNA extraction methods were employed in this study, the modified Zhou *et al.* (1996) DNA extraction method (used for Gobabeb) and the commercial kit, Ultraclean soil (MoBio Laboratories, Inc.) used for Swakopmund (Sps01 and Sps02). The DNA extraction methods employed in this study could have contributed to the low archaeal numbers detected in all the sampling sites. An investigation done by Wang and Edwards (2009) has shown that a more specialised approach should be employed to extract DNA from archaea because of the organism's cell wall structure which is more rigid than that of eubacteria (Wang and Edwards, 2009). The investigators advocated that combinations of chemical and mechanical cell lysis tools are required to obtain good quality archaeal DNA for downstream applications. Interestingly, the commercial kit (Ultraclean soil) utilised within this study, includes both chemical and mechanical lysis, and however was not stringent enough to remove the salt inhibitors to enable the extraction of archaea DNA from the saline rich environments. However as limited samples were used for this study alternative DNA extraction methods could not be tested for the different sediment types observed between study sites.

5.4 Concluding remarks

In conclusion, even though two different fingerprinting techniques (DGGE and T-RFLP) were used to assess archaea community profiles, the two techniques could not be directly compared due to differences in methodology applied.

Finally, archaea diversity of the Namibian salt pans, although low, is in agreement with previous investigations and the results illustrate that the prevalence of archaea in different geographical regions differs. These differences observed in the prevalence of archaea can be attributed to the physio -chemical and biogeographical features of the individual salt pans, since it has been shown that archaeal diversity in salt pans across geographical regions tends to differ (Ochsenreiter *et al.*, 2002; Bidle *et al.*, 2005).

Chapter 6: General Discussion

In this study three geographically separated salt pans were analysed within the terrestrial environment of the Namib.

Physio-chemical analysis of the salt pan soils from the three sampling regions (Gobabeb, Swakopmund, site 1 and Swakopmund site 2) revealed a difference in both the chemical composition and physical characteristics of the soils, which ultimately influenced the microbial diversities detected at these sites. Based on the mineral composition and conductivity readings, Gobabeb soil was found to be less saline than the two Swakopmund sites (Sps01 and Sps02). Other researchers have found that NaCl is the dominant ion in the Namib salt pans - which is supported by the precipitated gypsum at a salt pan at Hosbeeb, situated near the Gobabeb site, consisting mostly of NaCl (Day and Seely, 1988; 1993). However, the Gobabeb site investigated in this study contained no gypsum and the salinity measurements were lower than those recorded at Hosbeeb. Since the mineral composition of the Namib salt pans is affected by evaporation rates in the region (Day, 1993) it is not surprising to find a shift in environmental conditions in the Gobabeb region due to the fluctuating weather conditions of the desert (Eckardt *et al.*, 2012).

The two Swakopmund samplings sites used in this study formed part of the Silver Lake playas in Swakopmund (Eisfeld) region. These Silver Lake playas are part of an abandoned salt mining site (Eckardt and Drake 2011), which were used to filter out unwanted minerals such as Mg^{2+} , Ca^{2+} , SO_4 and S in order to obtain pure NaCl. The salt mining procedure involves the use of one pan to filter out unwanted minerals which is accomplished by the precipitation of gypsum ($CaSO_4 \cdot 2H_2O$). The water obtained from pan number one, now “purified” and only containing NaCl is then pumped to the crystallising pan where the NaCl salts crystallise (Javor, 2002). This may explain why gypsum was only found at Sps02 and not Sps01 sites, which are about 1km apart.

Since the three sampling sites shared different physiochemical properties it was difficult to apply the same DNA extraction methodologies for the individual sampling sites and therefore made it impossible to compare the sites.

Even though metagenomic sequencing is a fast growing method of exploring microbial diversity in human and environmental microbiomes, Next generation sequencing (NGS) is still relatively expensive. Therefore many microbial ecologists still use fingerprinting techniques as they are cost effective and can be used to obtain a snapshot of an unknown microbial environment relatively quickly and easily. Fingerprinting techniques have a number of advantages and disadvantages in the analysis of microbial diversity studies. One the most common short falls of fingerprinting techniques such as DGGE, T-RFLP and ARDRA is the possibility of either over- or under representing microbial communities (Sekiguchi *et al.*, 2001; Thies, 2007; Yu *et al.*, 2008; Sklarz *et al.*, 2009). While in this study the overall microbial representation of the sample communities detected with DGGE and T-RFLP was similar, there were some minor discrepancies. For example in the bacterial section, for sample GOB1 DGGE analysis identified 19 OTUs while only six OTUs were identified for T-RFLP analysis using *HpaII* and three OTUs from *HaeIII*. The discrepancies between the two fingerprinting techniques can be seen in Figure 52, where the DGGE was found to possibly over represent the diversity compared to T-RFLP analysis. However, one should bear in mind that one of the short falls of T-RFLP analysis is that one T-RF can represent more than OTU (a phenomena known as homoplasy) (Thies, 2007), and evidence of this can be seen in 16Sr RNA gene clone libraries constructed for bacterial section (Appendix A, B and C) where one T-RF (120) was found to associate to more than one sequence.

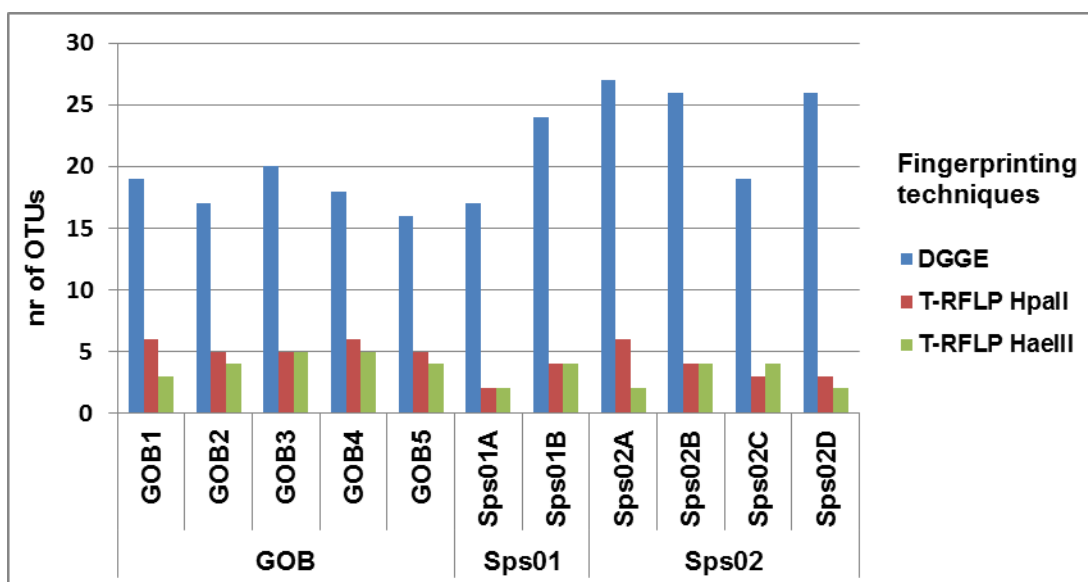


Figure 52: Comparison between the two different fingerprinting techniques (DGGE and T-RFLP) for three sampling sites. The OTUs obtained for DGGE is compared between the two restriction enzymes, *HpaII* and *HaeIII* used in T-RFLP analysis.

Similarly, ARDRA is known to over represent the number of taxa present within a sample site (Sklarz *et al.*, 2009). Theoretically, one restriction pattern should correspond to one phylotype, but the results obtained from ARDRA in this study clearly showed that the same phylotype was presented by several ARDRA patterns. This result can be seen in both 16S rRNA gene clone library construction for bacterial (Appendix A-C) and cyanobacterial sections (Appendix E-G) where ARDRA identified a diverse range of phylotypes, but on sequencing more than one restriction pattern was related to the same phylotype. ARDRA is unable to resolve intra species relationships, and can therefore present in more than one restriction pattern for the same species (Sklarz *et al.*, 2009).

As has been reported elsewhere, the majority of the 16S rRNA gene sequences were related to uncultured organisms. This is not surprising since it is estimated that 0.1 to 10% of the microbial population in a given habit are characterised (Panizzon *et al.*, 2015) with the majority of the known taxa being grouped into one of the four prominent bacterial phyla namely Proteobacteria, Firmicutes, Actinobacteria and Bacteroidetes (Rinke *et al.*, 2013). In this study Proteobacteria and Bacteroidetes were the most common phylotypes identified with Firmicutes, Cyanobacteria, Planctomycetes, Verrucomicrobia and *Nitrospira* forming minor groups. While for the Cyanobacterial analysis it was found that the majority of the phylotypes identified did not group with any known sequences on the reference databases (BLAST, SILVA and RDP).

In this study, two different DNA extraction methodologies was employed to analyse the different salt pans microbial communities thus prohibiting the direct correlation between these salt pan communities. In saying this, a common trend in microbial studies is to correlate the results obtained from the investigated site to other ‘similar’ referenced studies in which different DNA extraction methodologies, as well as analytical procedures, were employed especially for 16S rRNA gene-based studies (Kemp and Aller, 2004). Findings from this form of meta-analysis obtained from “pooling” data needs to be interpreted with some level of caution.

Other studies have found that salinity is the main driver of communities (Lopzupone and Knight, 2007), with the overall species diversity decreases and the archaeal diversity increases at higher saline concentrations (Nelson *et al.*, 2009). From the overall results obtained in this study (Figure 53) the less saline environment, Gobabeb, had a greater

bacterial and cyanobacterial species diversity, while the archaeal community was less abundant (Figure 53). Since archaea are more abundant in saline environments (Ventosa, 2006), it was not surprising to find the archaeal communities to be higher more abundant in the saline region of Swakopmund site 2 (Figure 53), although archaeal diversity was lower than expected. The number of archaea detected can be attributed to the DNA extraction methodology and to the primers used in this study (Pointing *et al.*, 2009; Singh, 2010). Since certain universal archaeal primers tend to bind to specific archaeal clades only (Baker and Cowan, 2004) and the use of degenerate primers were also found to influence primer specificity (Linhart and Shamir, 2002; Reed *et al.*, 2007).

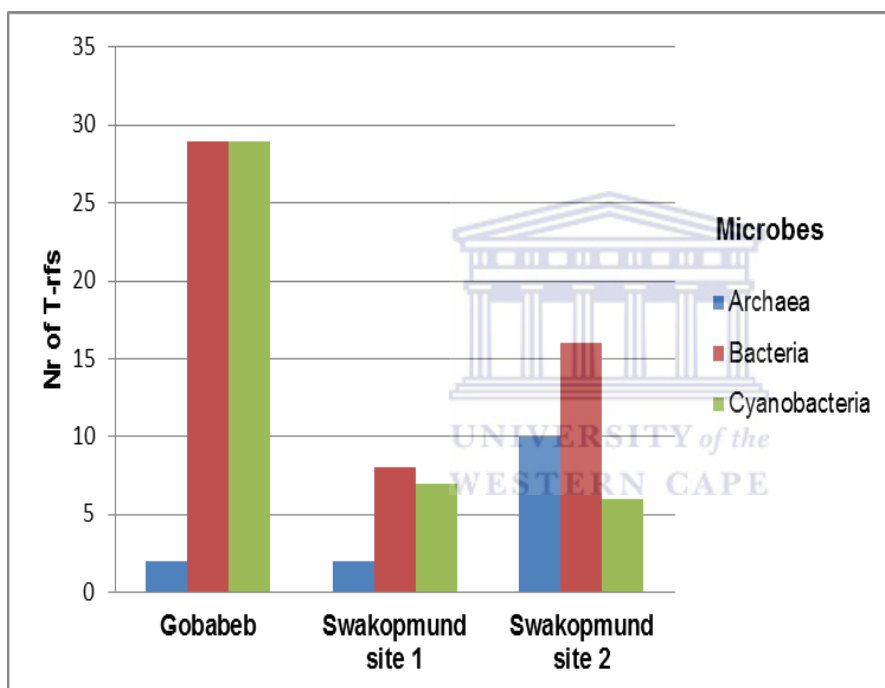


Figure 53: A summary of the number of archaea, bacteria and cyanobacteria OTU's obtained with T-RFLP analysis at the respective sampling sites.

Overall, the results obtained from this study indicated that the salt pans of Gobabeb site to be diverse, consisting of a rich bacterial population, dominated by one cyanobacterial community (*Cyanobacteria/Chloroplast*, Family VII). The salt pans of Swakopmund (Sps01 and Sps02) situated one kilometre away from one another were both found to contain small bacterial populations, with the two sites also dominated by the same cyanobacterial group(*Cyanobacteria/Chloroplast*, Family VII) as that of Gobabeb. Also, Sps01 was found to contain a larger group of unclassified bacteria or possibly a new cyanobacterial group compared to Sps02. Lastly, the fingerprinting techniques employed in this study provided a snapshot of the microbial biome encompassing the salt rich pans of the Namib.

6.1 Future Prospects

The focus of this study was to determine the microbial diversity of two Namib Desert salt ponds. The results obtained indicate that a diverse and unique microbial community is present in these extreme saline pools.

Although easily accessible and cost effective, fingerprinting techniques are now being replaced by 16S rRNA gene metagenomics and whole genome sequencing which provides for a more comprehensive view of the microbial communities. As this study is one of the first studies to identify archaea sequences using molecular methods within the Namib Desert environment, future studies could include NGS analysis of the archaea amplicons generated in order to obtain a more in depth analysis of the diversity present.

Even though, metagenomic sequencing has improved our way of studying microbial biomes of both the human and environmental sectors, it doesn't impact on the fact that a large number of microbes still remain uncultured. It is imperative that more emphasis should be placed on finding novel techniques as to improve the manner in which cultured techniques are approached and also, most importantly, the manner in which microbial diversity studies are carried out. Universal standards outlining how microbial studies should be conducted should be adopted to make it easier to directly compare further studies such as the human microbiome and earth microbiome projects.

This study faced many technical challenges, such as difficulties in extracting DNA from the highly saline samples and PCR anomalies. However, the findings did provide an overview of the rich microbial diversity present within the Namib Desert salt pans which can ultimately lead to the discovery of novel applications within the field of biotechnology.



Appendix A: Chapter 3-Gobabeb site. T-RFs matched to Blast results of clones obtained from Genbank for 16S rRNA gene bacterial libraries

T-RFs (bp)							
<i>Hae</i> III	<i>Hpa</i> II	Cluster	Clone	Accession nr of the closest phylogenetic ancestor	Sequence Affiliation	% Sequence similarity	Source of clone
		1	GOB38	EU246225.1	Uncultured organism clone MAT-CR-P5-E02 16S ribosomal RNA gene, part	99	Soil collected around the hospital Courtyard (Boston, MA)
			GOB120				
			GOB133				
			GOB32				
			GOB136				
		2	GOB4-11	AB078081.1	<i>Microscilla sericea</i> gene for 16S rRNA, strain:IFO 15983	99	cultured from strain
			GOB4-54				
			GOB4-32				
120		3	GOB4-14		Uncultured bacterium clone LGH02-B-071 16S ribosomal RNA gene, partial	99	Terrestrial mud volcano (Eastern Taiwan)
			GOB4-122				
			GOB4				
		4	GOB28	JN452340.1	Uncultured organism clone SBYG_6754 16S ribosomal RNA gene, partial sequence	94	Hypersaline Microbial mat (Guerrero Negro)
			GOB24				
		5	GOB4-29	JN811708.1	Uncultured bacterium clone LGH02-B-159 16S ribosomal RNA gene, partial sequence	99	sediment and water samples terrestrial mud volcano (Eastern Taiwan)
220		6	GOB4-2	EF190068.1	Uncultured <i>Psychroflexus</i> sp. clone GSX1 16S ribosomal RNA gene, partial sequence	95	Qinghai oilfield
			GOB4-123				
			GOB4-55				
202		7	GOB37	JN505140.1	Uncultured organism clone SBZA_6447 16S ribosomal RNA gene, partial se	99	Hypersaline Microbial mat (Guerrero Negro)
			GOB150				

120, 203	120	8	GOB4-10	AB247829.1	Uncultured <i>gamma proteobacterium</i> gene for 16S rRNA, partial sequence, clone: pLM5B-19	99	hydrothermal vents
			GOB9				
		9	GOB18	JN437385.1	Uncultured organism clone SBXZ_6344 16S ribosomal RNA gene, partial sequence	98	Hypersaline Microbial mat (Guerrero Negro)
			GOB4-39				
203		10	GOB23	AY344367.2	Unidentified bacterium clone K2-30-25 16S ribosomal RNA gene, partial sequence	96	marine water sample (Hawaiian Archipelago)
		11	GOB4-26	HQ190527.1	Uncultured bacterium clone BP47 16S ribosomal RNA gene, partial sequence	98	Zhongyuan oil field
		12	GOB129	AY711386.1	Uncultured bacterium clone SIMO-2020 16S ribosomal RNA gene, partial sequence	99	salt marsh
280		13	GOB102	JQ612262.1	Uncultured bacterium clone GBc134 16S ribosomal RNA gene, partial sequence	97	marine <i>Geodia barretti</i> sponge
			14	GOB4-34	NR_040918.1	<i>Marivirga tractuosa</i> DSM 4126 strain IFO 15989 16S ribosomal RNA, partial sequence	99
		GOB4-44					
		GOB4-129					
	85	15	GOB4-130	AB598223.1	Uncultured bacterium gene for 16S rRNA, partial sequence, clone: 357D_B9	99	sub seafloor sediments
		16	GOB123	JN881628.1	Uncultured <i>Planctomycetales</i> bacterium clone PNG_TBG_B38 16S ribosomal RNA gene, partial sequence	96	arsenic shallow sea hydrothermal vent (Papua New Guinea)
		17	GOB145	JF703676.1	<i>Leptolyngbya</i> sp. SM-13 16S ribosomal RNA gene, partial sequence	98	soil
220		18	GOB116	AM998246.1	Uncultured deep-sea bacterium partial 16S rRNA gene, clone Ulrdd_47	95	deep-sea surface sediments (South Atlantic)
			85	19	GOB146	JX162153.1	Uncultured bacterium clone CaletaPalS37 16S ribosomal RNA gene, partial
		20	GOB4-101	AB113191.1	Uncultured <i>epsilon proteobacterium</i> gene for 16S rRNA, partial sequence, clone:pCIRB-85	85	deep-sea hydrothermal field (slime)
		21	GOB134	JX047086.1	Uncultured bacterium clone KSB113 16S ribosomal RNA gene, partial sequence	92	marine hot springs (Indonesia)
		22	GOB17	JQ580165.1	Uncultured <i>planctomycete</i> clone RII-OX078 16S ribosomal RNA gene, partial	93	oil-polluted subtidal sediments

230		23	GOB4-47	JN443115.1	Uncultured organism clone SBYB_6632 16S ribosomal RNA gene, partial sequence	96	Hypersaline Microbial mat (Guerrero Negro)
76	76, 126	24	GOB4-114	JN436310.1	Uncultured organism clone SBXZ_5146 16S ribosomal RNA gene, partial sequence	99	Hypersaline Microbial mat (Guerrero Negro)
		25	GOB108	JN178461.1	Uncultured bacterium clone TX2_6D21 16S ribosomal RNA gene, partial sequence	93	saline-alkaline soil (lake Texcoco)
		26	GOB4-21	JN496973.1	Uncultured organism clone SBYZ_2383 16S ribosomal RNA gene, partial sequence	98	Hypersaline Microbial mat (Guerrero Negro)
202		27	GOB111	EU735674.1	Uncultured bacterium clone SN87 16S ribosomal RNA gene, partial sequence	88	oil-contaminated and pristine soils
		28	GOB33	JN432396.1	Uncultured organism clone SBXZ_2271 16S ribosomal RNA gene, partial se	99	Hypersaline Microbial mat (Guerrero Negro)
		29	GOB43	FM175466.1	Uncultured <i>Geothermobacter</i> sp. partial 16S rRNA gene, clone CL2.C166	93	tufa core (Hot springs) tufa formed due to the precipitation of carbonate minerals
		30	GOB103	JQ366607.2	Uncultured bacterium clone MD15h2_117 16S ribosomal RNA gene, partial	93	soil samples from Open Top Chamber
		31	GOB144	HQ857689.1	Uncultured <i>Bacteroidetes</i> bacterium clone BPS_H554 16S ribosomal RNA g	97	saline alkaline soil
		32	GOB39	DQ103635.1	Uncultured bacterium clone E4bF06 16S ribosomal RNA gene, partial sequence	86	salt crust from salterns (Eilat, Israel)
		33	GOB11	FM210986.1	Uncultured bacterium partial 16S rRNA gene, clone XH147	97	biomass from Salt lakes (Mongolia, China and Argentina)
		34	GOB15	JX162143.1	Uncultured bacterium clone CanalPalS28 16S ribosomal RNA gene, partial sequence	98	marine sediments (Chile)
		35	GOB29	FN553632.1	Uncultured sediment bacterium 16S rRNA gene, clone 285-57	97	Sediment from a hydrothermal flied
	120	36	GOB32	EU246225.1	Uncultured organism clone MAT-CR-P5-E02 16S ribosomal RNA gene, part	99	Soil collected around the hospital

							Courtyard (Boston)
		37	GOB4-131	JN683993.1	Uncultured bacterium clone M2_170_E5 16S ribosomal RNA gene, partial sequence	98	saline waste water
120		39	GOB4-60	JN418887.1	Uncultured soil bacterium clone B 16S ribosomal RNA gene, partial sequence	92	soil samples (Yamuna river)
		40	GOB4-3	FJ973579.1	Uncultured bacterium clone SS_WC_09 16S ribosomal RNA gene, partial sequence	98	water sample, hypersaline lake (California)
203	464	41	GOB26	HE662522.1	Uncultured bacterium partial 16S rRNA gene, clone S17	88	Rhizosphere of wheat
		42	GOB4-127	FJ717265.1	Uncultured bacterium clone B4_10.4_1 16S ribosomal RNA gene, partial sequence	87	isolated in a lugwurm, <i>Arenicola marina L.</i>
		43	GOB4-7	AY749436.1	<i>Sphingomonas</i> sp. SKJH-30 16S ribosomal RNA gene, partial sequence	99	Liquid nitrogen vessels
		44	GOB6	EU735689.1	Uncultured bacterium clone SN133 16S ribosomal RNA gene, partial sequence	95	oil-contaminated and pristine soils
		45	GOB46	FM214392.1	Uncultured bacterium partial 16S rRNA gene, clone Crozet_s_911	90	Marine sediments (Indian ocean)
		46	GOB27	JX391510.1	Uncultured bacterium clone N0074 16S ribosomal RNA gene, partial sequence	96	surface marine sediment
		47	GOB4-46	HQ183779.1	Uncultured <i>Clostridiisalibacter</i> sp. clone De242 16S ribosomal RNA gene, partial sequence	93	leachate sediment in a landfill waste site (China)

Appendix B: Chapter 3- Swakopmund site 1. T-RFs matched to Blast results of clones obtained from Genbank for 16S rRNA gene bacterial libraries

T-RFs (bp)							
<i>HaeIII</i>	<i>HpaII</i>	Cluster	Clone	Accession nr of the closest phylogenetic ancestor	Sequence Affiliation	% Sequence similarity	Source of clone
		1	Sps01-60	FM210946.1	Uncultured bacterium partial 16S rRNA gene, clone EN107	88	biomass from Salt lakes (Mongolia, China and Argentina)
			Sps01-165				
			Sps01-15				
			Sps01-5				
			Sps01-13				
120		2	Sps01-2	EU869403.1	Uncultured bacterium clone ARDBACWH3 16S ribosomal RNA gene, partial sequence	89	Hypersaline salt lakes (Algerian, Sahara)
			Sps01-10				
			Sps01-76			90	
			Sps01-55			89	
			Sps01-4			89	
			Sps01-77				
			Sps01-89				
		3	Sps01-68	AB533985.1	Uncultured bacterium gene for 16S rRNA, partial sequence, clone: 45-P2	96	Death Valley California
			Sps01-1				
			Sps01-16			95	
			Sps01-24				
			Sps01-92			97	
	489	4	Sps01-23	AB533936.1	Uncultured bacterium gene for 16S rRNA, partial sequence, clone: 19-P2	97	Death Valley California
			Sps01-53				
			Sps01-172				
	489	5	Sps01-18	AB533966.1	Uncultured bacterium gene for 16S rRNA, partial sequence, clone: 36-P1	98	Death Valley California
			Sps01-19				

			Sps01-31					
			Sps01-20					
		6	Sps01-74	JN435736.1	Uncultured organism clone SBXZ_4535 16S ribosomal RNA gene, partial se	97	Hypersaline Microbial mat (Guerrero Negro)	
			Sps01-88					
			Sps01-170					
		7	Sps01-29	DQ490464.1	<i>Sphingobacteriaceae</i> bacterium KVD-1969-11 16S ribosomal RNA gene, partial sequence	99	Hawaiian volcanic deposits	
			Sps01-72					
		8	Sps01-87	EU869422.1	Uncultured bacterium clone ARDBACWH88 16S ribosomal RNA gene, partial sequence	94	Hypersaline salt lakes (Algerian, Sahara)	
		9	Sps01-58	HM126955.1	Uncultured bacterium clone SINI583 16S ribosomal RNA gene, partial sequence	99	Tibetan Lake	
		10	Sps01-90	EU869422.1	Uncultured bacterium clone ARDBACWH88 16S ribosomal RNA gene, partial sequence	94	Hypersaline salt lakes (Algerian, Sahara)	
		11	Sps01-45	AB533965.1	Uncultured bacterium gene for 16S rRNA, partial sequence, clone: 35-P2	98	Death valley California	
		12	Sps01-69	AB533953.1	Uncultured bacterium gene for 16S rRNA, partial sequence, clone: 29-P1	90	Death valley California	
		13	Sps01-76	AB533957.1	Uncultured bacterium gene for 16S rRNA, partial sequence, clone: 31-P1	97	Death valley California	
		14	Sps01-96	DQ103665.1	Uncultured bacterium clone E2aE11 16S ribosomal RNA gene, partial sequence	92	hypersaline microbial mat (Eilat ,Israel)	
		15	Sps01-99	GU368364.1	Uncultured bacterium clone C28 16S ribosomal RNA gene, partial sequence	99	water samples collected from copper pipes	
		16	Sps01-81	KC160785.1	<i>Caulobacter</i> sp. SS14.14 16S ribosomal RNA gene, partial sequence	100	coastal sediments (Antarctica)	
		17	Sps01-91	JF343980.1	Uncultured <i>gamma proteobacterium</i> clone RODAS-002 16S ribosomal RNA gene, partial sequence	86	oil-polluted subtidal sediments	
		18	Sps01-78	HQ857647.1	Uncultured bacterium clone BPS_CK147 16S ribosomal RNA gene, partial sequence	83	Contaminated alkali saline soil	
		19	Sps01-39	AB533976.1	Uncultured bacterium gene for 16S rRNA, partial sequence, clone: 41-P1	97	Death valley California	

		20	Sps01-25	AY360587.1	Uncultured <i>Methylobacteriaceae</i> bacterium clone H5Ba35 small subunit rib	97	Soil samples collected from rice field in Italy
		21	Sps01-69	AB533953.1	Uncultured bacterium gene for 16S rRNA, partial sequence, clone: 29-P1	90	Death valley California



Appendix C: Chapter 3-Swakopmund site 2. T-RFs matched to Blast results of clones obtained from Genbank for 16S rRNA gene bacterial libraries

T-RFs (bp)							
<i>HaeIII</i>	<i>HpaII</i>	Cluster	Clone	Accession nr of the closest phylogenetic ancestor	Sequence Affiliation	% Sequence similarity	Source of clone
120		1	Sps02-7	EF409427.1	<i>Idiomarina</i> sp. BSw10113 16S ribosomal RNA gene, partial sequence	100	Polar region
			Sps02-5			99	
			Sps02-15				
			Sps02-32				
			Sps02-8				
		2	Sps02-6	JN437385.1	Uncultured organism clone SBXZ_6344 16S ribosomal RNA gene, partial sequence	99	Hypersaline Microbial mat (Guerrero Negro)
	Sps02-80						
		3	Sps02-14	AB243989.1	Uncultured bacterium gene for 16S rRNA, partial sequence, clone: Niigata-21	97	Death Valley California
	Sps02-18		96				
	Sps02-20		99				
	Sps02-21		99				
		4	Sps02-68	EU245063.1	Uncultured organism clone MAT-CR-H1-C12 16S ribosomal RNA gene, partial sequence	98	Soil collected around the hospital Courtyard (Boston, MA)
		5	Sps02-11	FJ404759.1	<i>Idiomarina</i> sp. SP96 16S ribosomal RNA gene, partial sequence	99	marine bacteria (East sea, China)
	Sps02-112						
	Sps02-43						
	81	6	Sps02-9	GQ441204.1	Uncultured bacterium clone GBI-13 16S ribosomal RNA gene, partial sequence	96	coastal microbial mats
	120	7	Sps02-3	GQ441204.1	Uncultured bacterium clone GBI-13 16S ribosomal RNA gene, partial sequence	96	coastal microbial mats
		8	Sps02-48	JQ975846.1	Bacterium enrichment culture clone 1E01 16S ribosomal RNA gene, partial	97	marine (Indian

					sequence		Ocean)
		9	Sps02-13	FJ516792.1	Uncultured <i>Erythrobacteraceae</i> bacterium clone TDNP_Bbc97_26_4_66 16S ribosomal RNA gene, partial sequence	99	soils from wetlands (Central Spain)
		10	Sps02-1	HM134559.1	Uncultured marine bacterium clone D15_12_AuS_163 16S ribosomal RNA gene, partial sequence	99	Coastal Seawater
	170	11	Sps02-67	EU245110.1	Uncultured organism clone MAT-CR-H2-C04 16S ribosomal RNA gene, partial sequence	99	Soil collected around the hospital Courtyard (Boston, MA)
		12	Sps02-42	EU917886.1	Uncultured bacterium clone Cyano2B08 16S ribosomal RNA gene, partial sequence	99	Stromatolites (Bahamas)



Appendix D: Chapter 3-Phylogenetic affiliation of bacterial 16S rR RNA gene clone based on RDP Classifier

Clone	Phylum	%	Class	%	Family	%	Genus	%
Sps01A-12	<i>Bacteroidetes</i>	97%	<i>Sphingobacteria</i>	74%	<i>Flammeovirgaceae</i>	45%	<i>Perexilibacter</i>	15%
Sps01A-15	<i>Planctomycetes</i>	36%	<i>Planctomycetacia</i>	36%	<i>Planctomycetaceae</i>	36%	<i>Blastopirellula</i>	26%
Sps01A_16	<i>Cyanobacteria/Chloroplast</i>	100%	<i>Cyanobacteria</i>	100%	<i>GpVII</i>	99%		
Sps01A_160	<i>Planctomycetes</i>	42%	<i>Planctomycetacia</i>	42%	<i>Planctomycetaceae</i>	42%	<i>Blastopirellula</i>	28%
Sps01A_165	<i>Planctomycetes</i>	42%	<i>Planctomycetacia</i>	42%	<i>Planctomycetaceae</i>	42%	<i>Blastopirellula</i>	28%
Sps01A_170	<i>Firmicutes</i>	100%	<i>Clostridia</i>	100%	<i>Clostridiaceae 3</i>	100%	<i>Sporosalibacterium</i>	99%
Sps01A_172	<i>Bacteroidetes</i>	100%	<i>Sphingobacteria</i>	100%	<i>Rhodothermaceae</i>	100%	<i>Salinibacter</i>	99%
Sps01A_18	<i>Bacteroidetes</i>	100%	<i>Sphingobacteria</i>	100%	<i>Rhodothermaceae</i>	100%	<i>Salinibacter</i>	94%
Sps01A_19	<i>Bacteroidetes</i>	100%	<i>Sphingobacteria</i>	100%	<i>Rhodothermaceae</i>	100%	<i>Salinibacter</i>	98%
Sps01A_20	<i>Bacteroidetes</i>	100%	<i>Sphingobacteria</i>	100%	<i>Rhodothermaceae</i>	100%	<i>Salinibacter</i>	98%
Sps01A_23	<i>Bacteroidetes</i>	100%	<i>Sphingobacteria</i>	100%	<i>Rhodothermaceae</i>	100%	<i>Salinibacter</i>	99%
Sps01A_24	<i>Cyanobacteria/Chloroplast</i>	83%	<i>Cyanobacteria</i>	83%	<i>GpVII</i>	76%		
Sps01A_25	<i>Proteobacteria</i>	100%	<i>Alphaproteobacteria</i>	98%	<i>Methylobacteriaceae</i>	39%	<i>Methylobacterium</i>	37%
Sps01A_29	<i>Bacteroidetes</i>	100%	<i>Sphingobacteria</i>	100%	<i>Sphingobacteriaceae</i>	100%	<i>Pedobacter</i>	100%
Sps01A_31	<i>Bacteroidetes</i>	100%	<i>Sphingobacteria</i>	100%	<i>Rhodothermaceae</i>	100%	<i>Salinibacter</i>	95%
Sps01A_39	<i>Bacteroidetes</i>	100%	<i>Sphingobacteria</i>	100%	<i>Rhodothermaceae</i>	100%	<i>Salinibacter</i>	100%
Sps01A_53	<i>Bacteroidetes</i>	100%	<i>Sphingobacteria</i>	100%	<i>Rhodothermaceae</i>	100%	<i>Salinibacter</i>	98%
Sps01A_69	<i>Bacteroidetes</i>	76%	<i>Sphingobacteria</i>	59%	<i>Chitinophagaceae</i>	34%	<i>Filimonas</i>	33%
Sps01A_69	<i>Bacteroidetes</i>	89%	<i>Sphingobacteria</i>	74%	<i>Chitinophagaceae</i>	21%	<i>Parasegetibacter</i>	9%
Sps01A_72	<i>Bacteroidetes</i>	100%	<i>Sphingobacteria</i>	100%	<i>Sphingobacteriaceae</i>	100%	<i>Pedobacter</i>	100%
Sps01A_74	<i>Cyanobacteria/Chloroplast</i>	100%	<i>Cyanobacteria</i>	100%	<i>GpVII</i>	100%		
Sps01A_76	<i>Bacteroidetes</i>	100%	<i>Sphingobacteria</i>	100%	<i>Rhodothermaceae</i>	100%	<i>Salinibacter</i>	100%
Sps01A_78	<i>Proteobacteria</i>	50%	<i>Epsilonproteobacteria</i>	26%	<i>Nautiliaceae</i>	20%	<i>Nitratiruptor</i>	14%
Sps01A_81	<i>Proteobacteria</i>	100%	<i>Alphaproteobacteria</i>	100%	<i>Caulobacteraceae</i>	100%	<i>Caulobacter</i>	100%
Sps01A_88	<i>Cyanobacteria/Chloroplast</i>	100%	<i>Cyanobacteria</i>	100%	<i>GpVII</i>	100%		
Sps01B_1	<i>Cyanobacteria/Chloroplast</i>	100%	<i>Cyanobacteria</i>	100%	<i>GpVII</i>	100%		
Sps01B_10	<i>Firmicutes</i>	47%	<i>Clostridia</i>	44%	<i>Clostridiales_Incertae Sedis XII</i>	20%	<i>Fusibacter</i>	13%
Sps01B_13	<i>Planctomycetes</i>	40%	<i>Planctomycetacia</i>	40%	<i>Planctomycetaceae</i>	40%	<i>Blastopirellula</i>	28%
Sps01B_2	<i>Firmicutes</i>	47%	<i>Clostridia</i>	43%	<i>Clostridiales_Incertae Sedis XII</i>	28%	<i>Fusibacter</i>	14%

Sps01B_28	Cyanobacteria/Chloroplast	96%	Cyanobacteria	96%	GpVII	89%		
Sps01B_35	Firmicutes	90%	Clostridia	86%	Thermoanaerobacteraceae	35%	Syntrophaceticus	31%
Sps01B_4	Proteobacteria	40%	Deltaproteobacteria	37%	Syntrophaceae	21%	Smithella	20%
Sps01B_45	Cyanobacteria/Chloroplast	100%	Cyanobacteria	100%	GpVII	99%		
Sps01B_5	Planctomycetes	34%	Planctomycetacia	33%	Planctomycetaceae	33%	Blastopirellula	21%
Sps01B_55	Proteobacteria	56%	Deltaproteobacteria	40%	Syntrophaceae	13%	Desulfobacca	10%
Sps01B_58	Proteobacteria	100%	Gammaproteobacteria	100%	Ectothiorhodospiraceae	53%	Thiohalospira	22%
Sps01B_68	Cyanobacteria/Chloroplast	100%	Cyanobacteria	100%	GpVII	100%		
Sps01B_76	Actinobacteria	12%	Actinobacteria	12%	Actinomycetales	11%	Streptosporangineae	4%
Sps01B_77	Proteobacteria	42%	Deltaproteobacteria	34%	Desulfobulbaceae	20%	Desulfofustis	18%
Sps01B_87	Bacteroidetes	27%	Sphingobacteria	25%	Flammeovirgaceae	22%	Flexithrix	20%
Sps01B_89	Firmicutes	47%	Clostridia	43%	Clostridiales_Incertae Sedis XII	28%	Fusibacter	14%
Sps01B_90	Proteobacteria	52%	Betaproteobacteria	25%	Comamonadaceae	17%	Pseudacidovorax	8%
Sps01B_91	Proteobacteria	94%	Gammaproteobacteria	85%	Thiotrichaceae	15%	Beggiatoa	15%
Sps01B_92	Cyanobacteria/Chloroplast	100%	Cyanobacteria	100%	GpVII	100%		
Sps01B_96	Proteobacteria	100%	Gammaproteobacteria	88%	Ectothiorhodospiraceae	44%	Thiorhodospira	41%
Sps01B_99	Proteobacteria	100%	Alphaproteobacteria	100%	Sphingomonadaceae	100%	Sphingomonas	100%
Sps02_1	Proteobacteria	100%	Gammaproteobacteria	100%	Idiomarinaceae	100%	Idiomarina	100%
Sps02_11	Proteobacteria	100%	Gammaproteobacteria	100%	Idiomarinaceae	100%	Idiomarina	100%
Sps02_112	Proteobacteria	100%	Gammaproteobacteria	100%	Alteromonadaceae	100%	Marinimicrobium	99%
Sps02_13	Proteobacteria	100%	Alphaproteobacteria	100%	Erythrobacteraceae	99%	Erythrobacter	90%
Sps02_14	Deinococcus-Thermus	15%	Deinococci	15%	Deinococcaceae	14%	Deinobacterium	14%
Sps02_15	Proteobacteria	100%	Gammaproteobacteria	100%	Idiomarinaceae	100%	Idiomarina	100%
Sps02_18	Bacteroidetes	29%	Sphingobacteria	6%	Saprospiraceae	2%	Haliscomenobacter	2%
Sps02_20	Chlamydiae	17%	Chlamydiae	17%	Parachlamydiaceae	16%	Parachlamydia	15%
Sps02_21	Bacteroidetes	26%	Sphingobacteria	9%	Saprospiraceae	6%	Haliscomenobacter	6%
Sps02_3	Proteobacteria	100%	Gammaproteobacteria	100%	Saccharospirillaceae	92%	Saccharospirillum	92%
Sps02_32	Proteobacteria	100%	Gammaproteobacteria	100%	Idiomarinaceae	100%	Idiomarina	100%
Sps02_42	Proteobacteria	100%	Alphaproteobacteria	99%	Phyllobacteriaceae	42%	Pseudaminobacter	19%
Sps02_43	Bacteroidetes	99%	Sphingobacteria	79%	Chitinophagaceae	22%	Parasetetibacter	17%
Sps02_48	Proteobacteria	100%	Gammaproteobacteria	100%	Alteromonadaceae	100%	Marinobacter	100%
Sps02_5	Proteobacteria	100%	Gammaproteobacteria	100%	Idiomarinaceae	100%	Idiomarina	100%

Sps02_6	<i>Bacteroidetes</i>	97%	<i>Sphingobacteria</i>	78%	<i>Cytophagaceae</i>	29%	<i>Persicitalea</i>	14%
Sps02_67	<i>Firmicutes</i>	100%	<i>Clostridia</i>	100%	<i>Clostridiaceae 3</i>	98%	<i>Sporosalibacterium</i>	84%
Sps02_68	<i>Firmicutes</i>	100%	<i>Clostridia</i>	100%	<i>Clostridiaceae 3</i>	94%	<i>Sporosalibacterium</i>	89%
Sps02_7	<i>Proteobacteria</i>	100%	<i>Gammaproteobacteria</i>	100%	<i>Idiomarinaceae</i>	100%	<i>Idiomarina</i>	100%
Sps02_8	<i>Proteobacteria</i>	100%	<i>Gammaproteobacteria</i>	100%	<i>Idiomarinaceae</i>	100%	<i>Idiomarina</i>	100%
Sps02_80	<i>Bacteroidetes</i>	100%	<i>Sphingobacteria</i>	89%	<i>Flammeovirgaceae</i>	29%	<i>Cesiribacter</i>	12%
Sps02_9	<i>Proteobacteria</i>	100%	<i>Gammaproteobacteria</i>	100%	<i>Saccharospirillaceae</i>	81%	<i>Saccharospirillum</i>	81%
Sps02_9	<i>Proteobacteria</i>	100%	<i>Gammaproteobacteria</i>	100%	<i>Saccharospirillaceae</i>	93%	<i>Saccharospirillum</i>	93%
GOB_102	<i>Nitrospira</i>	100%	<i>Nitrospira</i>	100%	<i>Nitrospiraceae</i>	100%	<i>Nitrospira</i>	100%
GOB_103	<i>Proteobacteria</i>	97%	<i>Deltaproteobacteria</i>	85%	<i>Geobacteraceae</i>	35%	<i>Geoalkalibacter</i>	28%
GOB_108	<i>Bacteroidetes</i>	100%	<i>Sphingobacteria</i>	100%	<i>Chitinophagaceae</i>	100%	<i>Gracilimonas</i>	89%
GOB_11	<i>Bacteroidetes</i>	100%	<i>Sphingobacteria</i>	100%	<i>Rhodothermaceae</i>	100%	<i>Salinibacter</i>	100%
GOB_111	<i>Proteobacteria</i>	93%	<i>Alphaproteobacteria</i>	91%	<i>Rhodobiaceae</i>	35%	<i>Afifella</i>	30%
GOB_116	<i>Proteobacteria</i>	100%	<i>Gammaproteobacteria</i>	99%	<i>Alcanivoracaceae</i>	66%	<i>Alcanivorax</i>	66%
GOB_120	<i>Bacteroidetes</i>	100%	<i>Sphingobacteria</i>	100%	<i>Saprospiraceae</i>	100%	<i>Haliscomenobacter</i>	99%
GOB_123	<i>Firmicutes</i>	73%	<i>Bacilli</i>	73%	<i>Pasteuriaceae</i>	73%	<i>Pasteuria</i>	73%
GOB_129	<i>Proteobacteria</i>	32%	<i>Gammaproteobacteria</i>	5%	<i>Halomonadaceae</i>	2%	<i>Modicisalibacter</i>	1%
GOB_133	<i>Bacteroidetes</i>	100%	<i>Sphingobacteria</i>	99%	<i>Saprospiraceae</i>	99%	<i>Haliscomenobacter</i>	98%
GOB_134	<i>Bacteroidetes</i>	80%	<i>Sphingobacteria</i>	79%	<i>Rhodothermaceae</i>	75%	<i>Salisaeta</i>	48%
GOB_136	<i>Bacteroidetes</i>	100%	<i>Sphingobacteria</i>	100%	<i>Saprospiraceae</i>	100%	<i>Haliscomenobacter</i>	99%
GOB_144	<i>Bacteroidetes</i>	100%	<i>Sphingobacteria</i>	100%	<i>Chitinophagaceae</i>	100%	<i>Balneola</i>	54%
GOB_145	<i>Cyanobacteria/Chloroplast</i>	100%	<i>Cyanobacteria</i>	100%	<i>GpIV</i>	48%		
GOB_146	<i>Proteobacteria</i>	100%	<i>Gammaproteobacteria</i>	100%	<i>Methylohalomonas</i>	38%		
GOB_15	<i>Proteobacteria</i>	43%	<i>Deltaproteobacteria</i>	32%	<i>Desulfarculaceae</i>	6%	<i>Desulfarculus</i>	6%
GOB_150	<i>Bacteroidetes</i>	100%	<i>Sphingobacteria</i>	100%	<i>Saprospiraceae</i>	97%	<i>Haliscomenobacter</i>	82%
GOB_18	<i>Bacteroidetes</i>	95%	<i>Sphingobacteria</i>	85%	<i>Cytophagaceae</i>	33%	<i>Persicitalea</i>	11%
GOB_23	<i>Proteobacteria</i>	100%	<i>Gammaproteobacteria</i>	100%	<i>Moraxellaceae</i>	36%	<i>Enhydrobacter</i>	30%
GOB_24	<i>Bacteroidetes</i>	100%	<i>Sphingobacteria</i>	100%	<i>Saprospiraceae</i>	99%	<i>Haliscomenobacter</i>	67%
GOB_26	<i>Verrucomicrobia</i>	100%	<i>Opitutae</i>	100%	<i>Puniceococcaceae</i>	99%	<i>Puniceococcus</i>	95%
GOB_27	<i>Proteobacteria</i>	100%	<i>Gammaproteobacteria</i>	100%	<i>Hahellaceae</i>	58%	<i>Hahella</i>	58%
GOB_28	<i>Bacteroidetes</i>	100%	<i>Sphingobacteria</i>	100%	<i>Saprospiraceae</i>	100%	<i>Haliscomenobacter</i>	55%
GOB_29	<i>Proteobacteria</i>	100%	<i>Gammaproteobacteria</i>	100%	<i>Coxiellaceae</i>	87%	<i>Coxiella</i>	87%

GOB_32	<i>Bacteroidetes</i>	100%	<i>Sphingobacteria</i>	100%	<i>Saprospiraceae</i>	100%	<i>Haliscomenobacter</i>	100%
GOB_32	<i>Planctomycetes</i>	39%	<i>Planctomycetacia</i>	39%	<i>Planctomycetaceae</i>	39%	<i>Blastopirellula</i>	24%
GOB_33	<i>Bacteroidetes</i>	100%	<i>Flavobacteria</i>	84%	<i>Cryomorphaceae</i>	39%	<i>Owenweeksia</i>	24%
GOB_37	<i>Bacteroidetes</i>	100%	<i>Sphingobacteria</i>	100%	<i>Saprospiraceae</i>	98%	<i>Haliscomenobacter</i>	82%
GOB_38	<i>Bacteroidetes</i>	100%	<i>Sphingobacteria</i>	100%	<i>Saprospiraceae</i>	100%	<i>Haliscomenobacter</i>	98%
GOB_39	<i>Bacteroidetes</i>	94%	<i>Sphingobacteria</i>	84%	<i>Flammeovirgaceae</i>	50%	<i>Limibacter</i>	27%
GOB_4	<i>Proteobacteria</i>	100%	<i>Gammaproteobacteria</i>	100%	<i>Idiomarinaceae</i>	100%	<i>Idiomarina</i>	100%
GOB_43	<i>Proteobacteria</i>	63%	<i>Deltaproteobacteria</i>	59%	<i>Syntrophaceae</i>	27%	<i>Smithella</i>	19%
GOB_46	<i>Gemmatimonadetes</i>	14%	<i>Gemmatimonadetes</i>	14%	<i>Gemmatimonadaceae</i>	14%	<i>Gemmatimonas</i>	14%
GOB_6	<i>Proteobacteria</i>	100%	<i>Gammaproteobacteria</i>	100%	<i>Thiohalomonas</i>	100%		
GOB_9	<i>Proteobacteria</i>	100%	<i>Gammaproteobacteria</i>	100%	<i>Methylohalomonas</i>	32%		
GOB_17	<i>Planctomycetes</i>	99%	<i>Planctomycetacia</i>	99%	<i>Planctomycetaceae</i>	99%	<i>Planctomyces</i>	96%
GOB4_10	<i>Proteobacteria</i>	100%	<i>Gammaproteobacteria</i>	100%	<i>Methylohalomonas</i>	16%		
GOB4_101	<i>Firmicutes</i>	20%	<i>Clostridia</i>	19%	<i>Incertae Sedis III</i>	11%	<i>Fervidicola</i>	11%
GOB4_11	<i>Bacteroidetes</i>	100%	<i>Sphingobacteria</i>	100%	<i>Flammeovirgaceae</i>	100%	<i>Marivirga</i>	100%
GOB4_114	<i>Proteobacteria</i>	100%	<i>Alphaproteobacteria</i>	100%	<i>Hypomonadaceae</i>	90%	<i>Woodsholea</i>	78%
GOB4_122	<i>Firmicutes</i>	99%	<i>Clostridia</i>	99%	<i>Peptococcaceae 1</i>	96%	<i>Desulfonispora</i>	96%
GOB4_123	<i>Bacteroidetes</i>	100%	<i>Flavobacteria</i>	100%	<i>Flavobacteriaceae</i>	100%	<i>Psychroflexus</i>	57%
GOB4_127	<i>Planctomycetes</i>	12%	<i>Planctomycetacia</i>	12%	<i>Planctomycetaceae</i>	12%	<i>Singulisphaera</i>	7%
GOB4_129	<i>Bacteroidetes</i>	100%	<i>Sphingobacteria</i>	100%	<i>Flammeovirgaceae</i>	100%	<i>Marivirga</i>	100%
GOB4_130	<i>Firmicutes</i>	100%	<i>Clostridia</i>	100%	<i>Clostridiaceae 4</i>	46%	<i>Geosporobacter</i>	16%
GOB4_131	<i>Planctomycetes</i>	97%	<i>Phycisphaerae</i>	87%	<i>Phycisphaeraceae</i>	87%	<i>Phycisphaera</i>	87%
GOB4_14	<i>Firmicutes</i>	100%	<i>Clostridia</i>	100%	<i>Peptococcaceae 1</i>	95%	<i>Desulfonispora</i>	95%
GOB4_19	<i>Firmicutes</i>	81%	<i>Clostridia</i>	80%	<i>Thermoanaerobacteraceae</i>	34%	<i>Syntrophaceticus</i>	30%
GOB4_2	<i>Bacteroidetes</i>	100%	<i>Flavobacteria</i>	100%	<i>Flavobacteriaceae</i>	100%	<i>Psychroflexus</i>	45%
GOB4_21	<i>Proteobacteria</i>	100%	<i>Alphaproteobacteria</i>	100%	<i>Rhodobiaceae</i>	53%	<i>Afifella</i>	32%
GOB4_26	<i>Proteobacteria</i>	55%	<i>Deltaproteobacteria</i>	51%	<i>Geobacteraceae</i>	13%	<i>Geothermobacter</i>	8%
GOB4_29	<i>Proteobacteria</i>	100%	<i>Gammaproteobacteria</i>	100%	<i>Alteromonadaceae</i>	100%	<i>Marinimicrobium</i>	100%
GOB4_3	<i>Proteobacteria</i>	100%	<i>Alphaproteobacteria</i>	100%	<i>Rhodobacteraceae</i>	100%	<i>Oceanicola</i>	41%

GOB4_32	<i>Bacteroidetes</i>	100%	<i>Sphingobacteria</i>	100%	<i>Flammeovirgaceae</i>	100%	<i>Marivirga</i>	100%
GOB4_34	<i>Bacteroidetes</i>	100%	<i>Sphingobacteria</i>	100%	<i>Flammeovirgaceae</i>	100%	<i>Marivirga</i>	100%
GOB4_39	<i>Firmicutes</i>	76%	<i>Clostridia</i>	75%	<i>Thermoanaerobacteraceae</i>	39%	<i>Syntrophaceticus</i>	35%
GOB4_44	<i>Bacteroidetes</i>	100%	<i>Sphingobacteria</i>	100%	<i>Flammeovirgaceae</i>	100%	<i>Marivirga</i>	100%
GOB4_46	<i>Firmicutes</i>	100%	<i>Clostridia</i>	100%	<i>Clostridiaceae 3</i>	100%	<i>Sporosalibacterium</i>	99%
GOB4_47	<i>Verrucomicrobia</i>	100%	<i>Opitutae</i>	100%	<i>Puniceicoccaceae</i>	100%	<i>Puniceicoccus</i>	88%
GOB4_54	<i>Bacteroidetes</i>	100%	<i>Sphingobacteria</i>	100%	<i>Flammeovirgaceae</i>	100%	<i>Marivirga</i>	100%
GOB4_55	<i>Bacteroidetes</i>	100%	<i>Flavobacteria</i>	100%	<i>Flavobacteriaceae</i>	100%	<i>Psychroflexus</i>	52%
GOB4_60	<i>Proteobacteria</i>	74%	<i>Deltaproteobacteria</i>	67%	<i>Desulfobacteraceae</i>	38%	<i>Desulforegula</i>	29%
GOB4_7	<i>Proteobacteria</i>	100%	<i>Alphaproteobacteria</i>	100%	<i>Sphingomonadaceae</i>	100%	<i>Sphingomonas</i>	99%



Appendix E: Chapter 4-T-RFs matched to Blast results obtained from GenBank for 16S rRNA clone library created for Gobabeb site

T-RFs (bp)		Cluster	Clone	Accession nr of the closest phylogenetic ancestor	Classification	% sequence similarity	Source of clones
<i>RsaI</i>	<i>AluI</i>						
		1	GOB49	AB694416.1	Uncultured bacterium 16S rRNA, partial sequence, clone: OTU147_Ref_Clone01	90	Marine deep sea sediment (Izu-Ogasawara trench slope)
			GOB56				
			GOB37				
			GOB41				
		2	GOB25	DQ058840.1	Uncultured <i>Synechococcus</i> sp. clone Sc22 16S ribosomal RNA gene, partial sequence	99	Microbial mat (Shark bay, Western Australia)
			GOB28				
			GOB34				
			GOB40				
			GOB60				
			GOB100				
			GOB92				
			GOB16				
		3	GOB57	DQ357946.1	Uncultured <i>Prochloron</i> sp. clone LI-93 16S ribosomal RNA gene, partial sequence	99	Colonies of <i>Prochloron</i> (coastal waters in Japan)
124	417	4	GOB59	DQ647099.1	Uncultured <i>Halanaerobiaceae</i> bacterium clone TCB22y 16S ribosomal RNA gene, partial sequence	90	Dahle <i>et al</i> , 2008
444		5	GOB7	DQ861117.1	Uncultured bacterium clone Sb21 16S ribosomal RNA gene, partial sequence	97	Microbial mat (Shark bay, Western Australia)
		6	GOB122	EU246016.1	Uncultured organism clone MAT-CR-P1-E11 16S ribosomal RNA gene, partial sequence	98	Soil Courtyard on hospital grounds (Boston, MA)
		7	GOB19	EU249119.1	<i>Leptolyngbya</i> sp. HBC8 16S ribosomal RNA gene, partial sequence	99	Stromatolites (Bahamas)
371		8	GOB62	FJ175512.1	Uncultured bacterium clone B1-74 16S ribosomal RNA gene, partial sequence	96	Marine sediments (Timor Sea, Australia)
			GOB20				

			GOB25				
			GOB78				
		9	GOB65	HM187283.1	Uncultured bacterium clone HDB_SIPP583 16S ribosomal RNA gene, partial sequence	86	Sub surface marine sediment (Hanford site, Washington)
69, 274		10	GOB18	JF948429.1	Uncultured gamma proteobacterium clone Pa06h08	99	Biofilm collected from a desalination plant
		11	GOB55	JF985302.1	Uncultured bacterium clone Upland_8_4600 16S ribosomal RNA gene, part	94	Soil samples from agricultural site
		12	GOB66	JN428950.1	Uncultured organism clone SBXY_3285 16S ribosomal RNA gene, partial sequence	94	Hypersaline Microbial mat (Guerrero Negro)
421		13	GOB27	JN881628.1	Uncultured Planctomycetales bacterium clone PNG_TBG_B38 16S ribosomal RNA gene, partial sequence	96	Shallow sea, hydrothermal vent (Papua, New Guinea)
		14	GOB63	JQ580371.1	Uncultured planctomycete clone RII-TR138 16S ribosomal RNA gene, part	97	Oil-polluted subtidal sediments
		15	GOB21	JQ889356.1	Uncultured planctomycete clone S-YY-29 16S ribosomal RNA gene, partial sequence	86	intertidal marine sediment (Yangtze Estuary)
			GOB54			86	
		16	GOB28	JX193385.1	Uncultured bacterium clone D30920 16S ribosomal RNA gene, partial sequence	95	intertidal marine sediment (China)

Appendix F: Chapter 4-T-RFs matched from Blast results obtained from GenBank for 16S rRNA clone library created for Swakopmund site 1

T-RFs (bp)		Cluster	Clone	Accession nr	Classification	% Sequence similarity	Source of clones
<i>RsaI</i>	<i>AluI</i>						
118, 415		1	Sps01-84	FJ536482.1	 Uncultured bacterium clone HS-ERV22B 16S ribosomal RNA gene, partial sequence	99	benthic surface from a crystallizer pond (Mediterranean)
			Sps01-74				
			Sps01_11				
			Sps01-16				
			Sps01-23				
			Sps01-29				
			Sps01-35				
			Sps01-47				
			Sps01-63				
			Sps01-70				
			Sps01-85				
			Sps01-87				
			Sps01-93				
			Sps01-110				
		2	Sps01-15	GU229750.1	Uncultured cyanobacterium isolate DGGE band RB2 16S ribosomal RNA gene, partial sequence	99	Intertidal hydrothermal springs (investigations of cyanobacteria)
			Sps01-40				
			Sps01-105				

Appendix G: Chapter 4-T-RFs matched to Blast results obtained from GenBank for 16S rRNA clone library created for Swakopmund site 2

T-RFs (bp)									
<i>RsaI</i>	<i>AluI</i>	Cluster	Clone	Accession nr of the closest phylogenetic ancestor	Classification	% Sequence similarity	Source of clones		
		1	Sps02-90	AM930333.1	Uncultured bacterium, clone SMQ57	88	Guo, 2007		
		2	Sps02-69	FJ536482.1	Uncultured bacterium clone HS-ERV22B 16S ribosomal RNA gene, partial sequence	99	Solar salterns, Mediterranean		
419		3	Sps02-74	FJ844124.1	Uncultured Verrucomicrobia bacterium clone Cy07-12 16S ribosomal RNA gene, partial sequence	99	Water samples obtained from lakes in Tibet		
			Sps02-9						
			Sps02-85						
			Sps02-18						
			Sps02-11						
			Sps02-17						
			Sps02-93						
			Sps02-38						
			Sps02-62						
			Sps02-43						
Sps02-38									
		4	Sps02-4	FJ844146.1	Uncultured Verrucomicrobia bacterium clone Cy07-34 16S ribosomal RNA gene, partial sequence	99	Water samples obtained from lakes in Tibet		
			Sps02-15						
		5	Sps02-78	HE604746.1	Uncultured bacterium partial 16S rRNA gene, hypersaline sediment, clone	97	Hypersaline sediments collected from lake Kasin (Southern Russia)		
			Sps02-52			97			
			Sps02-37			98			
		6	Sps02-100	HM480267.1	Uncultured Firmicutes bacterium clone Kir51gry B4.b35 16S ribosomal RNA	92	Microbial mat, marine origin, obtain from atoll of Kiritimati,		
		7	Sps02-63	JN499894.1	Uncultured organism clone SBZA_e706 16S ribosomal RNA gene, partial sequence	99	Hypersaline Microbial mat (Guerrero Negro)		

Appendix H: Chapter 4-Phylogenetic affiliation of 16r RNA gene clones based on RDP Classifier

Clone	Phylum	%	Class	%	Family	%	Genus	%
GOB-122	<i>Planctomycetes</i>	53%	<i>Phycisphaerae</i>	22%	<i>Phycisphaeraceae</i>	22%	<i>Phycisphaera</i>	22%
GOB-18	<i>Planctomycetes</i>	100%	<i>Planctomycetacia</i>	100%	<i>Planctomycetaceae</i>	100%	<i>Planctomyces</i>	99%
GOB-19	<i>Cyanobacteria/Chloroplast</i>	98%	<i>Cyanobacteria</i>	98%	<i>Family IV</i>	68%	<i>GpIV</i>	68%
GOB-20	<i>Proteobacteria</i>	46%	<i>Deltaproteobacteria</i>	29%	<i>Syntrophobacteraceae</i>	18%	<i>Desulfoglaeba</i>	15%
GOB-21	<i>Tenericutes</i>	10%	<i>Mollicutes</i>	10%	<i>Haloplasmataceae</i>	10%	<i>Haloplasma</i>	10%
GOB-25	<i>Proteobacteria</i>	39%	<i>Deltaproteobacteria</i>	27%	<i>Desulfarculaceae</i>	9%	<i>Desulfarculus</i>	9%
GOB-27	<i>Planctomycetes</i>	100%	<i>Planctomycetacia</i>	100%	<i>Planctomycetaceae</i>	100%	<i>Blastopirellula</i>	91%
GOB-28	<i>Verrucomicrobia</i>	22%	<i>Opitutae</i>	18%	<i>Puniceicoccaceae</i>	18%	<i>Cerasicoccus</i>	13%
GOB-37	<i>Planctomycetes</i>	40%	<i>Phycisphaerae</i>	35%	<i>Phycisphaeraceae</i>	35%	<i>Phycisphaera</i>	35%
GOB-41	<i>Planctomycetes</i>	45%	<i>Phycisphaerae</i>	42%	<i>Phycisphaeraceae</i>	42%	<i>Phycisphaera</i>	42%
GOB-54	<i>Tenericutes</i>	8%	<i>Mollicutes</i>	8%	<i>Haloplasmataceae</i>	8%	<i>Haloplasma</i>	8%
GOB-55	<i>Chloroflexi</i>	13%	<i>Thermomicrobia</i>	13%	<i>Thermomicrobiaceae</i>	13%	<i>Thermomicrobium</i>	13%
GOB-56	<i>Planctomycetes</i>	53%	<i>Phycisphaerae</i>	49%	<i>Phycisphaeraceae</i>	49%	<i>Phycisphaera</i>	49%
GOB-59	<i>Firmicutes</i>	100%	<i>Clostridia</i>	96%	<i>Halanaerobiaceae</i>	92%	<i>Halocella</i>	92%
GOB-62	<i>Acidobacteria</i>	53%	<i>Acidobacteria_Gp10</i>	37%	<i>Gp10</i>	37%	<i>Gp10</i>	37%
GOB-63	<i>Planctomycetes</i>	100%	<i>Planctomycetacia</i>	100%	<i>Planctomycetaceae</i>	100%	<i>Blastopirellula</i>	78%
GOB-78	<i>Cyanobacteria/Chloroplast</i>	100%	<i>Cyanobacteria</i>	98%	<i>Family IX</i>	43%	<i>GpIX</i>	43%
GOB-49	<i>Planctomycetes</i>	57%	<i>Phycisphaerae</i>	54%	<i>Phycisphaeraceae</i>	54%	<i>Phycisphaera</i>	54%
GOB-100	<i>Cyanobacteria/Chloroplast</i>	97%	<i>Cyanobacteria</i>	97%	<i>Family VII</i>	90%	<i>GpVII</i>	90%
GOB-16	<i>Cyanobacteria/Chloroplast</i>	94%	<i>Cyanobacteria</i>	94%	<i>Family VII</i>	83%	<i>GpVII</i>	83%
GOB-25	<i>Cyanobacteria/Chloroplast</i>	100%	<i>Cyanobacteria</i>	100%	<i>Family VII</i>	97%	<i>GpVII</i>	97%
GOB-28	<i>Cyanobacteria/Chloroplast</i>	99%	<i>Cyanobacteria</i>	99%	<i>Family VII</i>	93%	<i>GpVII</i>	93%
GOB-34	<i>Cyanobacteria/Chloroplast</i>	100%	<i>Cyanobacteria</i>	100%	<i>Family VII</i>	86%	<i>GpVII</i>	86%
GOB-40	<i>Cyanobacteria/Chloroplast</i>	100%	<i>Cyanobacteria</i>	100%	<i>Family VII</i>	81%	<i>GpVII</i>	81%
GOB-52	<i>Firmicutes</i>	44%	<i>Clostridia</i>	32%	<i>Peptococcaceae 2</i>	14%	<i>Desulfurispora</i>	14%
GOB-57	<i>Cyanobacteria/Chloroplast</i>	99%	<i>Cyanobacteria</i>	99%	<i>Family VII</i>	89%	<i>GpVII</i>	89%
GOB-59	<i>Cyanobacteria/Chloroplast</i>	99%	<i>Cyanobacteria</i>	99%	<i>Family VII</i>	89%	<i>GpVII</i>	89%
GOB-60	<i>Cyanobacteria/Chloroplast</i>	100%	<i>Cyanobacteria</i>	100%	<i>Family VII</i>	93%	<i>GpVII</i>	93%
GOB-65	<i>Proteobacteria</i>	26%	<i>Alphaproteobacteria</i>	20%	<i>Rhodospirillaceae</i>	14%	<i>Rhodovibrio</i>	10%

GOB-66	<i>Planctomycetes</i>	27%	<i>Phycisphaerae</i>	9%	<i>Phycisphaeraceae</i>	9%	<i>Phycisphaera</i>	9%
GOB-7	<i>Cyanobacteria/Chloroplast</i>	85%	<i>Cyanobacteria</i>	85%	<i>Family VII</i>	36%	<i>GpVII</i>	36%
GOB-92	<i>Cyanobacteria/Chloroplast</i>	96%	<i>Cyanobacteria</i>	96%	<i>Family VII</i>	67%	<i>GpVII</i>	67%
Sps01-105	<i>Cyanobacteria/Chloroplast</i>	100%	<i>Cyanobacteria</i>	100%	<i>Family VII</i>	100%	<i>GpVII</i>	100%
Sps01-11	<i>Cyanobacteria/Chloroplast</i>	100%	<i>Cyanobacteria</i>	100%	<i>Family VII</i>	100%	<i>GpVII</i>	100%
Sps01-110	<i>Cyanobacteria/Chloroplast</i>	100%	<i>Cyanobacteria</i>	100%	<i>Family VII</i>	100%	<i>GpVII</i>	100%
Sps01-16	<i>Cyanobacteria/Chloroplast</i>	100%	<i>Cyanobacteria</i>	100%	<i>Family VII</i>	100%	<i>GpVII</i>	100%
Sps01-23	<i>Cyanobacteria/Chloroplast</i>	100%	<i>Cyanobacteria</i>	100%	<i>Family VII</i>	100%	<i>GpVII</i>	100%
Sps01-29	<i>Cyanobacteria/Chloroplast</i>	100%	<i>Cyanobacteria</i>	100%	<i>Family VII</i>	100%	<i>GpVII</i>	100%
Sps01-35	<i>Cyanobacteria/Chloroplast</i>	100%	<i>Cyanobacteria</i>	100%	<i>Family VII</i>	100%	<i>GpVII</i>	100%
Sps01-40	<i>Cyanobacteria/Chloroplast</i>	100%	<i>Cyanobacteria</i>	100%	<i>Family VII</i>	100%	<i>GpVII</i>	100%
Sps01-47	<i>Cyanobacteria/Chloroplast</i>	100%	<i>Cyanobacteria</i>	100%	<i>Family VII</i>	99%	<i>GpVII</i>	99%
Sps01-63	<i>Cyanobacteria/Chloroplast</i>	100%	<i>Cyanobacteria</i>	100%	<i>Family VII</i>	100%	<i>GpVII</i>	100%
Sps01-70	<i>Cyanobacteria/Chloroplast</i>	100%	<i>Cyanobacteria</i>	100%	<i>Family VII</i>	100%	<i>GpVII</i>	100%
Sps01-74	<i>Cyanobacteria/Chloroplast</i>	100%	<i>Cyanobacteria</i>	100%	<i>Family VII</i>	100%	<i>GpVII</i>	100%
Sps01-84	<i>Cyanobacteria/Chloroplast</i>	100%	<i>Cyanobacteria</i>	100%	<i>Family VII</i>	100%	<i>GpVII</i>	100%
Sps01-85	<i>Cyanobacteria/Chloroplast</i>	100%	<i>Cyanobacteria</i>	100%	<i>Family VII</i>	100%	<i>GpVII</i>	100%
Sps01-87	<i>Cyanobacteria/Chloroplast</i>	100%	<i>Cyanobacteria</i>	100%	<i>Family VII</i>	100%	<i>GpVII</i>	100%
Sps01-93	<i>Cyanobacteria/Chloroplast</i>	100%	<i>Cyanobacteria</i>	100%	<i>Family VII</i>	100%	<i>GpVII</i>	100%
Sps02-100	<i>Firmicutes</i>	100%	<i>Clostridia</i>	95%	<i>Halanaerobiaceae</i>	93%	<i>Halocella</i>	71%
Sps02-11	<i>Lentisphaerae</i>	10%	<i>Lentisphaeria</i>	10%	<i>Lentisphaeraceae</i>	10%	<i>Lentisphaera</i>	10%
Sps02-15	<i>Verrucomicrobia</i>	37%	<i>Opitutae</i>	24%	<i>Puniceicoccaceae</i>	24%	<i>Cerasicoccus</i>	22%
Sps02-17	<i>Verrucomicrobia</i>	14%	<i>Opitutae</i>	13%	<i>Puniceicoccaceae</i>	12%	<i>Cerasicoccus</i>	11%
Sps02-18	<i>Verrucomicrobia</i>	12%	<i>Opitutae</i>	11%	<i>Puniceicoccaceae</i>	11%	<i>Cerasicoccus</i>	9%
Sps02-37	<i>Firmicutes</i>	100%	<i>Clostridia</i>	100%	<i>Halanaerobiaceae</i>	100%	<i>Halocella</i>	100%
Sps02-38	<i>Verrucomicrobia</i>	23%	<i>Opitutae</i>	15%	<i>Puniceicoccaceae</i>	15%	<i>Cerasicoccus</i>	13%
Sps02-04	<i>Verrucomicrobia</i>	30%	<i>Opitutae</i>	25%	<i>Puniceicoccaceae</i>	25%	<i>Cerasicoccus</i>	20%
Sps02-43	<i>Verrucomicrobia</i>	35%	<i>Opitutae</i>	29%	<i>Puniceicoccaceae</i>	28%	<i>Cerasicoccus</i>	21%
Sps02-52	<i>Firmicutes</i>	100%	<i>Clostridia</i>	100%	<i>Halanaerobiaceae</i>	100%	<i>Halocella</i>	100%
Sps02-62	<i>Verrucomicrobia</i>	7%	<i>Opitutae</i>	6%	<i>Puniceicoccaceae</i>	5%	<i>Cerasicoccus</i>	4%
Sps02-63	<i>Cyanobacteria/Chloroplast</i>	100%	<i>Cyanobacteria</i>	100%	<i>Family VII</i>	100%	<i>GpVII</i>	100%
Sps02-69	<i>Cyanobacteria/Chloroplast</i>	100%	<i>Cyanobacteria</i>	100%	<i>Family VII</i>	100%	<i>GpVII</i>	100%

Sps02-74	<i>Verrucomicrobia</i>	22%	<i>Opitutae</i>	17%	<i>Puniceococcaceae</i>	17%	<i>Cerasicoccus</i>	16%
Sps02-76	<i>Firmicutes</i>	100%	<i>Clostridia</i>	100%	<i>Halanaerobiaceae</i>	100%	<i>Halanaerobium</i>	88%
Sps02-78	<i>Firmicutes</i>	100%	<i>Clostridia</i>	99%	<i>Halanaerobiaceae</i>	98%	<i>Halocella</i>	98%
Sps02-85	<i>Verrucomicrobia</i>	6%	<i>Opitutae</i>	5%	<i>Puniceococcaceae</i>	5%	<i>Cerasicoccus</i>	5%
Sps02-9	<i>Verrucomicrobia</i>	18%	<i>Opitutae</i>	16%	<i>Puniceococcaceae</i>	16%	<i>Cerasicoccus</i>	15%
Sps02-90	<i>Firmicutes</i>	91%	<i>Clostridia</i>	90%	<i>Halanaerobiaceae</i>	89%	<i>Halocella</i>	88%
Sps02-93	<i>Verrucomicrobia</i>	31%	<i>Opitutae</i>	24%	<i>Puniceococcaceae</i>	24%	<i>Cerasicoccus</i>	20%



References

Aguilera A., Gómez F., Lospitao E. and Amils R. (2006). A molecular approach to the characterization of the eukaryotic communities of an extreme acidic environment: Methods for DNA extraction and denaturing gradient gel electrophoresis analysis. *Systematic and Applied Microbiology* **29**, 593-605

Ahmad N., Johri S., Sultan P., Abdin M. Z. and Qazi G. N. (2011). Phylogenetic characterization of archaea in saltpan sediments. *Indian Journal of Microbiology* **51**, 132-137

Altschul S.F., Gish W., Miller W., Myers E.W. and Lipman D.J., (1990). "Basic local alignment search tool." *Journal of Molecular Biology* 215:403-410

Amziane M., Metiaz F., Darenfed-Bouanane A., Djenane Z., Selama O., Abderrahmani A., Cayol J. and Fardeau M. (2013). *Virgibacillus natechei* sp. nov., A Moderately Halophilic Bacterium Isolated from Sediment of a Saline Lake in Southwest of Algeria. *Current Microbiology* (Epub ahead of print)

Anton J., Oren A., Benlloch S., Roderigues-Valera F., Amann R. and Rossello-Mora R. (2002). *Salinibacter ruber* gen. nov., sp. nov., a novel, extremely halophilic member of the Bacteria from saltern crystallizer ponds. *International Journal of Systematic and Evolutionary Microbiology* **52**, 485–491.

Ashelford K. E., Chuzhanova N. A., Fry J. C., Jones A. J. and Weightman A. J. (2006). New Screening Software Shows that Most Recent Large 16S rRNA Gene Clone Libraries Contain Chimeras. *Applied and Environmental Microbiology* **72**: 5734-5741

Averhoff V. and Muller B. (2010). "Exploring research frontiers in microbiology: recent advances in halophilic and thermophilic extremophiles." *Research in Microbiology* **161**, 506-514

Baker G. C., Smith J. J., and Cowan D. A. (2003). Review and reanalysis of domain specific 16S primers. *Journal of Microbiological Methods* **55**,541–555.

Baker G. C. and Cowan D. A. (2004). 16S rDNA primers and the unbiased assessment of thermophile diversity. *Biochemical Society Transactions* **32**, 218-221

Birge R. R., Gillespie N. B., Izaguirre E. W., Kusnetzow A., Lawrence A. F., Singh D., Song Q. W., Schmidt E., Stuart J. A., Seetharaman S. and Wise K. J. (1999). Biomolecular Electronics: Protein-Based Associative Processors and Volumetric Memories. *Journal of Physical Chemistry B* **103**, 10746-10766

Braid M. D., Nicholas L. M., Clement B. G. Kitner J. B. and Kitts C. L. (1999). Testing the UltraClean soil DNA purification kit on a diverse range of soils by PCR amplification of 16S rDNA. In: ASM General Meeting

Blackwood, C. B., Marsh T., Sang-Hoon P. and Eldor A. K. (2003). Terminal restriction fragment length polymorphism data analysis for quantitative comparison of microbial communities. *Applied and Environmental Microbiology* **69**, 926-932.

Bloom S. A. (1981). Similarity Indices in Community Studies: Potential Pitfalls. *Marine Ecology-Progress Series* **5**, 125-128

Boivin-Jahns V., Bianchi A., Ruimy R., Garcin J., Daumas S. and Christen R. (1995). Comparison of Phenotypical and Molecular methods for the identification of bacterial strains isolated from a deep subsurface environment. *Applied and Environmental Microbiology* **61**, 3400-3406

Brain C. K. (1980). Some Protozoans from saline pools in the Namib. *Namib Bulletin, Gobabeb*, 10-13

Brain C. K. and Koste W. (1993). Rotifers of the genus *Proales* from saline springs in the Namib Desert, with the description of a new species. *Hydrobiologia* **255**, 449-454.

Braun T., Backmann N., Vögli M., Bietsch A., Engel A., Lang H., Gerber C. and Hegner M. (2006). Conformational Change of Bacteriorhodopsin Quantitatively Monitored by Microcantilever Sensors. *Biophysical Journal* **90**, 2970-2977

Bukowska A., Bielczyńska A., Karnkowska A., Chróst R. J. and Jasser I. (2014). Molecular (PCR-DGGE) versus morphological approach: analysis of taxonomic composition of potentially toxic cyanobacteria in freshwater lakes. *Aquatic Biosystems* **10**: 1-10

Casamayor E. O., Massana R, Diez B., Goddard V. J., Gasol J. M. ,Joint I. , Rodriguez-Valera F. and Pedros-Alio C. (2002). Changes in archaeal, bacterial and eukaryal assemblages along a salinity gradient by comparison of genetic fingerprinting methods in a multipond solar saltern." *Environmental Microbiology* **4**, 338-348

Clayton R. A., Sutton G., Hinkle P. S., Bult C. and Fields C. (1995). Intraspecific variation in small-subunit rRNA sequences in Genbank: Why single sequences may not adequately represent prokaryotic taxa. *International Journal of Systematic Bacteriology* **45**, 595-599

Chao A. (1984). Non-parametric estimation of the number of classes in a population. *Scandinavian Journal of Statistics* **11**, 265-270.

Chao A., and Lee S. M. (1992). Estimating the number of classes via sample coverage. *Journal of the American Statistical Association* **87**, 210-217.

Chen M., Sheu S., Chiu T. and Chen W. (2012). *Neptuniibacter halophilus* sp. Nov., isolated from a salt pan, and emended description of the genus *Neptuniibacter*. *International Journal of Systematic and Evolutionary Microbiology* **62**, 1104-1109

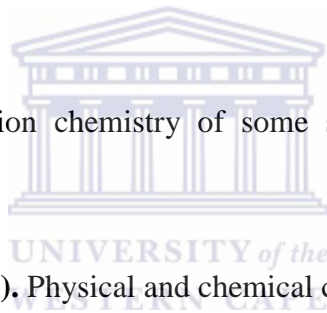
Cooke R., Warren A. and Goudie A. (1993). *Desert Geomorphology*. UCL press LTD, London, 32-34

Coronado M. J., Vargas C., Hofemeister J., Ventosa A. and Nieto J. J. (2000). Production and biochemical characterization of an K-amylase from the moderate halophile *Halomonas meridiana*. *FEMS Microbiology Letters* **183**, 67-71.

Costello E. K. and Schmidt S.K. (2006). Microbial diversity in alpine tundra wet meadow soil: novel Chloroflexi from a cold, water-saturated environment. *Environmental Microbiology* **8**,1471-1486

Curtis T. P., Sloan W. T. and Scannell J. W. (2002). Estimating prokaryotic diversity and its limits. *Proceedings of the National Academy of Sciences of the United States of America* **99**, 10494–10499

Day J. A. (1993). The major ion chemistry of some southern African saline systems. *Hydrobiologia* **267**, 37-59



Day J. A. and Seely M. K. (1988). Physical and chemical conditions in an hypersaline spring in the Namib Desert. *Hydrobiologia* **160**, 141-153

De longe E. F., Wickham G. S and Pace N. R. (1989). Phylogenetic stains: Ribosomal RNA -based probes for the identification of single cells. *Science* **243**, 1360-1363

de Liphay J. R., Enzinger C., Johnsen K., Aamand J. and Sorensen S. J. (2004). Impact of DNA extraction method on bacterial community composition measured by denaturing gradient gel electrophoresis. *Soil Biology and Biochemistry* **36**, 1607-1614

DeLonge E. F. (1992). Archaea in coastal marine environments. *Ecology* **89**,5685-5689

De Guzman M. N., Vargas V. G., Antezana H. and Svoboda M. (2008). Lipolytic enzyme production by halophilic/halotolerant microorganisms isolated from Laguna Verde, Bolivia. *Bolivian Journal of Chemistry* **25**, 14-23

de Lourdes Morenoa M., Garcíaa M. T., Ventosa A. , Iglesias-Guerrab F. and Melladoa E. (2010). The extremely halophilic bacterium *Salicola marasensis* IC10 accumulates the compatible solute betaine. *Systematic and Applied Microbiology* **33**, 308-310.

Díez B., Pedrós-Alió C., Marsh T. L. and Massana R. (2001). Application of Denaturing Gradient Gel Electrophoresis (DGGE) To Study the Diversity of Marine Picoeukaryotic Assemblages and Comparison of DGGE with Other Molecular Techniques. *Applied and Environmental Microbiology* **67**, 2942-2951

Dundas I. (1998). Was the environment for primordial life hypersaline. *Extremophiles* **2**, 375-377

Dopheide A., Lear G., Stott R. and Lewis G. (2009). Relative Diversity and Community Structure of Ciliates in Stream Biofilms According to Molecular and Microscopy Methods. *Applied and Environmental Microbiology* **75**, 5261-5272

Eckhardt F. D. and Drake N. (2011). Introducing the Namib Desert Playas. In *Sabkha Ecosystems Volume III: Africa and Southern Europa*, by Boer B., Barth H. J., Breckle S. W., Clusener-Godt M. and Khan M. A. and Ozturk M., 19-25. Springer Science and Business Media

Farris J. S. (1969). On the Cophenetic Correlation Coefficient. *Systematic Biology* **18**, 279-285

Fauth J. E., Bernardo J., Camara M., Resetarits W. J., Van Buskirk J. and McCollum S.A. (1996). Simplifying the jargon of community ecology: A conceptual approach. *American Naturalist* **147**, 282-286

Felsenstein J. (1981). Evolutionary Trees from DNA sequences: A Maximum Likelihood approach. *Journal of Molecular Evolution* **17**, 368-376

Faoro H., Alves A. C., Souza E. M., Rigo L. U., Cruz L. M., Al-Janabi S. M., Monteiro R. A., Baura V. A. and Pedrosa F. O. (2010). Influence of soil characteristics on the diversity of bacteria in the Southern Brazilian Atlantic forest. *Applied and Environmental Microbiology* **76**, 4744-4751

Fuhrman A., Hewson I, Schwalbach M. S., Steele J. A., Brown M. V. and Naeem S. (2006). Annually reoccurring bacterial communities are predictable from ocean conditions. *Proceedings of the National Academy of Science of the United States of America* **103**, 13104-13109

Grant, W. D. , Mcgenity R. T. and Gemmell T. J. (1998). “Halophiles.” In *Extremophiles, Microbial Life in Extreme Environments*, by K and Grant, W. D. (Edited) Horikoshi, 93-132. Canada: Wiley-Liss, Inc., 1998.

Grant W. D., Kamekura M., McGenity T. J. & Ventosa A. (2001). Class III. *Halobacteria* class. nov. In *Bergey's Manual of Systematic Bacteriology*, 2nd edn, vol. 1, pp. 294–301. Edited by D. R. Boone, R. W. Castenholz & G. M. Garrity. Springer, New York

Ghai R., Pasic L., Fernandez A. B., Martin-Cuadrado A., Mizuno C. M., McMahon K. D., Papke T., Stepanauskas R., Rodriguez-Brito B., Rohwer F., Sanchez-Porro C., Ventosa A. and Rodriguez-Valera F. (2011). New abundant Microbial Groups in Aquatic Hypersaline Environments. *Scientific Reports* **1**, 1-10

Galinski E. A., Pfeiffer H. P. and Truper H. G. (1985). 1,4,5,6-Tetrahydro-2-methyl-4-pyrimidinecarboxylic acid: A novel cyclic amino acid from halophilic phototrophic bacteria of the genus *Ectothiorhodospira*. *European Journal of Biochemistry* **149**, 135-139.

Gast R. J., Dennett M. R. and Caron D. A. (2004). Characterization of Protistan assemblages in the Ross Sea, Antarctica, by denaturing gradient gel electrophoresis. *Applied and Environmental Microbiology* **70**, 2028-2017

Graf R., Anzati S., Buenger J., Pfluecker F. and Driller H. (2008). The multifunctional role of ectoine as a natural cell protectant. *Clinics in Dermatology* **26**, 326-333

Hackl E., Zechmeister-Boltenstern S., Bodrossy L., and Sessitsch A. (2004). Comparison of Diversities and Compositions of Bacterial Populations Inhabiting Natural Forest Soils. *Applied and Environmental Microbiology* **70**, 5057-5065

Hatchfield B. (2000). Rain, fog and species richness in the Central Namib Desert in the exceptional rainy season of 1999/2000. *Dinteria* **26**, 113-146

Hansen M. C., Tolker-Nielsen T., Givskov M. C. and Molin S. (1998). Biased 16S rDNA PCR amplification caused by interference from DNA flanking the template region'. *Microbiology Ecology* **26**, 141-149.

Hartmann M., Frey B., Kolliker R and Widmer F. (2005). Semi-automated genetic analyses od soil microbial communités: comparison of T-RFLP and RISA based on descriptive and discriminative statistical approaches. *Journal of Microbiological Methods* **61**, 349-360

Hershey D. R. and Sand S. (1993). Electrical Conductivity (Measuring Activities for Elementary and Junior-high students). *Science Activities: Classroom Projects and Curriculum Ideas* **30**, 32-35

Hill G. T., Mitkowski N. A., Aldrich-Wolfe L. Emele L. R., Jurkonie D. D., Ficke A., Maldonado-Ramirez S., Lynch S. T. and Nelson E. B. (2000). Methods for assessing the composition and diversity of soil microbial communities. *Applied Soil Ecology* **15**, 25-36

Holmes S. (2003). Bootstrapping Phylogenetic Trees: *Theory and Methods. Statistical Science* **18**, 241-255

Ishahed M. S., Najar F. Z., Roe B. A., Oren A., Dewers T. A. and Krumholz L. R. (2004). Survey of Archaeal Diversity Reveals an Abundance of Halophilic Archaea in a Low-Salt, Sulfide- and Sulfur- rich Spring. *Applied and Environmental Microbiology* **70**, 2230-2239

Jackson C. R., Rodin E. E. and Churchill P. F. (2000). Denaturing Gradient Gel Electrophoresis Can Fail to Separate 16S rDNA Fragments with Multiple Base Differences. *Molecular Biology Today* **1**, 49-51

Jebbar M. , Talibart R. , Gloux K. , Bernard T . and Blanco C. (1992). Osmoprotection of *Escherichia coli* by Ectoine: Uptake and Accumulation Characteristics.” *Journal of Bacteriology* **174**, 5027-5035.

Jiang H., Dong H., Zhang G., Yu B., Chapman L. R. and Fields M. W. (2006). Microbial diversity in water and sediment of Lake Chaka, an Athalossohaline Lake in Northwest China. *Applied and Environmental Microbiology* **72**, 3832-3845

Julia R. de Liphthay J. R., Enzinger C., Johnsen K., Aamand J. and Sørensen S. J. (2004). Impact of DNA extraction method on bacterial community composition measured by denaturing gradient gel electrophoresis. *Soil Biology & Biochemistry* **36**, 1607-1614.

Kamat T. and Kerkar S. (2011). Bacteria from salt pans: A potential resource of antibacterial metabolites. *Recent Research in Science and Technology* **3**, 46-52

Kanapathipillaia M., Lentzenb G., Sierksa M. and Park C. B. (2005). Ectoine and hydroxyectoine inhibit aggregation and neurotoxicity of Alzheimer's Beta-amyloid. *FEBS Letters* **579**, 4775-4780.

Keyster M. (2007). Spatial distribution of cyanobacterial phylotypes in Antarctic Dry Valley soil biotopes (Unpublished Masters Thesis). Department of Biotechnology, University of the Western Cape. Bellville

Kimura M. (1980). A simple method for estimating evolutionary rates of base substitutions through comparative studies of nucleotide sequences. *Journal of Molecular Evolution* **16**, 111-120

Klappenbach J. A., Dunbar J. M. and Schmidt T. M. (2000). rRNA Operon copy number reflects ecological strategies of bacteria. *Applied and Environmental Microbiology* **66**, 1328-1333

Konstantinidis K. T. and Tiedje J. M. (2005). Genomic insights that advance the species definition for prokaryotes. *Proceedings of the National Academy of Sciences of the United States of America* **102**, 2567–2572

Kuhlmann E. and Bremer A. U. (2002). Osmotically Regulated Synthesis of the Compatible Solute Ectoine in *Bacillus pasteurii* and Related *Bacillus* spp. *Applied and Environmental Microbiology* **68**, 772-783.

Kurata S., Kanagawa T., Magariyama Y., Takatsu K., Yamada K., Yokomaku and Kamagata Y. (2004). Reevaluation and reduction of PCR bias caused by reannealing of templates. *Applied and Environmental Microbiology* **70**, 7545-7549

Lai M. C., Hong T. Y. and Gunsalus R. P. (2000). Glycine Betaine Transport in the Obligate Halophilic Archaeon: *Methanohalophilus portucalensis*. *Journal of Bacteriology* **182**, 520-524.

Lai M. C., Sowers K. R., Robertson D. E. , Roberts M. F. and Gunsalus R. P. (1991) Distribution of Compatible Solutes in the Halophilic Methanogenic Archaeobacteria. *Journal of Bacteriology* **173**, 5352-5358.

Lee J. C., Jeon C. O., Lim J. M., Lee S. M., Lee J. M., Song S. M., Park D. J., Li W. J. and Kim C. J. (2005). *Halomonas taeanensis* sp. nov., a novel moderately halophilic bacterium isolated from a solar saltern in Korea. *International Journal of Systematic and Evolutionary Microbiology* **55**, 2027-2032

Li W. and Godzik A. (2006). CD-hit: a fast program for clustering and comparing large sets of protein or nucleotide sequences. *Bioinformatics* **22**:1658-9

Li X. Sui X., Zhang Y., Zhou Y., Zhai Y. and Wang Q. (2010). An improved calcium chloride method preparation and transformation of competent cells. *African Journal of Biotechnology* **9**, 8549-8554

Lim J. M., Yoon J. H., Lee J. C., Jeon C. O., Park D. J., Sung C. and Kim C. J. (2004) *Halomonas koreensis* sp. nov., a novel moderately halophilic bacterium isolated from a solar saltern in Korea. *International Journal of Systematic and Evolutionary Microbiology* **54**, 2037-2042

Linhart C. and Shamir R. (2002). The degenerate primer design problem. *Bioinformatics* **18**, S172-S180

López-López A., Yarza P., Richter M., Suárez-Suárez A., Anton J., Niemann H. and Rossello-Moral R. (2010). Extremely halophilic microbial communities in anaerobic sediments from a solar saltern. *Environmental Microbiology Reports* **2**, 258–271

Luo W., Lei A., Lu J. and Hu Z. (2014). Estimating Cyanobacteria Community Dynamics and its Relationship with Environmental Factors. *International Journal of Environmental research and Public Health* **11**: 1141-1160

Maier R. M., Pepper I. L. and Gerba C. P. (2000). Environmental Microbiology. Aquatic and Extreme Environments. **Dowd S. E., Herman D. C. and Maier R. M.** Academic Press, London, UK. Chapter 6:123-146

Marsh T. L. (2005). Culture-Independent Microbial Community Analysis with Terminal Restriction Fragment Length Polymorphism. *Methods in Enzymology* **397**, 308-329.

Martin-Laurent F., Philippot L., Hallet S., Chaussod R., Germon J. C., Soulas G. and Catroux G. (2001). DNA extraction from soils: Old bias for new microbial diversity analysis methods. *Applied and Environmental Microbiology* **67**, 2354-2359

Maturrano L., Santos F., Rossello-Mora R. and Anton J. (2006). Microbial diversity in Maras salterns, a hypersaline environment in the Peruvian Andes. *Applied and Environmental Microbiology* **72**, 3887–3895

Maidak B. L., Olsen G. J., Larsen N., Overbeek R., McCaughey M. J. and Woese C. R. (1997). The RDP (Ribosomal Database Project). *Nucleic Acids Research* **25**, 109-110

MacDonell M.T. and Colwell R. R. (1984). The nucleotide sequence of 5S ribosomal RNA from *Vibrio marinus*. *Microbiological Sciences* **1**, 229-231

Meliani A., Bensoltane A. and Mederbel K. (2012). Microbial diversity and Abundance in Soil: Related to plant and soil type. *American Journal of Plant Nutrition and Fertilization technology* **2**, 10-18

Meyerhans A., Vartanian J. and Wain-Hobson S. (1990). DNA recombination during PCR. *Nucleic Acids Research* **18**, 1687-1691

Mevarech M., Hirsch-Twizer S., Goldman S., Yakobson E., Eisenberg H. and Dennis P. P. (1989). Isolation and characterization of the rRNA gene clusters of *Halobacterium marismortui*. *Journal of bacteriology* **171**, 3479-3485

Mikkat S., Hagemann S. and Schoor A. (1996). Active transport of glucosylglycerol is involved in salt adaptation of the cyanobacterium *Synechocystis* sp. strain PCC 6803. *Microbiology* **142**, 1725-1732.

Montoya I., Lozada-Chávez I., Amils R., Rodriguez N. and Marín I. (2011). The sulphate-rich and extreme saline sediment of the ephemeral Tirez lagoon: A biotype for acetoclastic sulphate-reducing bacteria and hydrogenotrophic methanogenic archaea. *International Journal of Microbiology*, 1-22

Muyzer G., De Waal E. C. and Uitterlinden A. G. (1993). Profiling of Complex Microbial Populations by Denaturing Gradient Gel Electrophoresis Analysis of Polymerase Chain Reaction-Amplified Genes Coding for 16S rRNA. *Applied and Environmental Microbiology* **59**, 695-700

Muyzer G. (1999). DGGE/TGGE a method for identifying genes from natural ecosystems. *Current Opinion in Microbiology* **2**, 317-322

Nagasathya A. and Thajuddin N. (2008). Cyanobacteria diversity in the hypersaline environment of the saltpans of Southeastern coast of India. *Asian Journal of Plant Sciences* **7**, 473-478

Narasingarao P., Podell S., Ugalde J. A., Brochier-Armanet C., Emerson J. B., Brocks J. J., Heidelberg K. B., Banfield J. F., and Allen E. E. (2012). De novo metagenomic assembly reveals abundant novel major lineage of Archaea in hypersaline microbial communities. *International Society for Microbial Ecology* **6**, 81-93

Nelson K. A., Moin N. S. and Bernhard A. E. (2009). Archaeal Diversity and the Prevalence of Crenarchaeota in Salt Marsh Sediments. *Applied and Environmental Microbiology* **75**, 4211-4215

Nicholson C. A. and Fathepurre B. Z. (2004). Biodegradation of benzene by halophilic and halotolerant bacteria under aerobic conditions. *Applied and Environmental Microbiology* **70**, 1222-1225

Nkem J. N., Virginia R. A., Barrett J. E., Wall D. H. and Li G. (2006). Salt tolerance and teh survival thersholds for two species of Antarctic soil nematodes.” *Polar Biology* **29**, 643-651

Nübel U., Garcia-Pichel F. and Muyzer G. (1997). PCR primers to amplify 16S rRNA genes from cyanobacteria. *Applied Environmental Microbiology* **63**, 3327-3332.

Olsen G. J., Lane D. J., Giovanni S. J. and Pace N. R. (1986). Microbial Ecology and Evolution: A ribosomal RNA approach. *Annual Reviews in Microbiology* **40**, 337-365

Olsen G. J., Larsen N. and Woese C. R. (1991). The ribosomal RNA database project. *Nucleic Acids Research* **19**, 2017–2021.

Osborn A. M., Moore E. R. and Timmis K. N. (2000). An evaluation of terminal-restriction fragment length polymorphism (T-RFLP) analysis for the study of microbial community structure and dynamics. *Environmental Microbiology* **2**, 39-50

Panizzon J. P., Pilz H.L., Knaak N., Ramos R.C., Ziegler D.R. and Fiuza. (2015). Microbial Diversity: Relevance and Relationship Between Environmental Conservation And Human Health. *Braziian Archives of Biology and Technology* **58**, 137-145

Pester M., Schleper C. and Wagner M. (2011). The Thaumarchaeota: an emerging view of their phylogeny and ecophysiology. *Current Opinion in Microbiology* **14**, 300-306

Pielou E. (1966). The measurement of diversity in different types of biological collections. *Journal of Theoretical. Biology* **13**, 131-144.

Polz M. F. and Cavanaugh C. M. (1998). Bias in template-to-product ratio in multitemplate PCR. *Applied Environmental Microbiology* **64**, 3724-3730

Pointing S. B., Warren-Rhodes K.A. Lacap D. C., Rhodes K. L. and McKay C. P. (2007). Hypolithic community shifts occur as a result of liquid water availability along environmental gradients in China's hot and cold hyperarid deserts. *Environmental Microbiology* **9**: 414-424

Pointing S. B., Chan Y., Lacap D. C., Lau M, C. Y., Jurgens J. A., and Roberta L. Farrell R. L. (2009). Highly specialized microbial diversity in hyper-arid polar desert. *Proceeding in the National Academy of Science USA* **106**: 19964–19969

Pruesse E., Quast C., Knittel K., Fuchs B.M., Ludwig W.G., Peplies J. and Glöckner F.O. (2007). SILVA: a comprehensive online resource for quality checked and aligned ribosomal RNA sequence data compatible with ARB. *Nucleic Acid Research* **35**, 7188-7196

Purdy K. J., Cresswell-Maynard T. D., Nedwell D. B., McGenity T. J., Grant W. D., Timmis K. N. and Embley T. M. (2004). Isolation of haloarchaea that grow at low salinities. *Environmental Microbiology* **6**,591-595

Rainey F. A., Ward-Rainey N. L., Janssen P. H., Hippe H. and Stackebrandt E. (1996). *Clostridium paradoxum* DSM 7308T contains multiple 16S rRNA genes with heterogeneous intervening sequences. *Microbiology* **142**, 2087-2095

Reed C., Fofanov V., Putonti C., Chumakov S., Slezak T. and Fofanov Y. (2007). Effect of the mutation rate and background size on the quality of pathogen identification. *Bioinformatics* **23**, 2665-2671

Reysenbach L., Giver L. J., Wickman G. S. and Pace N. R. (1992). Differential amplification of rRNA genes by Polymerase Chain Reaction. *Applied and Environmental Microbiology* **58**, 3417-3418

Ritika C., Suresh K. and Kumar P. A. (2012). *Caenispirillum salinarum* sp. nov., a member of the family *Rhodospirillaceae* isolated from a solar saltern. *International Journal of Systematic and Evolutionary Microbiology* **62**, 1698-1702

Robe P., Nalin R., Capellano C., Vogel T. M and Simonet P. (2003). Extraction of DNA from soil. *European Journal of Soil Biology* **39**, 183-190

Robinson P., Neelon K., Schreier H. J. and Roberts M. F. (2001). β -Glutamate as a substrate for Glutamine Synthetase. *Applied and Environmental Microbiology* **67**, 4458-4463

Sekiguchi H., Tomioka N., Nakahara T. and Uchiyama H. (2001). A single band does not always represent single bacterial strains in denaturing gradient gel electrophoresis analysis. *Biotechnology Letters* **23**, 1205-1208

Shannon C. E. (1948). A mathematical theory of communication. *The Bell System Technical Journal* **27**, 379-423

Sheffield V. C., Cox D. R., Lerman L. S. and Myers R. M. (1989). Attachment of a 40-base-pair G+C-rich sequence (GC-clamp) to genomic DNA fragments by the polymerase chain reaction results in improved detection of single-base changes. *Proceedings for the National Academic of Science USA* **86**, 232-236

Shaw P.A. and Bryant R. G. (2011). "Pans, playas and salt lakes". In *Arid Zone Geomorphology: Process, Form and Change in Drylands*, Third Edition. by Thomas D. S. G. (Editor). London: Wiley-Blackwell Ltd., 2011

Shyu C., Soule T., Bent S. J., James A. Foster J. A. and Larry J. Forney L. J. (2007). MiCA: A Web-Based Tool for the Analysis of Microbial Communities Based on Terminal-Restriction Fragment Length Polymorphisms of 16S and 18S rRNA Genes. *Microbial Ecology* **53**, 562-570

Simpson E. H., (1949). Measurement of diversity. *Nature* **163**, 688-688

Sipos R., Székely A. J., Palatinsky M., Révész S., Márialigeti K and Nikolausz M. The effect of primer mismatch, annealing temperature and PCR cycle number on 16S rRNA gene-targeting bacterial community analysis. *FEMS Microbial Ecology* **60**, 341-350

Sklarz M. Y., Angel R., Gillor O. and Soares M. I. M. (2009). Evaluating amplified rDNA restriction analysis assay for identification of bacterial communities. *Antonie Van Leeuwenhoek* **96**, 659-664

Srivastava A. K., Bharagava P., Kumar A., Rai L. C. and Neilan B. A. (2009). Molecular characterization and the effect of salinity on cyanobacterial diversity in the rice fields of Eastern Uttar Pradesh, India. *Saline Systems* **5**, 1-17

Stoica E. and Herndi G. J. (2007). Contribution of Crenarchaeota and Euryarchaeota to the prokaryotic plankton in the coastal northwestern Black Sea. *Journal of Plankton Research* **29**, 699-706

Sugumar R., Rammanathan G., Rajarthinam K., Jeevarathinam A., Abirami D. and Bhoothapandi M. (2011). Diversity of Saltpan marine Cyanobacteria from Cape Comorin Coast Tamilnadu. *Journal of Phytology* **3**, 01-04

Suzuki M. T. and Giovanni S. J. (1996). Biased caused by template annealing in the amplification of mixtures of 16S rRNA genes by PCR. *Applied and Environmental Microbiology* **62**, 625-630

Tamura K., Peterson D., Peterson N., Stecher G., Nei M. and Kumar S. (2011). MEGA5: Molecular Evolutionary Genetics Analysis using Maximum Likelihood, Evolutionary Distance, and Maximum Parsimony Methods. *Molecular Biology and Evolution* **28**: 2731-2739

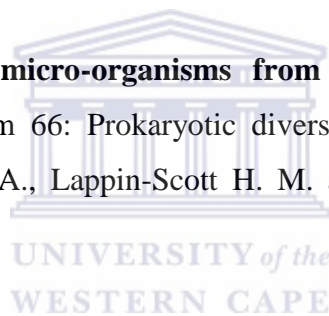
Tom A. Williams T. A., Foster P. G., Nye T. M. W., Cox C. J. and Embley M. T. (2012). A congruent phylogenomic signal places eukaryotes within the Archaea. *Proceedings of the Royal Society of Biological Sciences*. 1-12

Top B. (1992). A simple method to attach a universal 50bp GC-clamp to PCR fragments used for mutation analysis by DGGE. *Genome Research* **2**, 83-85

Torsvik L., Goksøyr J. and Daae F. L. (1990). High diversity in DNA of soil bacteria. *Applied and Environmental Microbiology* **56**, 782-787

Torsvik L. and Ovreas V. (2008). “Microbial diversity, Life Strategies, and Microbial Adaption to Life in Extreme Soils.” In *Microbiology of Extreme Soils*, by Dion P and Nautiyal C. S. (editors), 22-23. Germany: Springer-Verlag Berlin Heidelberg

Ventosa A. (2006). **Unusual micro-organisms from unusual habitats: hypersaline environments.** SGM Symposium 66: Prokaryotic diversity-mechanisms and significance. pp223-235. (Editors) Logan N. A., Lappin-Scott H. M. and Oysten P. C. F. Cambridge University Press



Viles H. A. (2005). Microclimate and weathering in the central Namib Desert, Namibia. *Geomorphology* **67**, 189-209

Viles H. A. and Goudie A. S. (2007). Rapid salt weathering in the coastal Namib desert: Implications for landscape development. *Geomorphology* **85**, 49-62

Wagner N. L., Greco J. A., Ranaghan M. J. and Birge R. R. (2013). Directed evolution of bacteriorhodopsin for applications in bioelectronics. *Journal of the Royal Society Interface* **10**, 1-15

Walsh D. A., Papke R. T. and Doolittle W. F. (2005). Archaeal diversity along a soil salinity gradient prone to disturbance. *Environmental Microbiology* **7**, 1655–1666

Wang G. C. Y. and Wang Y. (1996). The frequency of chimeric molecules as a consequence of PCR co-amplification of 16S rRNA genes from different bacterial species. *Microbiology* **142**, 1107-1114

Wang Q., Garrity G. M., J. M. Tiedje J. M., and J. R. Cole J. R. (2007). Naïve Bayesian Classifier for Rapid Assignment of rRNA Sequences into the New Bacterial Taxonomy. *Applied and Environmental Microbiology* **73**:5261-7

Warr S. R. C, Reed R. H. and Stewart W. D. P. (1984). Osmotic Adjustment of Cyanobacteria: the Effects of NaCl, KCl, Sucrose and Glycine Betaine on Glutamine Synthetase Activity in a Marine and a Halotolerant Strain. *Journal of General Microbiology* **130**, 2169-2175.

Warren-Rhodes K. A., Rhodes K. L., Pointing S. B. Ewing S.A., Lacap D.C., Go´mez-Silva B., Amundson R., Friedmann E. I. and McKay C. P. (2006). Hypolithic Cyanobacteria, Dry Limit of Photosynthesis, and Microbial Ecology in the Hyperarid Atacama Desert. *Microbial Ecology* **52**: 389-398

Williams T. A., Foster P. G., Nye T. M. W., Cox C. J. and Embley T. M. (2012). A congruent phylogenomic signals eukaryotes within the Archaea. *Proceedings of the Royal Society: Biological Sciences* **279**, 4870-4879

Wilson K. H., Blitchington R. B. and Greene R. C. (1990). Amplification of Bacterial 16S Ribosomal DNA with Polymerase Chain reaction. *Journal of Clinical Microbiology* **28**, 1942-194

Yahara K., Didelot X., Ansari M. A., Sheppard S. K. , and Falush D. (2014). Efficient Inference of Recombination Hot Regions in Bacterial Genomes. *Molecular Biology and Evolution* **31**, 1593-1605

Yutin N., Makarova K. S., Mekhedov S. L., Wolf Y. I. and Koonin E. V. (2008). The Deep Archaeal Roots of Eukaryotes. *Molecular Biology and Evolution* 25, 1619-1630

Zafrilla B., Martinez-Espinosa R. M., Alonso M. A. and Bonete M. J. (2010). Biodiversity of Archaea and floral of two inland saltern ecosystems in the Alto Vinalopó Valley, Spain. *Saline Systems* 6,1-12

Zhang X., Yan X., Goa P., Wang L., Zhou Z. and Zhou L. (2004). Optimized sequences retrieval from single bands of temperature gradient gel electrophoresis profiles of the amplified 16S rDNA fragments from an activated sludge system. *Journal of Microbiological Methods* 60, 1-11

Zhou J., Bruns M. A., and Tiedje J. M. (1996). DNA Recovery from Soils of Diverse Composition. *Applied and Environmental Microbiology* 62,316-322

